Russian Original Vol. 38, No. 5, May, 1975

November, 1975

SATEAZ 38(5) 361-468 (1975)

SOVIET ATOMIC ENERGY

АТОМНАЯ ЭНЕРГИЯ
(ATOMNAYA ÉNERGIYA)

TRANSLATED FROM RUSSIAN

CONSULTANTS BUREAU, NEW YORK

SOVIET ATOMIC ENERGY

Soviet Atomic Energy is a cover-to-cover translation of *Atomnaya Énergiya*, a publication of the Academy of Sciences of the USSR.

An agreement with the Copyright Agency of the USSR (VAAP) makes available both advance copies of the Russian journal and original glossy photographs and artwork. This serves to decrease the necessary time lag between publication of the original and publication of the translation and helps to improve the quality of the latter. The translation began with the first issue of the Russian journal.

Consultants Bureau journals appear about six months after the publication of the original Russian issue. For bibliographic accuracy, the English issue published by Consultants Bureau carries the same number and date as the original Russian from which it was translated. For example, a Russian issue published in December will appear in a Consultants Bureau English translation about the following June, but the translation issue will carry the December date. When ordering any volume or particular issue of a Consultants Bureau journal, please specify the date and, where applicable, the volume and issue numbers of the original Russian. The material you will receive will be a translation of that Russian volume or issue.

Subscription
$87.50 per volume (6 Issues)

Single Issue: $50
Single Article: $15

Prices somewhat higher outside the United States.

CONSULTANTS BUREAU, NEW YORK AND LONDON

227 West 17th Street
New York, New York 10011

4a Lower John Street
London W1R 3PD
England

Published monthly. Second-class postage paid at Jamaica, New York 11431.

Soviet Atomic Energy is abstracted or indexed in *Applied Mechanics Reviews, Chemical Abstracts, Engineering Index, INSPEC—Physics Abstracts and Electrical and Electronics Abstracts, Current Contents,* and *Nuclear Science Abstracts.*

SOVIET ATOMIC ENERGY

A translation of *Atomnaya Énergiya*

November, 1975

Volume 38, Number 5 May, 1975

CONTENTS

CONTENTS

(continued)

The Russian press date (podpisano k pechati) of this issue was 4/23/1975. Publication therefore did not occur prior to this date, but must be assumed to have taken place reasonably soon thereafter.

OBITUARY

VITALII VASIL'EVICH SHIPOV

Vitalii Vasil'evich Shipov, Director of Atomizdat and member of the Communist Party of the Soviet Union, passed away on April 22 after a prolonged illness.

V. V. Shipov was born in Moscow on April 12, 1911. After finishing his studies at the institute, he occupied the position of Chief Engineer of the Central Telegraph of the Buryyat-Mongol Autonomous Republic and then the post of Senior Engineer and Head of the Administration of the Main Communication Lines of the Ministry of Communication of the USSR.

Since 1949, V. V. Shipov combined his regular work with editorial activities. He was the Director of the Editorial Division of Svyaz'izdat, Editor of the journal Sovetskii Svyazist, and the Director of Svyaz'izdat. Vitalii Vasil'evich Shipov was intimately associated with the formation of the Atomizdat where he continued to work until his last moments of life. While acting as Director of the Atomizdat, Vitalii Vasil'evich carried out important work in smoothing out the editorial process, the preparation, publication, and dissemination of literature on atomic science and engineering.

As Chairman of the Editorial Committee of the Atomizdat, V. V. Shipov took pains to establish a wide authorial base for the Publishing House, and was instrumental in creating various Sections and Branches of the Editorial Committee through which the scientific community could participate in selecting and evaluating the submitted papers. He authored many popular science booklets and articles in periodical publications.

V. V. Shipov was a member of the Union of Journalists of the USSR and actively participated in its work as Deputy Chairman of the Section of Editorial and Publication Workers of the Moscow Division of the Union of Journalists.

For several years V. V. Shipov acted as a Member of the Kuibyshev Regional Committee of the Communist Party of the USSR and was elected Deputy of the Kuibyshev District Soviet. He was awarded the order for Valiant Labour in the Great Patriotic War, the anniversary medal "For Valiant Labour. In Commemoration the 100th Anniversary of the Birth of V. I. Lenin," the Gold and two Silver Medals

Translated from Atomnaya Énergiya, Vol. 38, No. 5, p. 282, May, 1975.

of the Exhibition of Achievement of the National Economy of the USSR, badges for Excellent Work in Publishing and for Distiguished Service in Civil Defence, a Diploma of the Presidium of the Supreme Soviet of the Buryat-Mongol Autonomous SSR, and other decorations.

For his outstanding contributions to the book publishing trade, V. V. Shipov has been given the honorary title of "Distiguished Worker of Culture of the RSFSR."

In all his professional and public activities, Vitalii Vasil'evich was noted for his communist principles, calm efficiency, professional skills, vitality and optimism, kindness and exactingness in work, competent leadership, and patience and persistence in educating his staff.

The great conviction, diligence, and modesty of Vitalii Vasil'evich always served as an example to all his collaborators.

The memory of Vitalii Vasil'evich will for ever remain in our hearts.

ARTICLES

NEUTRON-ABSORPTION ANALYZER OF BORON IN THE COOLANT OF THE PRIMARY CIRCUIT OF WATER-COOLED WATER-MODERATED POWER REACTORS

V. P. Bovin, V. L. Chulkin, and S. V. Shagov

UDC 621.039.562.2:621.039.562.26

Boric acid, added to the primary-circuit coolant of water-cooled, water-moderated power reactors (WWPR) for reactivity compensation, improves the energy release distribution in the core, improves the uniformity and depth of fuel burnup, and speeds up the reactor power operating conditions without affecting safety [1].

The advantages of boron control can be most fully utilized by monitoring boron concentration at various points of the circuit, in the purging and feed systems, and in the boric acid preparation units.

Chemical methods of analysis requiring sampling provide delayed information and do not reflect the dynamics of processes taking place in the reactor circuit.

Neutron-absorption methods used for the determination of elements with high thermal-neutron absorption cross sections, including boron, are now becoming very popular [2, 3]. The design of boron concentration meters for WWPR has been reported in [4, 5]. As a rule, special measuring chambers or lines which sample the coolant are used to provide optimum conditions for the measuring instrumentation.

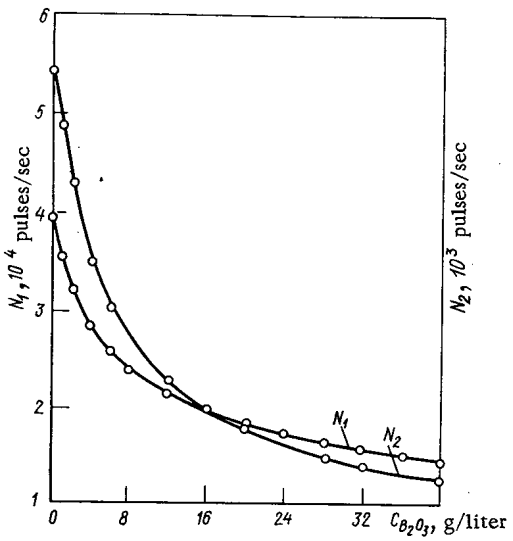

Fig. 1

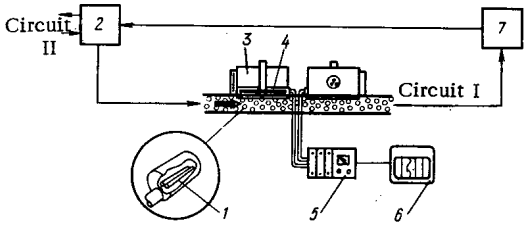

Fig. 2

Fig. 1. Count rate of a slow-neutron detector as a function of boron concentration with the detector and source located at the pipe center (N_1) and on the surface (N_2).

Fig. 2. Location of surface detectors of the boron analyzer on the primary-circuit piping of a WWPR: 1) neutron counter, 2) steam generator, 3) detector, 4) neutron source, 5) measuring panel, 6) potentiometer recorder, 7) WWPR.

Translated from Atomnaya Énergiya, Vol. 38, No. 5, pp. 283-286, May, 1975. Original article submitted April 15, 1974.

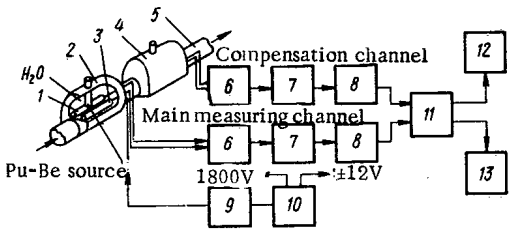

Fig. 3.

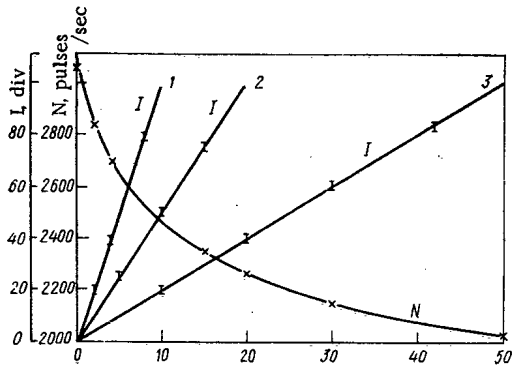

Fig. 4

Fig. 3. Block diagram of boron analyzer: 1) main counter SNM-16, 2) main detector, 3) stand-by SNM-16 counter, 4) compensation detector, 5) pipe with measured boric acid solution, 6) pulse amplifier, 7) threshold circuit, 8) shaper, 9) remote calibration control circuit, 10) counter and amplifier power supplies, 11) analog time interval meter, 12) computer, 13) potentiometer recorder.

Fig. 4. Count rate of SNM-16 counters as a function of H_3BO_3 concentration, and calibration curves of the time interval meter on all three ranges (1-3).

However, of most interest are methods and instruments for continuous on-line analysis of boron concentration which can be applied without affecting the pipeline network.

Two measuring methods can be used depending on the piping diameter and boron concentration: either counting of neutrons transmitted through a layer of the analyzed fluid, or counting reflected thermal neutrons. The first method is suitable for measuring boron concentration in small diameter piping. The second method can be used for boron analysis in a wider range of concentrations and in larger pipes (60 mm or more), the sensitivity of the method increasing with the diameter of piping up to about 100 to 150 mm and then remaining constant.

Figure 1 shows the neutron count rate as a function of B_2O_3 concentration, the Pu-Be source of fast neutrons with a yield of $5 \cdot 10^6$ neutr./sec and the thermal neutron counter (^3He filled SNM-16 detector) located on the surface and in the center of a 200 mm pipe. The count rate of reflected neutrons on the pipe surface decreases approximately by one order of magnitude. The loss of sensitivity caused by this geometry can be partially (approximately 1.5 to 2 times) compensated by placing both the counter and the source in a reflector (water or paraffin) or by using a source with a higher yield of neutrons. In addition, the application of high-efficiency, helium filled slow-neutron counters provides the necessary analytic accuracy with Pu-Be neutron sources with a yield of $5 \cdot 10^6$ neutr./sec.

In measuring the boron concentration in the primary circuit coolant one must take into account the possibility of errors caused by the variable background due to delayed neutrons produced in the decay

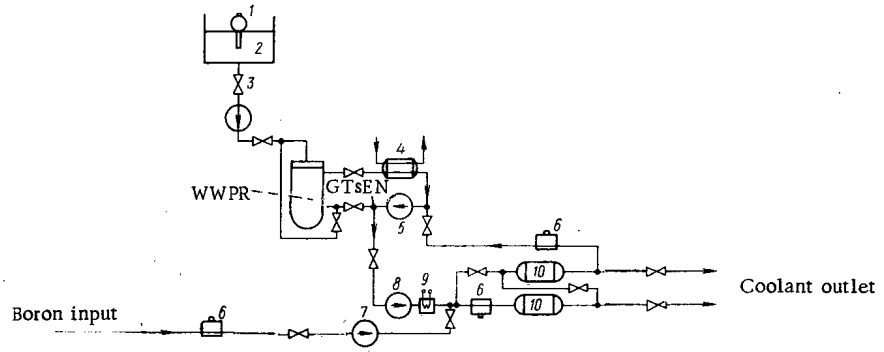

Fig. 5. Schematic drawing of detector mounting for measuring boron concentration in the purging—feeding system of the primary circuit and in emergency shielding tanks of a WWPR: 1) submersible boron-analyzer counter, 2) emergency H_3BO_3 supply tank, 3) valves, 4) steam generator, 5) main circulating pump, 6) surface boron-analyzer detectors, 7) feed pump, 8) purging circuit pump, 9) heat exchanger, 10) ion exchange filters.

TABLE 1. Analyzer Calibration Results

H_3BO_3 concentration, g/kg	Count rate at the main channel output, pulses/sec	H_3BO_3 concentration, g/kg	Count rate at the main channel output, pulse/sec
0	3042	4,77	2737
0,93	2965	7,99	2620
1,98	2891	11,4	2517
2,91	2831	14,0	2470
3.9	2773	50	2130

of fissionable elements and ^{17}Na. This background decreases appreciably several tens of seconds after the coolant leaves the core. If the necessary delay cannot be provided before analysis, the variable neutron background should be compensated in the measuring apparatus.

On the basis of these considerations we have designed a neutron-absorption boron concentration analyzer fitted with measuring and compensation detectors mounted side by side on the pipe surface (Fig. 2). Both detectors are structurally identical each containing two neutron counters, one operating and one stand-by, with the neutron source between them.

The compensation detector, which counts the background of delayed neutrons in the coolant, has no isotopic source. To improve sensitivity the detectors are provided with reflectors consisting of a stainless steel jacket filled with water. In operation on pipes carrying hot coolant, the reflector is used for cooling the counters and is connected to a circulating water system.

Periodical checking of the system operation is enabled by placing the counters into rotating cadmium shields with windows which can be remotely positioned to face the neutron reflector (reference point) or the analyzed solution (reading). Testing can also be provided by periodical connection of the stand-by counter.

It has been found that in this method of counting, the count rate of the main detector N less the count rate of background pulses due to delayed neutrons and the neutrons entering the counter without passing through the analyzed layer is inversely proportional to boric acid concentration C:

$$kC = \frac{N_0}{N} - 1 = QN_0 - 1,$$

where k is a proportionally factor, N_0 is the pulse count rate of the main detector at zero boric acid concentration minus background pulses, and Q = 1/N is the average interval between pulses.

Figure 3 shows the block diagram of the boron concentration meter. Pulses from the neutron counters are transmitted through a 100-200 m long cable and matching transformer to the measuring panel which has main and compensation channels. Each channel contains an amplifier, a threshold stage for noise suppression, and a pulse length and amplitude shaper.

Boron concentration is measured by an analog computing circuit consisting of a time interval meter with a linearized sensitivity characteristic [6]. The average time interval between pulses is determined by charging an integrating capacitor C_i, connected between the input and output of a dc operational amplifier, with a constant current and by discharging this capacitor by pulses N from the detector. The constant background is compensated by a feedback circuit through which the integrating capacitor is charged by a current inversely proportional to the output voltage. Solid-state integrated circuitry is used.

The analyzer has been designed to measure boric acid concentrations up to 50 g/kg and is provided with three ranges: 0-10, 0-20, and 0-50 g/kg. The measured results are applied to a potentiometer recorder and to a control and computing circuit. The accuracy is better than 4% of full range for time interval meter time constant τ = 50 sec. Figure 4 shows the analyzer calibration for type SNM-16 counters and the time interval meter response on all three measuring ranges.

A model of the instrument was tested at the Novovoronezh Atomic Power Plant. The detectors were mounted on the purging water line of the primary circuit of the VVER-440 water-cooled water-moderated power reactor following the heat exchanger and the water purification filters. The delayed-neutron background is practically zero at this point (about 7 pulses/sec) as it takes two minutes for the solution to pass from the reactor to this point. The compensation detector can thus be disconnected and used as a stand-by detector and for cases of emergency or fuel element leakage. The constant background in the main channel, due to neutrons that did not pass through the moderator, was 1500-2000 pulses/sec and

was compensated by feedback in the time interval measuring circuit thus providing a linear relationship between the output voltage or current and the boron concentration.

Table 1 shows the results of analyzer calibration in the boron acid concentration range up to 50 g/kg.

The operation included a check of the long-term reproducibility of results (after more than three weeks). The standard deviation of the obtained results $\delta = 1/\sqrt{2N\tau}$ did not exceed 2%. Other detector types as well as other mounting points can be employed depending on the measuring conditions (Fig. 5).

Submersible detectors are especially suitable for measuring boric acid concentration in solution preparation tanks. Neutron sources with a yield of $5 \cdot 10^5$ neutr./sec are sufficient for this purpose [6].

LITERATURE CITED

1. Operation of Reactor Facilities of the Novovoronezh Atomic Power Plant [in Russian], Atomizdat, Moscow (1972).
2. Yu. G. Fadeev and F. A. Sychev, in: Nuclear-Physics Methods of Analysis [in Russian], Atomizdat, Moscow (1971), p. 304.
3. M. A. Belyakov and É. V. Anchevskii, in: Nuclear-Physics Methods of Analysis [in Russian], Atomizdat, Moscow (1971), p. 156.
4. K. Fahrman and F. Jäpel, Kernenergie, 10, No. 11, 337 (1967).
5. R. Gopal, Trans. Amer. Nucl. Soc., 13, No. 1, 237 (1970).
6. V. P. Bovin et al., in: Radiation Engineering [in Russian], No. 11, Atomizdat, Moscow (1975), p. 263.

D. A. Kozhevnikov

NEUTRON CHARACTERISTICS OF ROCKS AND THEIR APPLICATIONS IN OIL AND GAS GEOLOGY*

Reviewed by E. M. Filippov

The book discusses one of the most important and timely topics: the energy, spatial, and time distribution of neutrons and capture γ quanta, and the measuring techniques used for the evaluation of neutron properties of rocks as applied to problems in oil field geophysics.

In the first chapter the author gives a simple and clear classification of neutron techniques, considers the scope of their application, and mentions the problems they are used to solve. This is followed by an exposition of nuclear properties of rock forming elements and of impurity elements having anomalous neutron properties. The chapter ends with a description of radioisotopic neutron sources. Here, and not in the second chapter, is the proper place to discuss californium sources which are now finding wide application in nuclear geophysics.

The second chapter is devoted to neutron moderation processes in rocks and describes elastic and inelastic neutron scattering, various simple methods of calculating the spatial and energy distribution of neutrons in rocks, and the effect of neutron absorption on their energy distribution. The concluding sections of this chapter contain a discussion of the time distribution of moderated neutrons provided by a pulse source and the relationships describing neutron moderation.

The age of neutrons, which is one of the most important characteristics of the spatial energy distribution of moderated neutrons, is discussed in the third chapter which also includes rules for calculating this parameter with various degrees of accuracy. The rules give results in good agreement with experimental data. Together with neutron age, the author discusses neutron migration using the term "neutron migration area" (pp. 74, 75). Actually, however, the discussion here concerns the square of this quantity, the term "area" being entirely inappropriate in this connection. The same can also be said about the migration length of γ radiation produced by radiative neutron capture (p. 105). If the term was adopted from literature this should have been stated explicitly and justified from a physical point of view. Moreover, similar quantities should have been termed uniformly: the squared diffusion length (p. 109) should rather be called the diffusion area.

The process of thermal neutron diffusion in matter is discussed in the fourth chapter. The energy spectrum of thermal neutrons is given, as is their spatial and space-time distribution and their radiative capture. Techniques are described for measuring the diffusion characteristics and their magnitude.

In the fifth chapter the author considers the possibilities of neutron methods in solving practical problems of oil and gas field geophysics and the nature of the dependence of NGM and NNM readings on the stratum porosity m. The author favors the É. Yu. Mikolaevskii formula and does not mention the relation $J_{n\gamma} = a + b \ln m$, where a and b are constants, which is most frequently used in practice. It would be desirable to discuss this relation in detail and compare it with the one cited in the book.

It would be more appropriate to discuss the problems associated with the effect of borehole radiation of NGM readings and methods of INNM measurement in the preceding chapter as they do not directly relate to the discussed problem. This is especially true of the material associated with the determination of diffusion parameters τ and D. The material presented in pp. 159-163 partly repeats the text in pp. 101-102.

It can be stated in conclusion that the book concerns itself mostly with the theory of neutron methods (chapters 2-4). Neutron properties proper are basically discussed in chapters 3-5, but even here they are

* Izd. Nedra, Moscow (1974), 184 pp.

Translated from Atomnaya Énergiya, Vol. 38, No. 5, p. 286, May, 1975.

for the most part treated rather schematically. For example, the methods of measuring diffusion characteristics, discussed in Chapter 4 (pp. 113-120), are only briefly described which is typical of theoretical courses. To make practical use of the described methods experimenters must turn to original works. This holds, for example, for the techniques proposed by V. V. Miller and Yu. S. Shimelevich, as well as for other techniques.

Thus, the book should have been more appropriately titled "Principles of the Theory of Neutron Methods as Applied to Oil and Gas Field Geophysics."

It can be stated in conclusion that the book is written in a clear language and is held on a high scientific level. It is very useful for geophysicists engaged in oil and gas prospecting and for nuclear geophysicists specializing in engineering, mining, and coal prospecting geology. A reader interested in the development and practical application of neutron methods will find the book most useful.

ARTICLES

MATHEMATICAL MODEL FOR DETERMINING UNIT POWERS OF ATOMIC POWER PLANTS AND VARIOUS REACTOR ASSEMBLIES

V. M. Chakhovskii and V. V. Matskov

UDC 621.311.2:621.039+001.58

There is still no firm stand as to the unit powers of atomic power plants and reactor assemblies using various reactor types to be put into operation till the year 2000. The need for a firm stand in this respect becomes clear if one considers that very large amounts of electric power, up to several gigawatts, are to be annually added till the end of this century. It is quite obvious that the realization of high-power units meets with many difficulties which have been covered in considerable detail in [1-5].

In solving this problem it is necessary to give due consideration to unit power levels economically feasible both in the immediate and the more distant future, and, on the other hand, to begin immediately the determination of such levels in a proper sequence so as to ensure a rational allocation of the available financial and manpower resources.

An estimation of the development of nuclear power engineering in the next 30 years requires the knowledge of the limits of optimum plant size and of economically warranted power levels. In addition, it is necessary to evaluate the most convenient from a technological and economical point of view, unit power levels of nuclear power plants within the scope of future power developments and also the terms when these new power levels are put into practice.

This problem must be considered and solved in parallel with the progress in conventional power engineering.

In this article the problems are solved with the aid of a dynamic optimization model. The main propositions of this model are:

1. The dynamics of growth of the total energy and of the power of thermal and atomic power plants individually is known. The growth of thermal and atomic plant powers are specified in terms of the number of hours of utilization.

2. Information on the fuel-energy balance is used to find the amount of each kind of fuel of thermal power plants which can be used for a given price per 1 ton of nominal fuel at point of use. Resources of fuel are divided in categories according to cost, the most cheap fuel being used first.

3. The transportation costs of nuclear fuel, raw materials, and used up fuel elements are not taken into account. The expenditure on fuel and its transportation for organic-fuel power plants are taken into account according to the cost of mineral fuel at the point of use.

TABLE 1. Predicted Growth of Unit Power of Generating Units of Atomic and Thermal Power Plants in the USA

Unit power of generating unit, MW	Number of units			
	1980		1990	
	APP	TPP	APP	TPP
601—1200	101	120	227	185
1201—1800	23	11	95	60
1801—2400	—	—	32	21
2401—3000	—	—	11	—

4. The cost of nuclear fuel and its cycling are determined in accordance with the type of atomic power plant. The consumption of fuel for any specific reactor type is assumed to remain fixed throughout the entire period of calculation. Reserves of natural uranium also are classified into categories depending on their costs, the cheapest being used up first [6, 7].

5. The time interval in the period of calculations is assumed as one year or more.

Translated from Atomnaya Énergiya, Vol. 38, No. 5, pp. 287-290, May, 1975. Original article submitted May 16, 1974.

6. The capital investment distribution over the years of power plant construction is allowed for by a resources-freezing coefficient throughout the construction period.

7. The reserve power is calculated on the basis of installed power-plant power at the beginning of the calculations period and taking into account the assumed growth of power in power systems.

8. The power of individual atomic and thermal power plants is assumed to remain constant over indefinitely long periods of time. Physically aging plants are replaced by equivelant ones (direct conversion). Atomic and thermal power plants put into operation during the calculations period are assumed to be utilized for a fixed number of hours at installed power throughout their entire exploitation period.

As input information to the model we use $X^{APP}_{\vartheta l}$, $X^{TPP}_{\vartheta l}$ ($\vartheta = 1, 2, \ldots, \theta$; $l = 1, 2, \ldots, L$) the total power of atomic (APP) and thermal (TPP) plants respectively, fed in the interval ϑ the number of utilization hours being h_l; G_s ($s = 1, 2, \ldots, S$) the amount of nuclear raw material received from the sources at the price of natural uranium s; B_z ($z = 1, 2, \ldots, Z$) the amount and kind of organic fuel used by thermal plants at the cost z per 1 ton of nominal fuel; W_q ($q = 1, 2, \ldots, Q$) the electrical power of the q-th construction site, M_ϑ ($\vartheta = 1, 2, \ldots, \theta$) the number of production workers engaged in electrical plant construction in the interval ϑ; $\wedge_\vartheta$ ($\vartheta = 1, 2, \ldots, \theta$) the number of production workers engaged in operating the power plants put into operation in the interval ϑ; $X^{max}_{i\vartheta_\tau}$, $x^{max}_{j\vartheta_\tau}$ ($i = 1, 2, \ldots, I$; $j = 1, 2, \ldots, J$; $\vartheta_\tau = 1, 2, \ldots, \vartheta$) the maximum possible production power of known types of respectively atomic and thermal power plant units in the interval of the calculations period (I, J is the number of typical sizes of atomic and thermal power plants respectively).

The above conditions can be formulated mathematically as follows. We have to find

$$\min \sum_{\vartheta=1}^{\theta} \sum_{q=1}^{Q} \sum_{l=1}^{L} \Big[\sum_{s=1}^{S} \sum_{i=1}^{I} E_{islq\vartheta} n_{islq\vartheta} N_i + \sum_{z=1}^{Z} \sum_{j=1}^{J} E_{jzlq\vartheta} n_{jzlq\vartheta} N_j \Big] (1+p)^{T-t_\vartheta} + p \sum_{\vartheta_\tau=1}^{\vartheta} \Big(\sum_{i=1}^{I} E^0_{i\vartheta_\tau} Y_{i\vartheta_\tau} + \sum_{j=1}^{J} E^0_{j\vartheta_\tau} Y_{j\vartheta_\tau} \Big) (1+p)^{T=t\vartheta_\tau}. \quad (1)$$

Here $\vartheta = 1, 2, \ldots, \theta$ is the number of time intervals in the calculations period, ϑ_τ is the interval of mastering type i, j plant; $E_{islq\vartheta}$, $E_{jzlq\vartheta}$ are the specific adduced expenditures of power plants using nuclear and organic fuel respectively with type i (j) units for a natural uranium price s and organic fuel price z, utilized for h_l hours at installed power at the q-th construction site in the interval ϑ of the calculations period; these expenditures include the cost of distribution lines, power plant construction, and building; $n_{islq\vartheta}$, $n_{jzlq\vartheta}$ are the desired variables which determine the number of generating units of atomic and thermal plants. The combination of subscripts (i, j, s, z, l, q, ϑ) indicates the i-th (j-th) type-size of the unit, s (z) is the type of fuel used with respect to its cost, h_l is the number of hours of utilization at installed power, ϑ is the interval of the calculations period, N_i, N_j is the unit power of type i (j) atomic and thermal power generating units in the interval ϑ; $E^0_{i\vartheta_\tau}$, $E^0_{j\vartheta_\tau}$ is the cost of mastering a new type of atomic or thermal generating unit put into operation at the beginning of ϑ_τ; $Y_{i\vartheta_\tau}$, $Y_{j\vartheta_\tau}$ is a Boolean variable (0 or 1, such that if $Y_{i\vartheta_\tau} = 1$ and $Y_{j\vartheta_\tau} = 1$, the unit can be introduced in the interval ϑ_τ (in the model)), p is a standardizing factor allowing for the noncoincidence of the various expenditures, T is the year of expenditure adduction, t_ϑ is the year preceding stage ϑ, and t_{ϑ_τ} is the year preceding stage ϑ_τ.

The minimum of function (1) is found under several constraints (either equalities or inequalities). The first group of constraints expresses the necessity of providing a given volume of atomic and thermal power inputs at all stages of the calculations period:

$$\sum_{q=1}^{Q} \sum_{s=1}^{S} \sum_{i=1}^{I} n_{islq\vartheta} N_i (1-\rho_i) \geqslant X^{APP}_{\vartheta l} \quad (\vartheta = 1, 2, \ldots \theta;\ l = 1, 2 \ldots, L); \quad (2)$$

$$\sum_{q=1}^{Q} \sum_{z=1}^{Z} \sum_{j=1}^{J} n_{jzlq\vartheta} N_j (1-\rho_j) \geqslant X^{TPP}_{\vartheta l} \quad (\vartheta = 1, 2 \ldots \theta;\ l = 1, 2 \ldots, L), \quad (3)$$

where ρ_i, ρ_j is the specific reserve of type i (j) plant determined in accordance with the systematic propositions put forward in [8].

The constraints reflecting the limited amount of nuclear raw materials at a fixed natural uranium price is written in the form

$$\sum_{\vartheta=1}^{\theta}\left(\sum_{q=1}^{Q}\sum_{l=1}^{L}\sum_{i=1}^{I}\beta_{il\vartheta}n_{islq\vartheta}N_i+G^0_{\vartheta s}\right)\leqslant G_s \qquad (4)$$
$$(s=1, 2\ldots, S),$$

where

$$\beta_{il\vartheta}=\beta'_{il}+\Delta\tau_{i\vartheta ls}\beta_{il} \qquad (5)$$

is the specific fuel consumption per 1 kW of electric power of type i generating unit with h hours of utilization put into operation in the interval ϑ (here β'_{il} is the specific nuclear fuel charge per 1 kW of electric power in the fuel cycle of an atomic power plant with type i generating units and h_l utilization hours, β_{il} is the specific nuclear fuel consumption per 1 kWh of an atomic power plant with type i units and h_ϑ utilization hours, $\Delta\tau_{i\vartheta ls}$ is the operating time of a type i unit with h_l utilization hours using uranium of price s in the interval ϑ of the calculations period); $G^0_{\vartheta s}$ is the consumption of uranium of price s of the existing units of an atomic power plant in the interval ϑ.

The constraints on the limitations of organic fuel at fixed costs is described by

$$\sum_{\vartheta=1}^{\theta}\sum_{q=1}^{Q}\sum_{l=1}^{L}\sum_{j=1}^{J}b_{jzl\vartheta}n_{jzlq\vartheta}N_j+B^0_{\vartheta z}\leqslant B_z \qquad (6)$$
$$(z=1, 2\ldots, Z),$$

where

$$b_{jzl\vartheta}=b'_{jzl}\Delta\tau_{j\vartheta lz} \qquad (7)$$

is the specific consumption of fuel of price z per 1 kW of electric power of a type j generating unit with h_l (here b'_{jlz} is the specific consumption per 1 kWh of organic fuel of price z per 1 ton of nominal fuel by a thermal generating unit of type j with h_l utilization hours, $\Delta\tau_{j\vartheta lz}$ is the operating time of a type j unit with h_l utilization hours using fuel of price z), $B^0_{\vartheta z}$ is the consumption of organic fuel of price z of the existing units of thermal power plants in the interval ϑ.

Electrical power plants put into operation in the calculations period should obey the following relationship which reflects the limiting power capacity of building sites:

$$\sum_{\vartheta=1}^{\theta}\sum_{l=1}^{L}\left(\sum_{s=1}^{S}\sum_{i=1}^{I}n_{islq\vartheta}N_i+\sum_{z=1}^{Z}\sum_{j=1}^{J}n_{jzlq\vartheta}N_j\right)\leqslant W_q \qquad (8)$$
$$(q=1, 2\ldots, Q).$$

The limitations of manpower in the construction of electrical power plants is written as

$$\sum_{l=1}^{L}\sum_{q=1}^{Q}\left(\sum_{s=1}^{S}\sum_{i=1}^{I}\mu_{i\vartheta}n_{islq\vartheta}N_i+\sum_{z=1}^{Z}\sum_{j=1}^{J}\mu_{j\vartheta}n_{jzlq\vartheta}N_j\right)\leqslant M_\vartheta \qquad (9)$$
$$(\vartheta=1, 2\ldots, \theta),$$

where $\mu_{i\vartheta}$, $\mu_{j\vartheta}$ is the specific number of personnel engaged in the construction of atomic and thermal power plants with type i (j) generating units in the interval ϑ per 1 kW of electrostatic power.

The limitations of manpower in operating electrical power plants is written as

$$\sum_{q=1}^{Q}\sum_{l=1}^{L}\left(\sum_{s=1}^{S}\sum_{i=1}^{I}\gamma_{i\vartheta}n_{islq\vartheta}N_i+\sum_{z=1}^{Z}\sum_{j=1}^{J}\gamma_{j\vartheta}n_{jzlq\vartheta}N_j\right)\leqslant\Lambda_\vartheta \qquad (10)$$
$$(\vartheta=1, 2\ldots, \theta),$$

where $\gamma_{i\vartheta}$, $\gamma_{j\vartheta}$ is the specific number of personnel engaged in running atomic or thermal power plants with type i (j) generating units in the interval ϑ per 1 kW of electric power.

The following constraints take into account the fact that a new type i of atomic generating unit can be put into operation after it is mastered at the following cost:

$$\sum_{q=1}^{Q}\sum_{l=1}^{L}\sum_{s=1}^{S}n_{islq\vartheta}N_i\leqslant\sum_{\vartheta_\tau=1}^{\vartheta}X^{\max}_{i\vartheta_\tau}Y_{i\vartheta_\tau} \qquad (11)$$
$$(i=1, 2\ldots, I;\ \vartheta=1, 2\ldots, \theta),$$

where

$$\sum_{\vartheta_\tau=1}^{\vartheta} Y_{i\vartheta_\tau} \leqslant 1. \tag{12}$$

The corresponding constraints for thermal power plants have the form

$$\sum_{q=1}^{Q}\sum_{l=1}^{L}\sum_{z=1}^{Z} n_{jzlq\vartheta} N_j \leqslant \sum_{\vartheta_\tau=1}^{\vartheta} X_{j\vartheta_\tau}^{\max} Y_{j\vartheta_\tau} \tag{13}$$
$$(j = 1, 2\ldots, J;\ \vartheta = 1, 2\ldots, \theta),$$

where

$$\sum_{\vartheta_\tau=1}^{\vartheta} Y_{j\vartheta_\tau} \leqslant 1. \tag{14}$$

The condition of nonnegativity of the introduced powers is written as

$$n_{islq\vartheta} \geqslant 0, \tag{15}$$
$$n_{jzlq\vartheta} \geqslant 0. \tag{16}$$

This method of including the cost of mastering the operation of generating units in the model has been accepted in accordance with the methods of solving combinatorial optimization problems [9]. In the general case the problem (Eqs. (1) through (16)) is nonlinear.

Taking into accout the facts that the cost of mastering new technology $E^0_{i\vartheta_T}$, $E^0_{j\vartheta_T}$ is known with little reliability, and also that the expenditure on machine building and site construction have been little studied, the first stage of the calculations for atomic power plants has been carried out neglecting these expenditures. In addition, to reduce the size of matrices, the development of atomic and thermal power plants has been treated separately in practical calculations. The form of the objective function (1), suitable for solving the problem of selecting the number of type-sizes of atomic power plants, is

$$\sum_{\vartheta=1}^{\theta}\sum_{q=1}^{Q}\sum_{l=1}^{L}\sum_{s=1}^{S}\sum_{i=1}^{I} E_{islq\vartheta} n_{islq\vartheta} \to \min, \tag{17}$$

where

$$E_{islq\vartheta} = E_{islq\vartheta} N_i (1+p)^{T-t_\vartheta}.$$

The minimum of the function (17) is sought under the constraints (2), (4), (8)-(10) and (15).

The described model has been applied to a study of the feasible power levels of generating units and power plants operating with nuclear fuel. The purpose of the study was to establish the effectiveness of the model in solving problems associated with the determination of the technical policy in the field of further increases of unit power of generating units and plants, with equipment structure, and with the selection of the most desirable number of different type-sizes of atomic power plant equipment. The model has been used in a run of calculations for different versions of the predicted growth of nuclear energy with different starting technical and economical indicators. The calculations were carried out with a BÉSM-6 computer using a modified simplex program. The size of the computation matrix was 29 constraints, and 520 unknowns. The computing time was 60 sec.

The basic results obtained at this stage can be reduced to the following. The computations confirmed the stability of results as applied to atomic power plants with thermal reactor concerning the increase of unit power of generating units from 440-500 to 3000 MW. The economically desirable scale of generating units power has been established in the following order: 1000 MW units till 1985, 2000 MW units till the year 2000, and 3000-4000 MW units at the end of the 90's and after the year 2000. The economical effect of increasing unit power of atomic power plants with fast reactors is still higher. Considering that such power plants will be in commercial use in the late 80's, they should be even now designed for unit powers in the 1500 to 3000 MW range. Unit powers of atomic power plants both with thermal and fast reactors should be at the 6000 to 12,000 MW level. The most optimistic version of the growth of nuclear power in the early 90's indicates that the best solution for thermal-reactor plants is to use generating units of 3000-4000 MW unit power and plants of 12-16 GW unit power.

A provisional study of parameters of atomic power plants with thermal reactors indicates that in view of the difficulties involved in building sufficiently strong housings of very large dimensions one can hardly count on a significant increase of pressure. This means that the parameters of the turbine loop will remain unchanged, i.e., the saturated steam supplied to the turbine will have a pressure of 60-65 atm. With increasing unit power of fast reactors with liquid-metal coolant, the steam parameters will remain

subcritical [10-11]. The temperature at the reactor inlet and outlet will be 380-400 and 570°C respectively. Optimum steam parameters lie in the 130-160 atm and 490-530 °C range.

It is interesting to consider the predicted increase of unit power of atomic and thermal power plant units in the USA [12]. The predicted data are listed in Table 1. As seen in the table, the unit power of atomic generating units will exceed the unit power of thermal generating units.

Calculations indicate that, in view of the expected growth of the total annual power input in the country, the increase of unit power of generating units and power plants is an essential condition for satisfying the growing need for electric power in the national economy. In developing a program for the future growth of nuclear power one should proceed on the basis of the most effective unit powers of generating units and power plants which should correspond to the high prediction levels of electric energy production.

LITERATURE CITED

1. M. P. Kostenko and E. Ya. Kazovskii, Énergetika i Transport, No. 6, 18 (1973).
2. I. K. Terent'ev and L. D. Frenkel', ibid., p. 26.
3. E. T. Doblenko and N. N. Zorev, ibid., p. 31.
4. L. Ya. Stanislavskii et al., ibid., p. 50.
5. A. M. Petros'yanis, From Scientific Research to Atomic Industry [in Russian], Atomizdat, Moscow (1972).
6. V. P. Brailov, At. Énerg., 32, 401 (1972).
7. A. D. Virtser, G. B. Levental', and S. Ya. Chernavskii, At. Énerg., 33, 955 (1972).
8. G. N. Lyalik and V. I. Urvantsev, Élektricheskie Stantsii, No. 1, 7 (1972).
9. V. N. Burkov and S. E. Lavetskii, Avtomat. i Telemekhan., No. 11, 68 (1968).
10. V. M. Chakhovskii, in: Methods of Estimating the Growth of Electric Power [in Russian], Nauka, Moscow (1973).
11. Gasuhiro Koayshi, J. Nucl. Sci. Technol., 10, No. 10, 607 (1973).
12. Electrical Rev., 191, No. 14, 441 (1972).

ABSORPTION OF THERMAL NEUTRONS IN MEDIA WITH LOCALIZED INHOMOGENEITIES

A. V. Stepanov

UDC 539.125.52:621.039.51.12

In the analytical approach to the study of neutron distribution functions in nuclear reactors, wide use is now made of the theory of a heterogeneous reactor with small blocks [1-3]. In this theory, analysis of the neutron transfer equation in the diffusion-age approximation reduces to solving the so-called characteristic equation for the critical dimension of the periodic lattice of the reactor. One of the essential constraints assumed in the theory of the heterogeneous reactor is the assumption of strict periodicity in the positioning of the blocks. Allowance for random deviations of the block coordinates from the lattice points implies the inclusion of elements of statistical averaging in the theory. This approach to the problem of neutron transfer in a heterogeneous medium with an arbitrary structure was developed in a previous paper [4]. The method reduces to finding the mean macroscopic neutron flux. It is effective in solving that class of problems in which, despite marked oscillations in the diffusion characteristics of the medium, the fluctuations of the neutron flux are small so that we can use the theory of perturbations. In the cases of practical interest, the scatter of the block coordinates is small, and the theory of perturbations can be used [4]. However, the initial stage of the calculation is an expression for the flux in a medium without perturbations, i.e., in this case, a medium with a strictly periodic arrangement of blocks. Finding this flux is itself a complex problem and leads to cumbersome expressions [1-3]. Therefore we shall use a different method in which the dimensions of the blocks are assumed to be small.

We shall draw a formal analogy between this problem and the well-known theory of multiple scattering [5, 6]. Let us write an expression for the neutron flux $G(x \mid y)$ from an elementary source in a medium with an irregular arrangement of N blocks:

$$G(x \mid y) = G_0(x \mid y) + \int\int dx'\, dx''\, G_0 \times (x \mid x') \sum_{n=1}^{N} Q_n(x' \mid x'')\, G_0(x'' \mid y). \tag{1}$$

Here $G_0(x \mid y)$ is the Green's function of the kinetic equation for a homogeneous moderator, $\{x\}$ is the set of variables in the problem, and y represents the variables characterizing the neutron source. The components of the kernel of the integral term $Q_n(x \mid y)$, which depend on the block coordinates $R_1, \ldots, R_n, \ldots, R_N$ and on the parameters, in turn satisfy the following system of equations:

$$Q_n(x \mid y) = t(x \mid y) + \int\int dx'\, dx''\, t_n(x \mid x') \sum_{m \neq n} G_0(x' \mid x'')\, Q_m(x'' \mid y), \tag{2}$$

where $t_n(x \mid y)$ denotes the perturbation of the neutron flux by the n-th block when the undisturbed flux is incident on it. Equation (2) represents the fact that the total disturbance due to the n-th block results from the action of this block on the undisturbed flux and the disturbance due to all the other blocks.

Averaging of expression (1) over the configurations of the blocks will obviously affect only the values of the Q_n. It is easily verified that owing to the correlation between t_n and Q_m, direct averaging of Eq. (2) does not lead to a closed equation for $\langle Q_n \rangle$, the mean of the Q_n. Therefore we shall use the following approximate procedure [5, 6]. Let $\ll \ldots \gg_{n \ldots k}$ denote the result of incomplete averaging when the coordinates of the n...k-th blocks are fixed. We write down the obvious equation

Translated from Atomnaya Énergiya, Vol. 38, No. 5, pp. 291-294, May, 1975. Original article submitted April 15, 1974; revision submitted December 3, 1974.

$$\langle\langle Q_m(x \mid y,\ R_n)\rangle\rangle_m = \int d\mathbf{R}_m\, \Gamma^{(2)}(\mathbf{R}_n\mathbf{R}_m)\, \langle\langle Q_m(x \mid y;\ \mathbf{R}_n,\ \mathbf{R}_m)\rangle\rangle_{m,\,n}. \tag{3}$$

Here $\ll Q_m(x \mid y; R_n, R_m)\gg$ is an operator forming the disturbance to the neutron flux by the n-th block when the positions of the n-th and m-th blocks are fixed; $\Gamma^{(2)}(\mathbf{R}_n, \mathbf{R}_m)$ is the conditional probability that the m-th block is at point $\mathbf{R}_m$ if the n-th block is already at point $\mathbf{R}_n$. The form of function $\Gamma^{(2)}$ is determined by the configuration of the medium. Let us make use of the following approximate relation:

$$\langle\langle Q_m(x \mid y;\ \mathbf{R}_n,\ \mathbf{R}_m)\rangle\rangle_{m,\,n} \approx \langle\langle Q_m(x \mid y\mathbf{R}_m)\rangle\rangle_m, \tag{4}$$

which is strictly true in two limiting cases [5, 6]: 1) when the medium has a periodic structure, and 2) when the blocks are chaotically arranged in the medium. Approximation (4) enables us to obtain for $\ll Q(R_n)\gg$ the closed equation

$$\begin{aligned}\langle\langle Q_n(x \mid y;\ \mathbf{R}_n)\rangle\rangle_n &= t_n(x \mid y,\ \mathbf{R}_n)\\ &+ \sum_{m\neq n}\int dx' \int dx'' \int d\mathbf{R}_m \Gamma^{(2)}(\mathbf{R}_n,\ \mathbf{R}_m)\, t_n\\ &\times (x \mid x',\ \mathbf{R}_n)\, G_0(x' \mid x'')\, \langle\langle Q_m(x'' \mid y,\ \mathbf{R}_m)\rangle\rangle_m.\end{aligned} \tag{5}$$

Averaging the solution of this equation relative to the law of distribution of the R_n, we find $\langle Q_n\rangle$ and, with the aid of Eq. (1), the macroscopic flux $\langle G(x \mid y)\rangle$.

Let us use these general relations to solve the problem of the absorption of thermal neutrons in a system of irregularly arranged cylindrical blocks which we shall for simplicity assume to be identical, where N is the number of blocks. If the parameters of the blocks are different, then we can approximately use their mean values. In the diffusion-age approximation, the Laplacian of the critical system p is the root of the equation

$$1 - k(\mathbf{p}) = 0, \tag{6}$$

where

$$k(\mathbf{p}) = \frac{N-1}{(2\pi)^2}\int d\mathbf{p}_1 \gamma^{(2)}(\mathbf{p}-\mathbf{p}_1)\, \tilde{t}(\mathbf{p}_1)\, g_0(\mathbf{p}_1). \tag{7}$$

Equation (6) determines the position of the poles of the mean Green function $\langle g(\mathbf{p})\rangle$ in the complex plane p. Here

$$\begin{aligned}\gamma^{(2)}(\mathbf{p}) &= \int \Gamma^{(2)}(\mathbf{R})\, e^{i\mathbf{p}\mathbf{R}}\, d\mathbf{R};\ \Gamma^{(2)}(\mathbf{R})\\ &= \Gamma^{(2)}(\mathbf{R}_1 - \mathbf{R}_2);\end{aligned} \tag{8}$$

$$g_0(\mathbf{p}) = \int G_0(\mathbf{r})\, e^{i\mathbf{p}\mathbf{r}}\, d\mathbf{r} = \frac{1}{p^2 + \varkappa_0^2} \tag{9}$$

(where $G_0(\mathbf{r})$ is the Green's function of the diffusion equation for the pure moderator, $\varkappa_0^2 = L_0^{-2}$, and L_0 is the diffusion length of neutrons in the moderator), and

$$\tilde{t}(\mathbf{p}) = \int d(\mathbf{r}-\mathbf{r}')\, t(\mathbf{r} \mid \mathbf{r}')\, e^{i\mathbf{p}(\mathbf{r}-\mathbf{r}')}. \tag{10}$$

From the definition of $t(\mathbf{r} \mid \mathbf{r}_1)$ (see above), it follows that the distribution function of neutrons from the source at the point $\mathbf{r}_0$ can be expressed in terms of $t(\mathbf{r} \mid \mathbf{r}_1)$ with the aid of the expression

$$G_1(\mathbf{r} \mid \mathbf{r}_0) = G_0(\mathbf{r} \mid \mathbf{r}_0) + \int d\mathbf{r}'\, G_0(\mathbf{r} \mid \mathbf{r}')\, t(\mathbf{r}' \mid \mathbf{r}_1)\, G_0(\mathbf{r}_1 \mid \mathbf{r}_0). \tag{11}$$

At point $\mathbf{r}_1$ we find a small cylindrical block. To find $\tilde{t}(\mathbf{p})$, we write down the equation of neutron transfer in terms of the Green's function $G_1(\mathbf{r} \mid \mathbf{r}_0)$. This [1-3] takes the form

$$\begin{aligned}&\nabla^2 G_1(\mathbf{r} \mid \mathbf{r}_0) - \varkappa_0^2 G_1(\mathbf{r} \mid \mathbf{r}_0)\\ &+ \eta\gamma W(\mathbf{r} \mid \mathbf{r}_1)\, G_1(\mathbf{r}_1 \mid \mathbf{r}_0) - \gamma\delta(\mathbf{r}-\mathbf{r}_1)\, G_1\\ &\times (\mathbf{r}_1 \mid \mathbf{r}_0) = -\delta(\mathbf{r}-\mathbf{r}_0),\end{aligned} \tag{12}$$

where $\gamma = \tilde{\gamma}(3\Sigma t/v)$. Here Σ_t is the total macroscopic cross section for thermal neutrons, v is the neutron velocity, * γ is the thermal constant equal to the ratio of the number of neutrons absorbed in a block per unit time to the density of neutrons at the surface of the block, η is the number of fast neutrons arising in the block when one thermal neutron is absorbed in it, and $W(\mathbf{r} \mid \mathbf{r}_1)\, d\mathbf{r}$ is the probability that a fast neutron produced at point $\mathbf{r}_1$ is moderated to thermal energies at point $\mathbf{r}$.

* We regard the thermal neutrons as one monoenergetic group.

We can find the solution to Eq. (12) as follows:

$$G_1(\mathbf{r}\,|\,\mathbf{r}_0) = G_0(\mathbf{r}\,|\,\mathbf{r}_0) + \frac{\int d\mathbf{r}'\, G_0(\mathbf{r}\,|\,\mathbf{r}')\,\pi(\mathbf{r}'\,|\,\mathbf{r}_1)}{1-\int d\mathbf{r}'\, G_0(\mathbf{r}_1\,|\,\mathbf{r}')\,\pi(\mathbf{r}'\,|\,\mathbf{r}_1)}\, G_0(\mathbf{r}_1\,|\,\mathbf{r}_0). \tag{13}$$

Here

$$\pi(\mathbf{r}\,|\,\mathbf{r}_1) \equiv \pi(\mathbf{r}-\mathbf{r}_1) = \eta\gamma W(\mathbf{r}\,|\,\mathbf{r}_1) - \gamma\delta(\mathbf{r}-\mathbf{r}_1). \tag{14}$$

Comparing Eqs. (11), (13), and (14), we easily find the expression

$$t(\mathbf{r}\,|\,\mathbf{r}_1) \equiv t(\mathbf{r}-\mathbf{r}_1) = \frac{\pi(\mathbf{r}-\mathbf{r}_1)}{1-\int d\mathbf{r}'\, G_0(\mathbf{r}')\,\pi(\mathbf{r}')}. \tag{15}$$

Correspondingly, the Fourier transform of this quantity, $\tilde{t}(\mathbf{p})$, for a Gaussian function $W(\mathbf{r}-\mathbf{r}')$, takes the form

$$\tilde{t}(\mathbf{p}) = \frac{\eta\gamma e^{-p^2\tau} - \gamma}{1 - \frac{\gamma}{(2\pi)^2}\int \frac{d\mathbf{q}\,(\eta e^{-q^2\tau}-1)}{q^2+\varkappa_0^2}}, \tag{16}$$

where τ is the age of the neutrons.

Let us now analyze the characteristic equation. Let us first consider a system in which the blocks are located close to the points of a regular periodic lattice. We shall assume that a block with radius ρ can, with probability $f_l(\mathbf{r})\,d\mathbf{r}$, occupy any position in a cylindrical channel of radius R_1 near the l-th lattice point ($\mathbf{r} \le \mathbf{R} = \mathbf{R}_1 - \rho$; $\int f_l(\mathbf{r})d\mathbf{r} = 1$). Then for this model of the medium,

$$\Gamma^{(2)}(\mathbf{R}-\mathbf{R}') = \frac{1}{N-1}\sum_{\rho_l}{}' f_l(\mathbf{R}-\mathbf{R}'-\boldsymbol{\rho}_l) \tag{17}$$

and

$$\gamma^{(2)}(\mathbf{p}) = \frac{1}{N-1}\tilde{f}(\mathbf{p})\sum_{\rho_l}{}' e^{i\mathbf{p}\boldsymbol{\rho}_l}. \tag{18}$$

Here ρ_l is the radius vector of the lattice points (the prime on the summation sign denotes that we must exclude the term with $\rho_l = 0$);

$$\tilde{f}(\mathbf{p}) = \int f(\mathbf{r})\, e^{i\mathbf{p}\mathbf{r}}\, d\mathbf{r}. \tag{18a}$$

Clearly, in the case of a regular periodic structure $f(\mathbf{p}) \equiv 1$ and

$$\gamma^{(2)}(\mathbf{p}) = \frac{1}{N-1}\sum_{\rho_l}{}' e^{i\mathbf{p}\boldsymbol{\rho}_l}. \tag{19}$$

We easily evaluate the integral in (19) with $f_l(\mathbf{r}) = \text{const}$. As a result,

$$\tilde{f}(\mathbf{p}) = \frac{2}{R^2}\int_0^R r\,dr\,J_0(rp) = \frac{2}{Rp}J_1(rp). \tag{20}$$

Using Eqs. (9), (16), (18), and (19), from Eqs. (6) and (7) we obtain the following characteristic equation for a lattice with deviations from strictly periodic block positions:

$$\begin{aligned} &1 - \frac{\gamma}{(2\pi)^2}\int \frac{d\mathbf{q}\,(\eta e^{-q^2\tau}-1)}{q^2+\varkappa_0^2} \\ &= \frac{1}{(2\pi)^2}\sum_{\rho_l}{}' e^{i\mathbf{p}\boldsymbol{\rho}_l}\int d\mathbf{p}_1\, e^{-i\mathbf{p}_1\boldsymbol{\rho}_l} \\ &\times \frac{2J_1(R\,|\,\mathbf{p}-\mathbf{p}_1\,|)}{R\,|\,\mathbf{p}-\mathbf{p}_1\,|}\,\frac{\eta\gamma e^{-p_1^2\tau}-\gamma}{p_1^2+\varkappa_0^2}. \end{aligned} \tag{21}$$

To both sides of this equation we add the term

$$\frac{\eta\gamma}{(2\pi)^2}\int \frac{d\mathbf{p}_1}{p_1^2+\varkappa_0^2}J_0(p_1\rho)\,\frac{2J_1(R\,|\,\mathbf{p}-\mathbf{p}_1\,|)}{R\,|\,\mathbf{p}-\mathbf{p}_1\,|}\,(\eta e^{-p_1^2\tau}-1).$$

As a result we get

$$\begin{aligned} &1 + \frac{2\gamma}{R^2}\int_0^R r\,dr\,\frac{1}{2\pi}\int_0^\infty \frac{q\,dq}{q^2+\varkappa_0^2}J_0(\rho q)\,[1-J_0(qr)] \\ &-\frac{2\gamma\eta}{R^2}\int_0^R r\,dr\,\frac{1}{2\pi}\int_0^\infty \frac{q\,dq}{q^2+\varkappa_0^2}J_0(\rho q)\,e^{-q^2\tau} \end{aligned}$$

$$\times [1-J_0(rq)] = \gamma \sum_{\rho_l} e^{-i\mathbf{p}\rho_l} \frac{1}{(2\pi)^2} \int \frac{d\mathbf{p}_1}{p_1^2+\varkappa_0^2} \times J_0(\rho p_1)[\eta e^{-p_1^2\tau}-1]\, e^{-i\mathbf{p}_1\rho_l} \frac{2J_1(Rp_{-1})}{Rp_1}. \quad (22)$$

In writing Eq. (22) we have neglected terms of order pR ~R/B (where B is the size of the system as a whole), and have included in the integrand the factor $J_0(\rho p_1)$ which ensures convergence of the integrals.* The first integral A_1 on the left-hand side of Eq. (22) can be reduced to tabulated functions and, in the case of practical interest ($R > \rho$, $\varkappa_0 R \ll 1$),

$$A_1 = \frac{\gamma}{2\pi}\left(\ln\frac{R}{\rho} - \frac{R^2-\rho^2}{2R^2}\right). \quad (23)$$

The second integral A_2 can, when $\sqrt{\tau} \gtrsim R$, be written in the form of a rapidly-convergent series in powers of R^2/τ. Approximately we get

$$A_2 = -\frac{R^2}{16\tau}\frac{\gamma\eta}{2\pi}. \quad (24)$$

We transform the right-hand side of Eq. (22) as follows. Using the relation

$$\sum_{\rho_l} e^{i\mathbf{k}\rho_l} = \frac{(2\pi)^2}{S_{cr}} \sum_{s} \delta(\mathbf{k}-\mathbf{s}), \quad (25)$$

where S_{cr} is the area of a reactor cell, s is the reciprocal lattice vector (for a square cell with sides $2a$, $|\mathbf{s}| = \pi/a\sqrt{n^2+m^2}$, where n and m are integers). Substitute (25) into the right-hand side of Eq. (22). If $e^{-s^2\tau} \lesssim e^{-\pi^2(\tau/a^2)} \ll 1$, we get

$$\frac{1}{q_0}\left[\frac{\eta e^{-p^2\tau}-1}{p^2/\varkappa_0^2+1} - \frac{2\varkappa_0^2}{R}\sum_s{}' = \frac{J_0(s\rho)J_1(Rs)}{s^3}\right]; \quad (26)$$

$$q_0 = S_{cr}\frac{\varkappa_0^2}{\gamma}. \quad (27)$$

We calculate the sum of the reciprocal lattice vectors; the result † is as follows:

$$\frac{2}{R}\sum_s{}' \frac{J_0(s\rho)J_1(sR)}{s^3} = \begin{cases} \frac{a^2}{\pi}\left(\ln\frac{4a^2}{\pi\rho^2}-\frac{3}{2}\right), & R<\rho; \\ \frac{a^2}{\pi}\left(\ln\frac{4a^2}{\pi R^2}-\frac{1}{2}-\frac{\rho^2}{R^2}+\frac{\pi R^2}{8a^2}\right); & R>\rho. \end{cases} \quad (28)$$

Where $R \to 0$ we go over to a system of periodically located blocks. In this case the characteristic equation (22) [1-3] becomes

$$\frac{\eta e^{-p^2\tau}-1}{p^2/\varkappa_0^2+1} = q_0 + \frac{a^2\varkappa_0^2}{\pi}\left(\ln\frac{4a^2}{\pi\rho^2}-\frac{3}{2}\right). \quad (29)$$

Where $R > \rho$, by (23), (24), and (26)-(28), we can write Eq. (22) in the form

$$\frac{\eta e^{-p^2\tau}-1}{p^2/\varkappa_0^2+1} = q_0 + \frac{a^2\varkappa_0^2}{\pi}\left(\ln\frac{4a^2}{\pi\rho^2}-\frac{3}{2}\right) + \frac{\varkappa_0^2R^2}{8}\left(1-\frac{a^2}{\pi\tau}\eta\right). \quad (30)$$

The correction to the block effect in the thermal absorption will clearly be

$$\Delta q = \frac{\varkappa_0^2R^2}{8}\left(1-\frac{a^2}{\pi\tau}\eta\right). \quad (31)$$

Thus when $(a^2/\pi\tau)\eta < 1$, the correction for irregularity in the positions of the blocks will be positive, and the block effect in the thermal absorption will be increased. If, on the other hand, $(a^2/\pi\tau)\eta > 1$, then $\Delta q < 0$, and the block effect will be reduced by disorder in the arrangement of the blocks. From Eq. (31) it follows that Δq is small in the cases presenting practical interest.‡

Now let us consider the case in which the coordinates of the blocks are totally uncorrelated. Then [8]

* This method of regularizing the integrals is the standard method in the theory of a heterogeneous reactor with small blocks [1,2].

† A method for calculating sums of this kind is given in [7].

‡ Analysis reveals that the influence of disorder in the positions of the blocks is more marked when we are calculating the probability of avoiding resonance capture. This problem will be discussed in detail in a later article.

$$\gamma^{(2)}(\mathbf{p}) = \frac{(2\pi)^2}{S_{\text{syst}}}\,\delta(\mathbf{p}), \tag{32}$$

where S_{syst} is the cross-sectional area of the system as a whole, and

$$k(\mathbf{p}) = \frac{N}{S_{\text{syst}}}\,\tilde{t}(\mathbf{p})\,g_0(\mathbf{p}). \tag{33}$$

The values of $\tilde{t}$ and g_0 are respectively given by Eqs. (16) and (9).

The characteristic equation for this system is

$$\frac{\eta e^{-p^2\tau}-1}{p^2/\varkappa_0^2+1} = q_0\left[1-\frac{\gamma}{(2\pi)^2}\int\frac{d\mathbf{q}}{q^2+\varkappa_0^2}\,(\eta e^{-q^2\tau}-1)\right]. \tag{34}$$

After evaluating the integral we get

$$\frac{\eta e^{-p^2\tau}-1}{p^2/\varkappa_0^2+1} = q_0\left[1-\frac{\eta\gamma}{4\pi}\,e^{\tau\varkappa_0^2}E_1(\tau\varkappa_0^2)+\frac{\gamma}{2\pi}\,K_0(\rho\varkappa_0)\right]. \tag{35}$$

Here

$$E_1(x) = \int_x^\infty e^{-v}\frac{dv}{v}.$$

As shown by numerical estimates, for equal block densities N/S_{syst} and with parameter values of practical interest, a periodic lattice will have a smaller block effect in thermal absorption than a system of chaotically arranged blocks. For example, $q = (\eta e^{-p2\tau}-1)/p^2/\varkappa_0^2+1)$ is equal to $0.483\cdot10^{-2}$ for a periodic lattice, but $0.646\cdot10^{-2}$ ($q_0 = 0.405\cdot10^{-2}$) for a system of chaotically arranged blocks. This calculation was carried out with the following values: $\eta = 1.33$; $\gamma = 2.20$; $\tau\varkappa_0^2 = 1.25\cdot10^{-2}$; $S_{cr}\varkappa_0^2 = 0.81\cdot10^{-2}$; $\pi\rho^2/S_{cr} = 3.88\cdot10^{-2}$; $\rho\varkappa_0 = 10^{-2}$.

In conclusion we may note that the above method of solving the kinetic equation can find other applications. For instance, a similar procedure could simplify the solution to the problem of the energy dependence of the neutron distribution function in the resonance energy region, where the cross sections are oscillatory functions of the neutron energy.

The author thanks A. P. Rudik, who suggested this work, and A. D. Galanin for helpful advice.

LITERATURE CITED

1. A. D. Galanin, The Theory of Nuclear Reactions with Thermal Neutrons [in Russian], Atomizdat, Moscow (1959).
2. A. D. Galanin, The Theory of the Heterogeneous Reactor [in Russian], Atomizdat, Moscow (1971).
3. S. M. Feinberg, in: Reactor Construction and the Theory of Reactors: Proceedings of First Geneva Conference [in Russian], Izd-vo AN SSSR, Moscow (1955), p. 152.
4. A. V. Stepanov, At. Énerg., 22, 271 (1967); Kernenergie, 11, 125, 148 (1968); in: Theoretical and Experimental Problems of Nonsteady Neutron Transfer [in Russian], Atomizdat, Moscow (1972), p. 66.
5. M. Goldberger and K. Watson, The Theory of Collisions [Russian translation], Mir, Moscow (1967).
6. [Omitted from Russian original — Consultants Bureau].
7. A. V. Stepanov, Preprint FIAN, No. 139 (1969).
8. K. D. Ilieva and A. V. Stepanov, Kratkie Soobshcheniya po Fizike, No. 4, 65 (1972); Preprint IYaI, No. 93 (1973).

EXPERIMENTAL STUDY OF NEUTRON THERMALIZATION BY THE PULSED-SOURCE METHOD

A. Stanolov and V. Khristov

UDC 539.125.52:621.039.51.12

Many authors have studied neutron thermalization, steady-state diffusion, and transient diffusion in homogeneous moderators [1-3].

Only a few such investigations have been carried out in moderators containing inhomogeneities of various kinds [4, 5]. It is sufficient to point out that, if a moderator contains an absorbing particle with a cross section not obeying the 1/v law (a "non-1/v" particle), the asymptotic neutron distribution, even in an infinite homogeneous medium containing uniform sources, will deviate from the Maxwell distribution, and the corresponding neutron pulse attenuation factor λ will be a nonlinear function of the concentration of the absorbing substance N. In view of its low curvature, the function λ (N) is difficult to analyze in the range accessible to experiment. It should furthermore be emphasized that any experimental study of transient neutron thermalization in systems comprising inhomogeneous moderators (and of the asymptotic neutron distributions in such systems) will considerably widen the possibility of verifying the theoretical models and determining the neutron parameters in moderators of various configurations and compositions; such studies are thus of great practical interest [6].

The aim of the present investigation was to make an experimental determination of several neutron diffusion and thermalization parameters in a water lattice containing empty aluminum tubes, using a pulsed neutron source and a strong absorbing medium with a cross section not varying in accordance with the 1/v law.

TABLE 1. Measured Values of λ in Water and in Lattices of Empty Channels for Various Concentrations of the "Non-1/v" Absorbent, sec^{-1}

Size of medium, cm	B_g^2, cm^{-2}	N_{Cd} = 0, nuclei/cm^3	$N_{Cd} = 5.2 \cdot 10^{18}$, nuclei/$cm^3$	$N_{Cd} = 1.04 \cdot 10^{19}$, nuclei/$cm^3$	$N_{Cd} = 1.56 \cdot 10^{19}$, nuclei/$cm^3$	$N_{Cd} = 2.08 \cdot 10^{19}$, nuclei/$cm^3$
10×10×10	0,2614	Water 14 260±228 Lattice 16 945±220	18 010±212 18 018±236	21 433±283 20 400±295	22 257±295 21 380±268	24 712±318 22 628±270
12×12×12	0,1853	Water 11 860±178 Lattice 13 725±178	15 652±189 16 683±194	19 213±213 19 644±252	22 139±199 20 257±222	23 953±291 22 178±292
14×14×14	0,1381	Water 9 650±145 Lattice 11 662±117	14 449±171 14 410±187	19 234±186 17 797±195	21 665±256 19 230±167	22 925±284 21 473±335
16×16×16	0,1069	Water 8 667±113 Lattice 10 110±111	13 407±161 12 561±138	17 876±136 16 345±181	20 710±312 18 567±152	20 742±103 20 712±313
18×18×18	0,0852	Water 8 0202±112 Lattice 9 320±128	11 678±132 11 550±233	17 503±120 15 310±175	19 800±401 17 612±238	20 452±173 20 100±281
20×20×20	0,0695	Water 7 468±134 Lattice 8 124±101	11 647±123 10 516±167	16 386±113 14 425±168	18 812±138 17 194±201	19 381±186 19 602±192

Institute of Nuclear Studies and Nuclear Power, Bulgarian Academy of Sciences, Sofia. Translated from Atomnaya Énergiya, Vol. 38, No. 5, pp. 295-298, May, 1975. Original article submitted June 6, 1974.

TABLE 2. Results of the Measurements of M_2

$B_g^2 = 0$	λ_a, sec^{-1}	a., cm^3/sec	b, cm^6/sec	$N'M_2$, cm^{-1} experiment	$N'M_2$, cm^{-1} caluclation [15]
Water	4910±15	(7,2±0,1)·10^{-16}	(2,1±0,8)·10^{-37}	5,1±4	5,23 b
Lattice a	4305	5,96·10^{-16}	2,57·10^{-37}	2,92	3,85 c 3,34 d 0,67 e

[a] Errors not given, in view of the great indeterminacy of the extrapolated value of λ_a.
[b] Model of the tree rotator [16, 17].
[c] Model of an ideal monatomic gas [18].
[d] Model of Nelkin [19].
[e] Model of the water molecule [15].

Theory of a Pulse Experiment Using a "Non-1/v" Neutron Absorber

It is well known [7, 8] that, if the flux from a short neutron pulse falling on to a moderator satisfies the relationship $\Phi(E, r, t) = \Phi(E)\, R(r)\, e^{-\alpha t}$, the diffusion approximation of the neutron transport equation for the fundamental space harmonic takes the following form:

$$\left[\Sigma_a'(E) - \frac{\lambda}{v} + B^2 D(E)\right]\Phi(E) = \int_0^\infty \alpha E' \left[E_s(E' \to E)\,\Phi(E') - \Sigma_s(E \to E')\,\Phi(E)\right] \quad (1)$$

(generally-accepted notation).

Following the "diffusion—cooling" approach, we obtain the following expression for the neutron-pulse damping decrement λ in the form of a series in powers of B^2:

$$\lambda = \lambda_0 + D_0 B^2 - CB^4 + FB^6 + \ldots \quad (2)$$

In this way an analysis of the diffusion—cooling coefficient C will provide useful information as to the thermalization properties of the moderator.

Friedman [8] considers that difficulties arising in this method of analysis may be avoided if a small quantity (N atoms/cm^3) of a "non-1/v" absorbent with a microscopic absorption cross section $\sigma_a(E)$ is added to an infinite moderator with 1/v absorption. In this case the spectrum of the thermalized neutrons in the moderator deviates substantially from the Maxwell distribution, and the damping decrement λ may be expressed in the form:

$$\lambda = \lambda_a + N\frac{\bar{\sigma}_a}{(1/v)} = \lambda_a + \frac{2v_0}{\sqrt{\pi}} N(\alpha + \beta N + \ldots), \quad (3)$$

where β serves as a measure of the distortion of the spectrum due to the "non-1/v" absorber.

It may be shown [8, 9] that Eq. (1) remains valid even if B^2 is replaced by N and D(E) by $\sigma_a(E)$, and that there is a mathematical similarity between the equations describing the damping of the thermalized neutron pulse in moderators of finite and infinite dimensions with variable concentrations of the additional absorbing medium.

For a finite medium Eq. (3) takes the form:

$$\lambda = \lambda' + \frac{2v_0}{\sqrt{\pi}} N(\alpha' + \beta' N + \ldots), \quad (4)$$

where λ' is the damping decrement for a medium consisting of the pure moderator.

Making use of this method, we may determine the diffusion and thermalization characteristics of the medium under consideration by measuring the damping decrement λ as a function of N, which gives $\alpha'(B^2)$ and $\beta'(B^2)$. By determining $\beta'(B^2)$ for several values of B^2 and extrapolating the curve to $B^2 = 0$ we may determine β. By extrapolating $\alpha'(B^2)$ to $B^2 = 0$ we also obtain $\bar{\sigma}_a$, which may be used for verification purposes since σ_a is determinable from other experiments.

Results of the Experiments

Experiments were carried out in the third horizontal beam of the IRT-2000 reactor in Sofia. The collimated neutron beam from the reactor was interrupted by the steel rotor of a mechanical selector, and the resultant pulses fell on the center of the lateral surface of the water lattices under consideration. For a rotor turning at 6000 rpm, neutron pulses 160 μsec long were obtained at intervals of 5 msec. As detector of the thermalized neutrons we used a ^{3}He SNM-17 counter. The pulses were analyzed with a 400-channel French analyzer of the SA-40B type having a time adapter. In order to eliminate the background from the scattered neutrons, the lattices being measured were placed in a paraffin/boric acid housing, screened from within by a cadmium sheet 1 mm thick. The systems under examination consisted of cubic aluminum containers filled with distilled water to which the absorbent was added in various proportions. In order to form a periodic lattice, a system of hollow aluminum tubes 0.5 cm in radius was lowered into the water container, their upper and lower ends being fixed in apertures in two Plexiglas plates. The lattice spacing was 2 cm. The porosity p, i.e., the ratio of the volume of the cavities to the volume of matter in the lattice, equalled 0.2442. The volumetric proportion of water in the lattice was 0.7174.

Using a 2 MW reactor and a measuring time of 5-8 h, the channels of the time analyzer collected sufficient pulses to ensure a high accuracy of the experimental results (800 thousand and 60 thousand pulses respectively at the maximum and minimum of the attenuation curve).

First of all we made a series of control measurements with pure water in order to compare with our own earlier results [10] and those of other authors [11]. As absorbent we used cadmium chloride $CdCl_2 \cdot 2.5H_2O$ in four concentrations: 4, 8, 12, and 16 g/liter.

In order to determine λ the experimental pulse attenuation curves were approximated by means of a linear combination of exponentials (allowing for background) as follows

$$N(t_i) = A_0 + \sum_{k=1}^{j} A_k e^{-\lambda_K t_i}, \tag{5}$$

where $N(t_i)$ is the number of pulses in the i-th channel of the analyzer, $\tilde{t_i} = i\Delta$ is the time interval ($i = 1, 2, \ldots, n$), while λ_K is the attenuation constant. For $t_i > 400$ μsec only one exponential and the background remained. Calculations were carried out in the GIER computer, using the SHE program and the regularization method given in full detail in [10, 12, 13]. In order to choose the most reliable values of λ we used two independent criteria: maintenance of a constant value of $\lambda = f(t_i)$ on successively discarding the initial points $i = i_0[1]$, and preservation of the best agreement between these values and the values obtained by the approximation of Eq. (5) for all the damping curves studied [13]. The first method gave an accuracy of 2% in determining λ.

Table 1 gives the measured λ values in relation to N and B^2 for homogeneous and heterogeneous media.

No measured λ values relating to analogous lattices (suitable for comparing with our present results) have apparently been published. We may simply note that in lattices containing hollow tubes the rate of attenuation is reduced by virtue of the reduction in the amount of absorbent (for the same total volume of the medium). We also find excellent agreement between the results obtained for a water medium containing a "non-1/v" absorbent and the results of [9], calculated on the basis of the Nelkin model for $B^2 = 0.1$ cm^{-2} and $N_{Cd} = 6.692 \cdot 10^{19}$ nuclei/cm^3. The calculated value of λ equals 13.125 sec^{-1}; our measured value for $B^2 = 0.1069$ cm^{-2} and $N_{Cd} = 5.2 \cdot 10^{18}$ nuclei/cm^3 is 13,407 sec^{-1}.

Using the measured values of λ for the lattice (R = 0.5 cm, p = 0.2442) with $N_{Cd} = 0$, together with the approximation to Eq. (2), we calculated the mean diffusion and diffusion—cooling coefficients as follows:

$$\overline{D} = 66\,921 \pm 920 \quad \text{cm}^2 \cdot \text{sec}^{-1} \text{ and } \quad \overline{C} = 83052 \pm 12\,400 \quad \text{cm}^4 \cdot \text{sec}^{-1}.$$

The results were analyzed by the regularization method of [14], using the quantity $\lambda_0 = 3779$ sec^{-1} as additional information while retaining the values of $\overline{D}$ and $\overline{C}$.

An analysis of the experimental curves of $\lambda = f(N)$ also enabled us to determine the thermalization parameter M_2 (the mean square of the energy exchange in a single act of thermal-neutron scattering). We then extrapolated the $\lambda_i = f(B^2, N_i)$ curves to $B^2 = 0$. The points $\lambda_i(B^2 = 0, N_i)$ only enabled us to analyze the dependence of λ on N. For convenience we may write this relationship in the form [2, 3, 4]:

$$\lambda = \lambda_a + aN - bN^2, \tag{6}$$

where $a = \bar{V}\bar{\sigma_a}$ and $b = (\bar{V}\bar{\sigma_a}/2N'M_2)\bar{\sigma_s}$; N' is the concentration of the scattering nuclei.

The coefficients a and b were calculated by the regularization method, using additional information as to the value of λ_a obtained by extrapolating the experimental relationships $\lambda = f(N_{Cd})$ for $B^2 = 0$. The extrapolated values were $\lambda_a = 4305\ \text{sec}^{-1}$ for the lattice and $\lambda_a = 4910\ \text{sec}^{-1}$ for water.

The average value of the microscopic absorption cross section of cadmium $\bar{\sigma}_{Cd}$ was calculated from the well-known equation

$$\bar{\sigma}_{Cd} = g(T_n)\frac{\sqrt{\pi}}{2}\sigma_{Cd}(293)\sqrt{\frac{293}{T}} \quad \text{for } g(T_n) = 1{,}3,$$

$$T_0 = 293^\circ\text{K and } \sigma_{Cd}(293) = 2537\text{ b}.$$

The results obtained for the homogeneous solutions and the lattices under consideration are presented in Table 2, in which the last column gives the calculated values of $N'M_2$ obtained by Honeck [15] for four different moduli of the scattering nuclei in water $\Sigma_{s0}(E' \to E)$, using the equation

$$M_2 = \frac{1}{T^2}\int_0^\infty dE' M(E') \times \int_0^\infty dE \Sigma_{s0}(E' \to E)(E' - E)^2. \tag{7}$$

Nelkin's relationship between the thermalization parameter M_2 and the diffusion—cooling coefficient C takes the following form for a heavy gas:

$$C = \sqrt{\pi} D^2/v_0 N' M_2. \tag{8}$$

The value of $N'M_2$(5.1 cm^{-1}) obtained for water agrees with the theoretical value (5.23 cm^{-1}) calculated by Honeck for the model of a free rotator, but differs from the value calculated by the Nelkin model (3.34). In view of the absence of experimental data from other authors in relation to the value of $N'M_2$ for heterogeneous systems, we simply note that the value of $N'M_2$ obtained for the lattice (2.92 cm^{-1}) is smaller than the experimental value (5.1 cm^{-1}), since $N'M_2$ depends on the concentration of scattering nuclei N'. If we allow for porosity, we obtain 2.92/1—p = 3.87, in agreement with the calculated value for the model of [18] (Table 2). A more rigorous comparison should also allow for the change in the spectrum due to the effect of diffusion cooling in the lattice spaces.

This relationship is indicated indirectly by Eq. (8). Substituting the measured values of $\bar{D}$ and $\bar{C}$ for the lattice into (8), we obtain $N'M_2 = 4.35\ \text{cm}^{-1}$, which agrees in a reasonable manner with the calculated value of 3.87 within the limits of computing error characterizing the approximation of Eq. (8), due allowance being made for the porosity of the medium.

LITERATURE CITED

1. Proc. Brookhaven Conf. on Neutron Thermalization, BNL-719 (1962).
2. Proc. IAEA Symp. on Pulsed Neutron Research Vol. 1, Karlsruhe, May 10-14 1965.
3. Proc. IAEA Symp. on Neutral Thermalization and Reactor Spectra, Vol. 1, Ann Arbor, July 17-21 1967, p. 11.
4. E. Arai and M. Kuhle, Nukleonik, 7, 416 (1965).
5. H. Honeck and B. Quiguemelle, [2], p. 309.
6. M. V. Kazarnovskii, [3], Vol. 2, p. 287.
7. K. Bekurtz and K. Wirtz, Neutron Physics [Russian translation], Atomizdat, Moscow (1968), p. 218.
8. E. Friedman, Nucl. Sci. and Engng., 14, 420 (1962); 19, 203 (1964).
9. G. Calame, Nucl. Sci. and Engng., 20, 352 (1964).
10. V. Khristov, Dissertation, Akad. Nauk, Bulg. Nar. Rep. (1969).
11. M. Paiano and S. Paiano [3], p. 395.
12. L. Aleksandrov, Izvest. Fiz. Inst. ANEB (Bulg.), 19, 102 (1969).
13. L. Aleksandrov, Dissertation, UINR, Dubna (1973).
14. L. Aleksandrov, A. Stanolov, and V. Khristov, At. Énerg., 29, No. 4, 284 (1970).
15. H. Honeck, Nucl. Sci. and Engng., 18, 49 (1964).
16. H. Brown and D. John, Savannah River Rep., DP-33 (1954).
17. H. Brown, Savannah River Rep., DP-64 (1956).
18. F. Wigner and J. Wilkins, AECD-2275 (1944).
19. M. Nelkin, Phys. Rev., 119, 791 (1960).

GAMMA SPECTROMETRY AND METALLOGRAPHY OF THE FUEL ELEMENTS IN THE WORKING CASSETTE OF THE IVV-2 REACTOR

V. V. Bychenkov, V. I. Zelenov, S. G. Karpechko, E. N. Pankov, and A. N. Timokhin

UDC 621.039.665:620.18

After a four-year period of service, the working cassette of the IVV-2 research reactor became dehermetized; over the next three days there was a gradual increase in the specific γ activity of the coolant of the first circuit and gas activity in the special ventilation (blowing) system. Gamma spectrometry of the dry residue obtained from coolant samples revealed the presence of the following isotope fragments: ^{140}La, ^{132}Te, ^{141}Ce, ^{143}Ce, ^{144}Ce, ^{103}Ru, ^{137}Cs, ^{134}Cs, ^{91}Sr, ^{95}Zr. The high specific activity of the coolant ($2.7 \cdot 10^{-4}$ Ci/liter) for a total volume of the water in the vessel equal to 60 m^3 indicated that fission products with a total activity of ~20 Ci had passed into the coolant. The absence of uranium from the water and the zero α activity of the dry residue suggested that the fuel had not been in direct contact with the coolant. The dehermetized cassette was extracted by means of a special channel system and transferred to a holding tank. Some of the characteristics of the IVV-2 reactor and the service conditions of the dehermetized cassette are given in Table 1 as well as in [1, 2].

TABLE 1. Cassette Working Conditions

Feature	Characteristic
Type of fuel composition	Dispersion of the uranium-aluminum alloy in the aluminum matrix
Material of can	Aluminum alloy SAV-1
Type of fuel element	Ribbed rod
Enrichment with respect to ^{235}U, %	90
Number of fuel elements in the cassette, items	42
Burn-up at the time of dehermetization (average for cassette, wt. -%	51,9
Integrated thermal-neutron flux, neutrons/cm^2	$3,3 \cdot 10^{21}$
Maximum and mean temperature of the can during service, °C	98; 55
Average chemical conditions of the water	pH = 5.5-6.5; hardness 3 $\mu g \cdot eq$/liter Resistivity $3 \cdot 10^5$-$2 \cdot 10^6$ $\Omega^{-1} \cdot cm^{-1}$ Chloride content 0.03-0.36 mg/liter

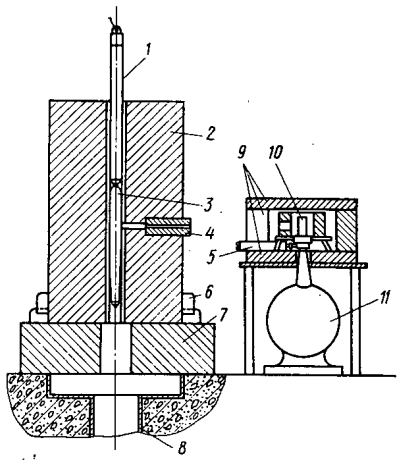

Fig. 1. Experimental apparatus for the γ scanning of the fuel elements: 1) clamp (holder) for fuel element; 2) container; 3) fuel element; 4) collimator; 5) preamplifier; 6) centering parts; 7) support; 8) hot-chamber hatch; 9) Pb shield of detector; 10) detector; 11) cryostat.

Translated from Atomnaya Énergiya, Vol. 38, No. 5, pp. 299-303, May, 1975. Original article submitted July 15, 1974; revision submitted January 9, 1975.

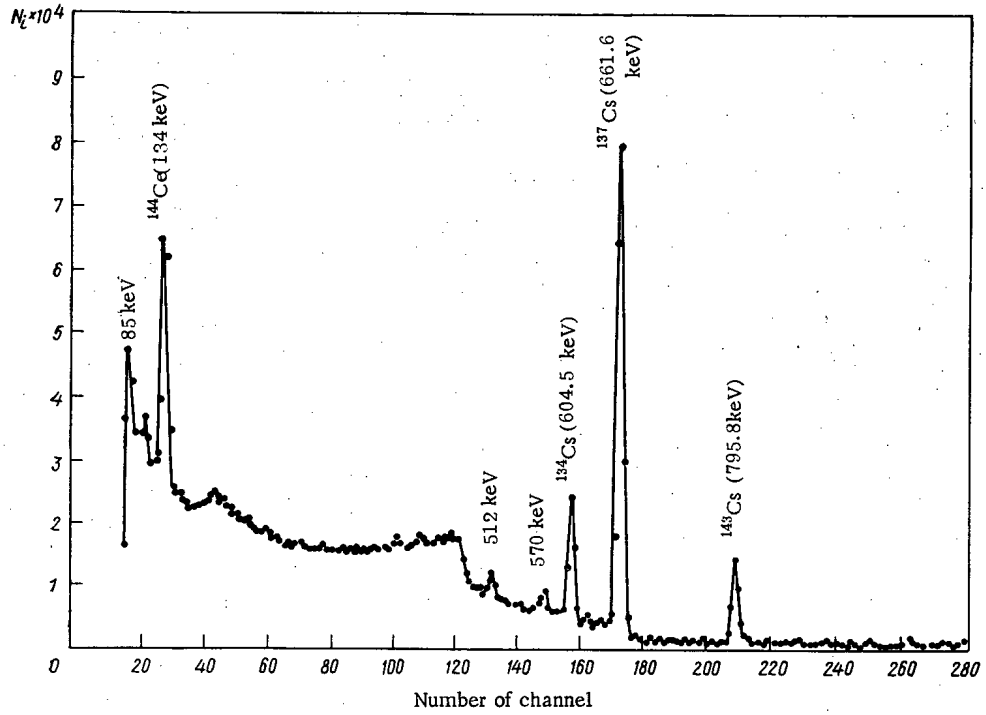

Fig. 2. Spectrum of fission products in the fuel elements of the cassette.

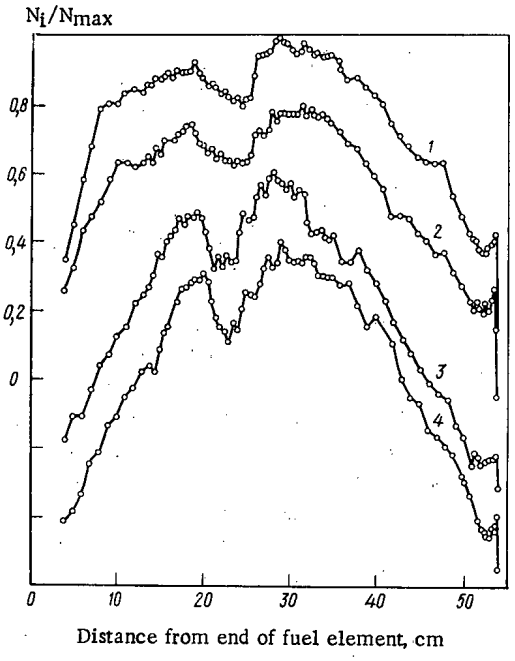

Fig. 3

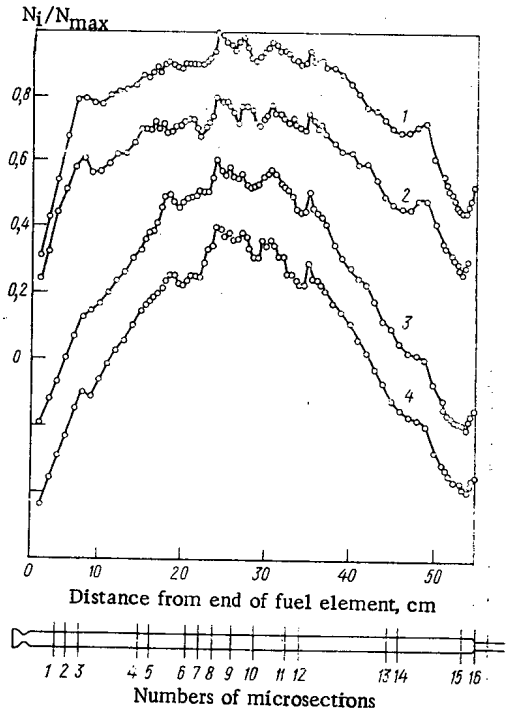

Fig. 4

Fig. 3. Relative distribution of long-lived fission products along fuel element No. 31. Slit (slot) collimator. Exposure 655.4 sec: 1) ^{137}Cs (661.6 keV); 2) ^{144}Ce (134 keV; 3 and 4) ^{134}Cs (604.5 and 795.8 keV respectively).

Fig. 4. Scheme of preparation and relative distribution of the fission products along fuel element No. 25. Slit collimator. Exposure 1310.7 sec (notation of curves as in Fig. 3).

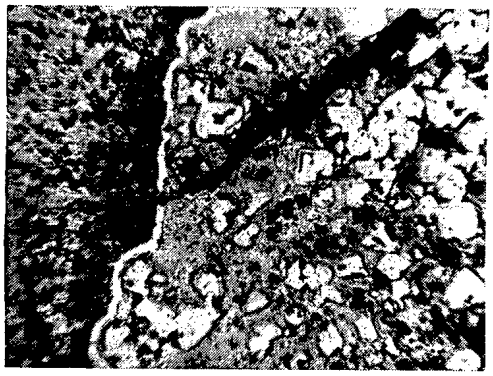

Fig. 5.

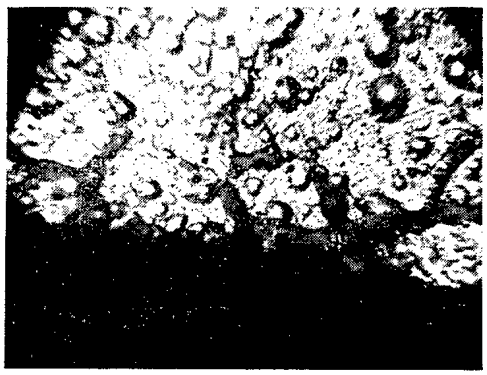

Fig. 6

Fig. 5. Microsection No. 9. Radiation damage to the core and can (× 100).

Fig. 6. Microsection No. 1. Can on the coolant side. Intercrystallite corrosion. Erosive wear (× 500).

After a three-year holding period the cassette was dismantled to study the fuel elements by γ spectrometry and optical metallography.

Experimental Apparatus for the Gamma Scanning of the Fuel Elements

The apparatus consists of a lead-filled protective cylindrical container having a channel along its axis for moving the clamp holding the fuel element relative to the collimator (Fig. 1). The container is placed on the hatch of the hot chamber, being set in special sockets provided to ensure the strict orientation of the collimated beam relative to a specified point in the sensitive volume of the detector. The dimensions of the central channel and the clamp are chosen in such a way that the maximum deviation of the axis of the fuel element relative to the axis of the slot collimator (size 6 × 0.8 mm) during the motion should never exceed ± 0.3 mm. The clamp is furnished with a scale for recording the position of the fuel element along the vertical. A Ge (Li) detector is placed 710 mm from the collimator and has a lead screen up to 200 mm thick in order to reduce the background. The total resolution of the spectrometer is 0.8 and 1.0% for the 661.6 and 1330 keV lines respectively. We used an AI-4096-2-AB-100 amplitude analyzer and a PP-12 scaler. The principal requirement laid upon the experimental apparatus (high accuracy of relative measurement) was satisfied by virtue of the stable geometry of the system, the high Compton peak ratio for the γ lines of the spectrum, the use of an adequate exposure, and the exact positioning of the fuel element in the container.

Relative Distribution of Long-Lived Fission Products along the Fuel Elements

In the γ spectrum of the fuel elements recorded after a three-year holding period, we identified the lines of ^{137}Cs, ^{134}Cs, ^{144}Ce and ^{144}Pr (Fig. 2). The relative distributions of the long-lived fission products along all 42 fuel elements were recorded. Allowance for the photo-peaks was made by the Covell method by reference to the lines 661.6 (^{137}Cs); 604.5 (^{134}Cs); 795.8 (^{134}Cs) and 134 keV (^{144}Ce).

The statistical accuracy of the results of the measurements was determined experimentally by making repeated measurements with the same exposure for the same part of the fuel element, the fuel element being displaced and returned to its original position after each measurement. The mean square error so determined includes the error involved in reproducing the geometry after the movement of the fuel element, the statistical error of the apparatus in recording the γ quanta, the probability of the actual decay process, and the error committed in determining the area of the photo-peak. For a 50-fold measurement with an exposure of 5.45 min, the mean square error equals ± 0.7% for the 661.6 keV line. For an exposure of 21.8 min the statistical accuracy increases to ± 0.4%; in measuring the 134, 604.5, and 795.8 keV lines it is slightly worse, but the error never exceeds ± 1.5%.

In the majority of the fuel elements studied (Figs. 3 and 4), a number of special characteristics were revealed in the fission-product distributions, and there were some anomalies corresponding to the central part of the fuel elements, i.e., the regions of maximum burn-up. The number, form, and depth of the anomalies were peculiar to every fuel element. The anomalies were usually located in regions

with dimensions of 0.8 to 3.0 cm, and amounted to 18-20% relative to the maximum of the distribution curve. The special characteristics of the distribution curves were associated with technological and radiative factors. The gravimetric proportion of ^{235}U in the core amounts to 35 ± 1.5%, i.e., a local nonuniformity of the energy evolution may occur within the limits indicated. The thickness of the core varies monotonically, and in considering the localized anomalies in the distribution curves this is not taken into account. Technological factors lead to a ±4.5% nonuniformity in the distribution relative to the maximum. The anomalies may also be attributed to the outflow of fission products at the point of dehermetization of the fuel-element can. For fission products to be produced it is by no means essential to have direct contact between the fuel and the coolant; it is sufficient that there should be weak regions due to intercrystallite corrosion, technological defects, or radiation damage to the matrix and the can. It is reasonable to assume that anomalies exceeding 4.5% are due to the transfer of fission products to the coolant at the point of can dehermetization. Thus the method of γ spectrometry may be used for identifying the point of damage to the fuel-element can. The effectiveness of the method will be greater for fuel elements with a relatively low nonuniformity of their ^{235}U distribution. The interpretation of anomalies in the fission-product distribution in high-temperature oxide fuel irradiated to high degrees of burn-up is impeded by the influence of cracks and other structural defects. Investigations into the use of γ spectrometry for extimating the state of other types of fuel element are to be continued.

Metallographic Study of a Fuel Element

For purposes of metallographic examination we selected fuel element No. 25. Cutting was carried out in the hot chamber, using a diamond wheel and intensive water cooling. The relative distributions of the fission products and the scheme of preparation (cutting of microsections) are shown in Fig. 4. After grinding and polishing, the samples were treated with Keller's solution (1% HF; 1.5% H_2SO_4; 2.5% HNO_3; 95% H_2O) for 2-10 sec and inspected under the microscope at a magnification of 100-500 times. On visual inspection no can damage appeared. However, there was a considerable loss of ductility and an increase in the elastic modulus [3].

A comparison between the microsections of the central and peripheral parts of the fuel element showed that with increasing burn-up the spaces formed at the boundaries between the dispersed fuel particles and the matrix as a result of bombardment with fission fragments increased in size. There is a clear relationship between the degree of radiation damage to the matrix, the size of the fuel particles, and the volumetric proportion of the fissile isotope. The fuel particles of various shapes have dimensions varying from 0.04 to 0.25 mm. An analysis of the structure showed that, for the same degree of burn-up, an increased porosity of the matrix occurred at the points of aggregation of the finer particles. These results agree with published data [4]. The considerable porosity of the matrix which occurs in regions of high burn-up is also associated with the presence of a eutectic (up to 11 wt. %). In the central part of the fuel element close to the boundary between the core and the can (Fig. 5) we see a crack at least 40 mm long, up to 2.5 mm wide, and up to 0.2 mm deep. The formation of a crack at the point of maximum burn-up is no chance matter. The core material is subject to cyclical thermal stresses during its service life. As the burn-up increases the temperature gradient in the fuel element does likewise by virtue of the creation of porosity and the accumulation of gaseous and solid fission products. The mechanical stresses are exacerbated by the static pressure of the gaseous fragments and the difference in thermal expansion coefficient between the core and the can.

The formation of pores also clearly occurs in the intermetallic compound particles as a result of the accumulation and diffusion of gaseous and solid fission products. We note the good state of diffusion contact between the can and the core.

Metallographic analysis of the fuel-element can revealed the presence of intermetallic (Mg_2Si) particles 3-20 μ in diameter (Fig. 6). The inner surface of the can (the fuel side) was bombarded with fussion nuclei from adjacent fuel particles and also subjected to the chemical action of active fission products. Pore formation accordingly took place at depths of up to 0.2 mm (Fig. 5). From the coolant side the can was subjected to intercrystallite corrosion (Fig. 6) to depth of 0.2-0.3 mm. We notice erosive wear of the surface in the turbulized flow of coolant, leading to a breakdown in the continuity of the oxide film and an increase in corrosion rate. Metallographic analysis revealed no "through" damage; however, the depth of the anomalies on the fission-element distribution curves and the manner in which these elements passed into the coolant at the time of dehermetization indicated the presence of weakened parts of the can. Technological defects (ellipticity of the core, eccentric displacement of the core relative to the axis of the fuel element, dents in the can up to a depth of 0.5 mm, chips and cuts in the ribbing)

inevitably lead to nonuniformity in the can thickness. At the thin points of the can the zones of radiation damage on the outside and inside may overlap, and this will facilitate the escape of fission products into the coolant.

Thus the apparatus which we have devised for the γ scanning of the rod-type fuel elements in the IVV-2 reactor enables us to detect singularities in the distribution of the long-lived fission products and so to identify the points of can damage subject to metallographic examination.

In conclusion, the authors wish to express their sincere thanks to A. M. Demidov for discussing the results of the work and for making some valuable comments, and also V. P. Krivorotova, V. N. Novichikhin, and Z. B. Slepukhina for help in the metallographic analysis and the processing of the results.

LITERATURE CITED

1. B. N. Goshchitskii et al., At. Énerg., 25, No. 1, 21 (1968).
2. A. P. Veselkin et al., in: Physics of Reactor Shielding, No. 5 [in Russian], Atomizdat, Moscow (1972), p. 251.
3. A. P. Kuznetsova and B. V. Sharov, At. Énerg., 21, No. 1, 58 (1966).
4. K. E. Weber and G. G. Hirsh, in: Metallurgy of Nuclear Power and the Effects of Irradiation on Materials [Russian translation], Metallurgizdat, Moscow (1956), p. 298.

I. S. Krashemikov, S. S. Kurochkin, A. V. Matveev, et al.

MODERN NUCLEAR ELECTRONICS. VOL. 1. MEASURING SYSTEMS AND INSTRUMENTS *

Reviewed by I. V. Shtranik

Modern nuclear electronics (which was originally undertaken with a view to solving particular problems in nuclear physics) is now becoming more and more an individual branch of general electronics rather than an auxiliary or subsidiary discipline.

The book under review differs from many of its predecessors by virtue of its more rigorous scientific approach to the exposition of the themes and the presentation of the contents. This is not by any means a reference book, but the material which it contains may prove extremely useful to physicists, engineers, and instructors working in this field or using electronics for scientific and technical purposes.

The first volume contains two chapters. The first generalizes and redevelops fundamental material relating to the theoretical analysis of factors determining the physical nature and character of the flows of data recorded from ionizing-radiation detectors. This material is of vital significance, since it provides a strict scientific basis for the ranges of validity and accuracy of the recorded data, characteristics which in the actual process of measurement are subject to the influence of detecting, shaping, coding, amplifying, and other processing stages. At the same time the actual flows of data presented at the input may be characterized by complex statistical laws in respect of a large number of parameters (for example, amplitude, time distribution, and others), while the reaction of the counting and scaling devices (apart from the specific transmission functions) may be complicated by many additional factors, such as noise fluctuations, the statistical scatter of the parameters, and so forth. The systematization, generalization, and scientific justification of all this information, drawn from a large number of literary sources, are greatly to the credit of the authors.

Slight demerits of this chapter include the absence of complete information relating to adjustable and optimum filters facilitating the creation of a greater signal/noise ratio. In addition to this, it would be desirable in later editions to give a greater number of separate examples and numerically-solved problems illustrating the theoretical conclusions.

The second chapter is devoted to an examination of the elements and components making up the most recent electronic instruments employed in nuclear physics, which are characterized by the extensive use of microelectronics, greatly advanced parameters by comparison with nuclear electronics of the second generation, a large quantity of coded data, and technical means of direct coupling to electronic computers.

It should be noted that the rapid development of the basic electronic principles has sharply altered the structure of nuclear-electronic instruments and necessitated new approaches to their creation. This development is fully reflected in the book, and at the present time no more complete exposition of such material exists. The book indicates all the special operating characteristics of the circuits, as well as the actual structure of the latter, and considers the circuit technology and methods required in order to realise specified parameters, and the operating accuracy of the amplifying, shaping, and amplitude-and-time coding units, together with analog operations and other signal-processing procedures characteristic of nuclear electronics. These data are extremely useful to developers of electronic apparatus,

*Atomizdat, Moscow (1974); (2 vols.), Vol. 1. 20 pp.

Translated from Atomnaya Énergiya, Vol. 38, No. 5, p. 303, May, 1975.

including nonnuclear applications, since they correlate the present scattered information and provide an analysis of the causes and factors on which the resultant characteristics depend.

Shortcomings of this section (and of the general setting-out of the material) include the rather "sharp" transition from the strict exposition of theoretical problems in the first chapter to the examination of specific apparatus elements in the second. It would have better to incorporate an additional section showing the formulation of the systems and components in the electronic apparatus as a consequence of the theoretical expositions. In addition to this, the second chapter contains a certain duplication in the description of noise processes in amplifiers.

At the present time it is impossible within the limited space of a book to give the whole range of constructions of every individual instrument; the important requirement is to present the basic principles and methods which are unlikely to alter with time, and in this respect the authors have coped excellently.

The book here reviewed will prove extremely useful to a wide circle of readers; it makes a major contribution to the development of Soviet science and instrument-making.

ARTICLES

CHANGE IN THE STRUCTURE OF CARBON MATERIALS UNDER NEUTRON IRRADIATION

Yu. S. Virgil'ev, I. P. Kalyagina,
T. K. Pekal'n, and T. N. Shurshakova

UDC 621.039:532.21

The physical properties of graphite (strength, thermophysical, etc.) are largely determined by its crystallographic structure. When using graphite in atomic technology its properties undergo major changes as a result of its subjection to neutron irradiation. It is well known that when neutrons interact with matter they create zones with a high concentration of simple defects (displaced atoms and vacancies), which as a result of local heating undergo partial recombination. On prolonged irradiation a certain constant defect concentration becomes established, the chief result of this being a change in the crystal structure of the graphite. This appears as a increase in the dimensions of the unit cell along the crystallographic C axis and a contraction along the A axis, a reduction in the crystallite size as determined from the width of the x-ray diffraction lines, and a fall in the degree of order. Hence the establishment of the general laws governing the changes taking place in the structural characteristics of carbon materials in relation to the conditions of irradiation (dose and temperature) and their original values will provide a better understanding of the mechanism underlying the radiation-induced changes in those properties of structural graphite which are of greatest practical importance.

In the present investigation the x-ray structural characteristics were determined in URS-50IM diffractometers, operating in conjunction with an SRS-1-0 scintillation counter and an SSS recording and measuring system. The recordings were made in copper radiation, using powder samples. The (002), (004), (110), and (112) diffraction lines were recorded on a point-by-point basis. The intervals between the points were 2' at the maximum and 10' at the minimum of the intensity curve, the count time being 100 sec.

TABLE 1. Comparison between the Diameters of the Crystallites Determined by the X-Ray Method L_a and from the Temperature Dependence of Thermal Conductivity L_λ*

Material	Crystallite diameter Å	
	L_a	L_λ
GMZ	600—800	800
VPG type	600—800	1200
Compact (VPP)	1000	2200

*Results obtained by B. K. Dymov.

TABLE 2. Relative Falls in the Diameter and Height ($\Delta L/L_a$) and ($\Delta L/L_c$) of the Coherent Scattering Regions on Irradiating Semifinished Samples of GMZ and KPG Under Various Conditions, %

Temp. of heat treatment	GMZ 200°C; $5\cdot10^{20}$ neutrons/cm²		KPG 400-500°C; $3\cdot10^{20}$ neutrons/cm²		
	J_{112}/J^*_{110}	$\Delta L/L_c$	J_{112}/J_{110}	$\Delta L/L_a$	$\Delta L/L_c$
1800	0	0	0	0	0
1900	—	—	0	0	0
2000	0,10	38	0,05	0	7
2100	0,19	56	0,10	32	21
2300	0,21	66	0,17	53	17
2400	—	—	0,31	72	33
2600	0,36	—	0,43	83	32
2800	0,40	70	0,47	83	32

*J_{112}/J_{110} is the degree of graphitization of the material.

Translated from Atomnaya Énergiya, Vol. 38, No. 5, pp. 304-308, May, 1975. Original article submitted June 6, 1974.

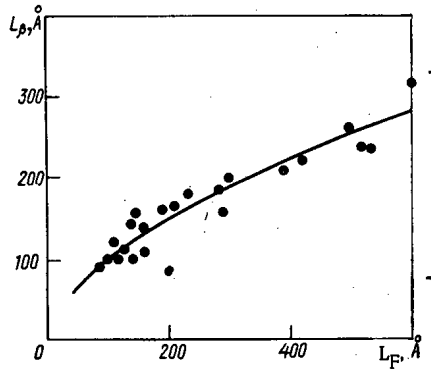

Fig. 1. Relation between the heights of the coherent scattering regions calculated by the Selyakov-Scherrer equation (L_β) and the Fourier method, before and after irradiation of the graphites.

In order to eliminate instrumental broadening, the line profiles were corrected by comparison with standard lines obtained from natural graphite. The absolute error in measuring the lattice parameters c and a was no greater than $2\text{-}3 \cdot 10^{-3}$ and $0.5 \cdot 10^{-3}$ Å respectively.

The dimensions of the crystallites (diameter and height) were determined by means of the Selyakov-Scherrer equation, assuming, in accordance with [1], that they took the form of fairly short cylinders. It was further assumed that the physical broadening was due simply to the block nature of the structure. However, an application of the Fourier-analysis method, in which the coefficients were calculated with a BÉSM-2M computer, showed that such an assumption led to an underestimation of the results, since the contribution of microdeformations to the broadening of the diffraction lines was not taken into account. This underestimate may be evaluated from the curve of Fig. 1, which relates the heights of the crystallites determined by the two methods. For this purpose we used samples of two brands of graphite (GMZ and highly-anisotropic recrystallized graphite) in the irradiated and unirradiated states.

We see from Fig. 1 that, for a crystallite height less than 100-150 Å, the difference in the results is no greater than 10-15%, i.e., it lies within the measuring error. With increasing height of the crystallities (i.e., perfection of the material) the difference increases; for L_β = 300 Å it reaches 100%. The crystallite dimensions determined on the basis of the temperature dependence of the thermal conductivity and the x-ray method in materials obtained by the ordinary electrode technology (the GMZ brand and various modified versions of this) are quite close together (Table 1). For materials with a higher degree of perfection in the crystal structure the difference between the diameters may be considerable.

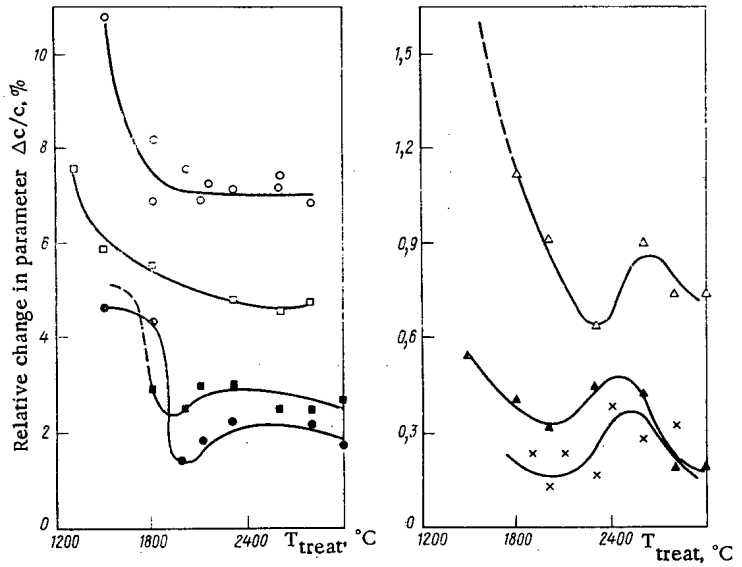

Fig. 2. Relative change in the crystal lattice parameters of semifinished GMZ after irradiation, expressed as a function of the heat-treatment temperature: ○, □) irradiation at 150-200°C with 2.7 and $2.3 \cdot 10^{20}$ neutrons/cm^2; ■, ●) 200-240°C; 4.6 and $3.8 \cdot 10^{20}$ neutrons/cm^2; △, ×) 400-500°C; 5 and $2 \cdot 10^{20}$ neutrons/cm^2; ▲) 600-700°C; $9.8 \cdot 10^{20}$ neutrons/cm^2.

TABLE 3. Change in the Crystal-Lattice Parameter of GMZ Graphite for Low Levels of Irradiation*

φt, 10^{19}, neutrons/cm^2	c, Å
0	6,779
0,6	6,774
2,1	6,750
2,7	6,737
5,5	6,774
12	6,805
20	6,825

*Irradiation temperature 200-220°C. Error in measuring the c parameter ±0.005 Å.

TABLE 4. Experimentally-Determined Constants of Eq. (2)

Lattice parameters	A_{0i}	E_i, eV	α_{0i}	Q_i, eV
c	$6,5\cdot10^{-5}$	0,26	10^4	0,21
a	$2\cdot10^{-5}$	0,32	$1,5\cdot10^3$	0,11
L_a	0,34	0,09	10	0,09
L_c	0,05	0,14	14	0,08

Thus the determination of the diameter and height of the crystallites from the Selyakov-Scherrer equation is valid for irradiated materials and others not having a very high degree of perfection. In this case it is more correct to speak not of the dimensions of the crystallites but of the diameter and height of the regions of coherent scattering.

The influence of the degree of perfection of the crystal lattice on the changes taking place in its parameters under irradiation was studied in coke powders (KNPS, pitch), natural graphite of the Taiginsk region, and material of the GMZ type formed from petroleum coke. The degree of perfection of these materials could be varied over a wide range from 0 to 0.84 by heat treatment of the semifinished product* at various temperatures between 1300 and 3000°C. Each series of samples was irradiated under identical conditions.

As a result of irradiation the lattice parameter increased, the more strongly the lower the irradiation temperature and the greater the accumulated dose (Fig. 2). The general character of the relationship between the c parameter and the processing temperature remained the same as in the unirradiated material. At the same time, the relative increment in the parameter $\Delta c/c$ was considerably higher in the nongraphitized samples than in the graphitized, at any rate up to an irradiation temperature of ~200°C. For graphitized samples the $\Delta c/c$ ratio depends little on the perfection of the crystal structure, and to a first approximation may be regarded as being the same for all the different materials. On plotting the dose dependences, not of the actual lattice parameters, but of their relative values, it was therefore perfectly legitimate to make use of data relating to various brands of graphite, including those produced outside the Soviet Union [2-4].

A minimum appears on the curves relating to samples irradiated at temperatures over 200°C and heat-treated at 1800-2100°C. This may be explained by the fact that, on irradiation, some of the displaced atoms migrate into the vacancies left after the removal of the peripheral atoms. This occurs after heat treatment at 1800-2000°C [5]. Corresponding to the minimum change $\Delta c/c$ we find a maximum change in the volume of the submicropores with dimensions of 50-250 Å [6], i.e., the large volume of the submicropores has accommodated a considerable proportion of the expansion of the crystal lattice.

*Material obtained after roasting at 1000-1300°C.

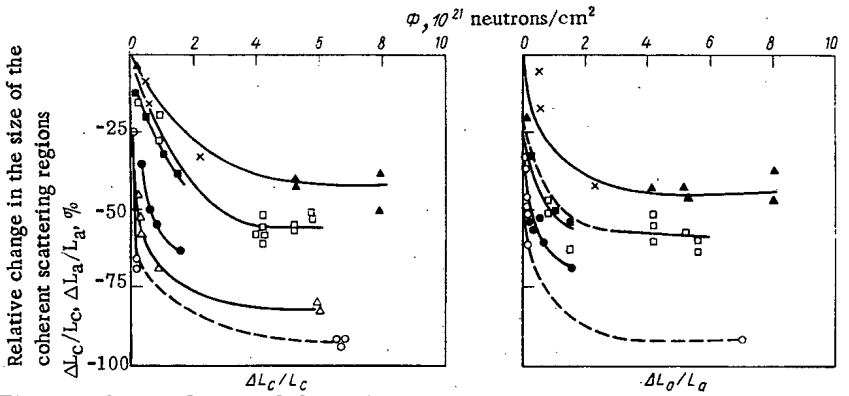

Fig. 3. Dependence of the relative change in the diameter L_a and height L_c of the crystallites (coherent scattering regions) on the integrated flux at various temperatures, °C: ○) 90-150; Δ) 150-170; ●) 170-200; ■) 300; □) 450-650; ▲) 800-950; ×) 480

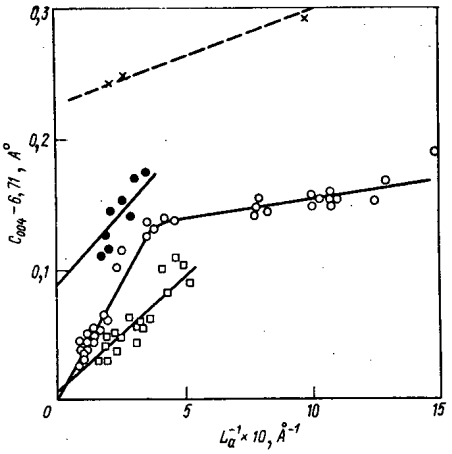

Fig. 4. Relationship between the c parameter and the diameter of the coherent scattering regions (for materials differing in their degree of crystal–lattice perfection) before (○) and after irradiation with doses of over 10^{21} neutrons/cm^2 at the following temperature: below 150 (×), at 140-150 (●), above 300°C (□)

The relative change in the dimensions of the coherent scattering regions in materials with a considerably disordered structure (those treated below 2000°C) is close to zero. As the perfection of the crystal lattice increases, the $\Delta L/L$ does likewise, and for graphite it becomes practically constant. An increase in the irradiation temperature reduces the extent of this effect (Table 2, Fig. 3).

The poor accuracy achieved in determining the dimensions of the coherent scattering regions in irradiated nongraphitized samples, which have very diffuse diffraction lines, prevents any quantitative analysis of this effect.

For irradiation temperatures of 140-200°C the lines (110) and (112) vanish, which indicates the existence of considerable distortions, worsening the three-dimensional ordering of the graphite. For irradiation temperatures above 400°C there is hardly any change in the spectrum of the diffraction lines, and the degree of crystallinity varies very little.

The relationships so obtained may be explained as follows: the defects created by low-temperature irradiation (displaced atoms and small complexes of these) in nongraphitized materials increase the distance between the strongly-curved and weakly-bound (00l) planes very little. If any additional curvature is created, it can hardly be recorded at all. In graphite itself after graphitization, however, the curvature of the (00l) planes and the distance between them diminish sharply, while the bond is strengthened. For this reason the increment in the interplane distance becomes smaller and the planes themselves curve easily.

For high-temperature irradiation the complexes of the defects become larger and the radiation effect diminishes.

The change in the structural characteristics which occurs on irradiation starts from doses of $\sim 10^{19}$ neutrons/cm^2 and amounts to a reduction in the parameter c (Table 3). Only when a dose of some 10^{20} neutrons/cm^2 has accumulated is this reduction replaced by an increase. A similar anomaly appears for the dimensions of the coherent scattering regions. It would appear that this effect is due to the removal of internal microstresses in the graphite.

The fall in the c parameter preceding the general rise (i.e., the apparent improvement in the structure) in graphite filaments irradiated at 420°C with doses of 10^{18}-10^{19} neutrons/cm^2 was considered in [7]. Irradiation with doses above $1 \cdot 10^{20}$ neutrons/cm^2 causes a rise in the parameter and a reduction in the size of the coherent scattering regions. Then the process stabilizes [5]. The coherent scattering regions are characterized by a rapid reduction in their dimensions, with a subsequent stabilization of this process also (Fig. 2). The change in the lattice parameters and the dimensions of the coherent scattering regions diminishes sharply with rising irradiation temperature. For graphite the relative change in the lattice parameters and the dimensions of the coherent scattering regions is approximately given by an expression of the form [8]

$$\frac{\Delta p}{p_i} = \frac{A_i D}{1 + A_i \alpha_i D}, \qquad (1)$$

where $D = \varphi t$ is the dose accumulated in a time t (in units of 10^{20} neutrons/cm^2) for an intensity φ of the damaging flux, A_i is a constant characterizing the intensity of defect development, allowing for the recombination between vacancies and interstitial atoms, α_i is a coefficient allowing for the probability of complex formation, p_i is the property under consideration: c, a, L_c, L_a.

$$\Delta p/p_i = (p_i)_{irr}/(p_i)_{orig} - 1.$$

Since the dimensions of the coherent scattering regions and the magnitude of the a parameter diminish on irradiation, the quantities A_i and α_i for these are negative. For the level of radiation corresponding to the stabilization of the process, the relative change in the structural characteristics will no longer depend on the dose, so that Eq. (1) will simplify

$$\Delta p/p_i \approx 1/\alpha_i. \tag{1a}$$

We may thus assume that the change taking place in the crystal-lattice parameters of graphite is mainly associated with the accumulation of point defects, their recombination, and the formation of complexes. The parameters of Eqs. (1) and (1a) are related exponentially to the irradiation temperature:

$$A_i = A_{0i} \exp(E_i/RT); \quad \alpha_i = \alpha_{0i} \exp(-Q_i/RT), \tag{2}$$

where A_{0i}, α_{0i} are constants, E_i and Q_i are the total activation energies, T is the absolute temperature, and R is the gas constant. The exponential relationships of Eq. (2) are, at all events, valid for the range of irradiation temperatures 100-800°C (Table 4).

The value of A_{0c} is greater than A_{0a} owing to the difference in the lattice-vibration eigenfrequencies for the a and c directions [8].

Making use of existing data regarding the activation energy of individual defects [9], together with our present values for the mean activation energies of defect migration to the complexes, it is reasonable to assume that the main defect which arises in graphite subjected to irradiation involves twinned atoms (C_2). The dynamics of the motion of these defects determine the changes taking place in the dimensions of the coherent scattering regions and the parameter a. The more complicated C_4 defects make a contribution to the change taking place in the parameter c, which is characterized by a high total activation energy.

It is well known that the C_2 molecules have two unpaired spins, which may be confirmed by the method of electron spin resonance. Measurements on samples irradiated at various temperatures, in fact, showed [10] the existence of such spins with a concentration of $\sim 10^{-2}$ per neutron. The activation energy was here also about 0.05 eV.

The total activation energy of recombination was higher than that of the growth of complexes. However, it was some two or three times lower than that of the thermal annealing of the defects, i.e., recombination takes place more easily on irradiation.

A relationship was established in [11] between certain parameters of the crystal structure of graphite (interplane distance and diameter of the coherent scattering regions); for $L_a > 110$ Å this was given by

$$d = N + (M/L_a),$$

where N and M are constants equal to 3.354 and 9.5 Å respectively.

Data obtained for a wide range of Soviet materials confirmed the validity of such a mutual relationship. However, for graphitized materials the constant M was approximately equal to 18. A similar relationship was also established for nongraphitized materials in which $L_a < 280$ Å. In this case M = 1.5 Å and N = 3.42 Å (Fig. 4).

After the irradiation of graphitized materials, the linear relationship between the quantities under consideration remained intact, but the constants changed. For fairly high values of irradiation doses (over 10^{21} neutrons/cm^2), from Eqs. (3) and (1a) we have

$$d_{irr} = 3.35[1 + \alpha_c^{-1}] + 18(1 - \alpha_L^{-1}) L_{irr}^{-1} \tag{3a}$$

The difference between α_{0c}, α_{0L} and Q_c, Q_L is due to the displacement of the lines in Fig. 4. For irradiation temperatures of under 150°C the factor $(1-\alpha_L^{-1})$ is practically zero, i.e., there is no relationship between the size of the coherent scattering regions and the interplane distance; the structure becomes turbostratic.

CONCLUSIONS

For graphite materials produced by electrode technology, the radiation-induced changes in the structural characteristics [the crystal-lattice parameters, and the dimensions of the crystallites (coherent scattering regions)] at irradiation temperatures of up to 700-800°C are mutually related, and are determined by the dynamic characteristics of the accumulation and transformation of defects of the C_2 type.

The interaction of these defects with the strongly-curved graphite-like layers of the carbon materials is responsible for the sharp increase in the c parameter (greater than for graphite) and the almost zero change in crystallite dimensions.

In the three-dimensionally ordered structure of graphite the relative changes in the parameters and the crystallite dimensions are, to a first approximation, independent of the degree of perfection.

LITERATURE CITED

1. B. Warren and B. Averbach, J. Appl. Phys., 21, No. 6, 545 (1965).
2. W. Reynolds and J. Simmons, in: Proc. Fifth Conf. on Carbon, Pergamon Press, New York, Vol. 1, p. 255.
3. E. Fitzer, in: Proc. IAEA Symp. on Radiation Damage in Reactor Materials, Vol. 2, Vienna (1963), p. 593.
4. R. Henson, R-5489, Harwell (1967).
5. S. V. Shulepov, Physics of Carbon-Graphite Materials [in Russian], Chelyabinsk (1965), p. 200.
6. Yu. S. Virgil'ev, E. V. Zelentsova, and E. I. Kurolenkin, Izv. Akad. Nauk SSSR, Neorg. Mat., 9, 1264 (1973).
7. J. Peggs and R. Mils, Tenth Conf. on Carbon, Buffalo (1971), Rep. RD119.
8. Yu. S. Virgil'ev, At. Énerg., 30, No. 3, 312 (1971).
9. T. Jwata and M. Suzuki, [3], p. 565.
10. A. S. Kotosonov and Yu. S. Virgil'ev, in: Construction Materials Based on Graphite, No. VI [in Russian], Metallurgiya, Moscow (1971), p. 77.
11. B. Richards, J. Appl. Cryst., 1, 35 (1968).

CERTAIN LAWS REGARDING TRANSIENT RADIATION-INDUCED CREEP IN CONSTRUCTION GRAPHITE

Yu. S. Virgil'ev

UDC 621.039.532.21

In order to ensure a long and reliable life for construction graphite subjected to severe temperature, loads, and neutron irradiation, it is essential to take due account of creep processes, including those induced by radiation. Models of radiation-induced creep proposed in [1-5] only describe individual results, and offer no means of interpreting all the data which have now been accumulated.

In this paper we shall consider certain laws governing the transient low-temperature creep of graphite.

Measurements of the thermal creep of several types of low-anisotropy Soviet graphites at temperatures above 2000°C [1, 2] agree satisfactorily with the Andrade equation for high-temperature creep.

It was shown earlier [3] that the transitional stage of radiation-induced creep could properly be described by logarithmic or exponential relationships between the relative deformation and the dose of irradiation. The inaccuracy involved in determining the deformation at moderate doses made it virtually impossible to assign preference to either one of these relationships. It was established on the basis of experimental data that the creep rate depended linearly on the applied stress and was independent of the irradiation temperature in the range 150-350°C.

The transient stage of creep was explained in [4] on the basis of a mechanism involving the climbing of edge dislocations as a result of the absorption of mobile interstitial atoms, which led to the following equation for the rate of transient radiation-induced creep:

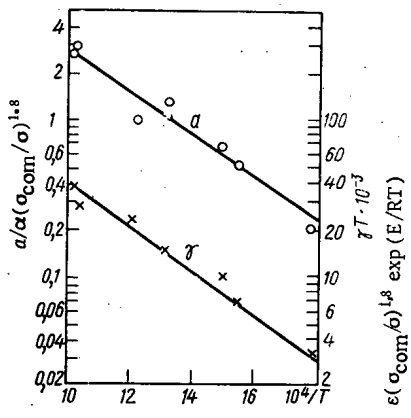

Fig. 1

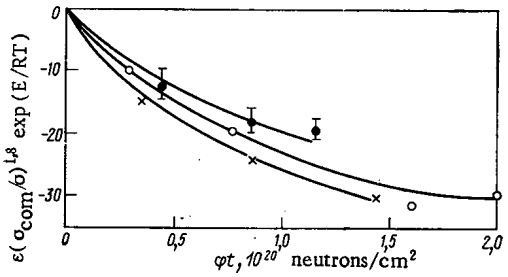

Fig. 2

Fig. 1. Dependence of the parameters of Eqs. (2') and (4), a_{red} and γ, on the irradiation temperature (GMZ graphite, dose given with respect to neutrons having energies E > 0.18 MeV).

Fig. 2. Creep deformation of semifinished GMZ material (reduced to unit stress and unit compressive strength) after treatment at temperatures 1300 (●), 2300 (○) and 2800°C (×). Tests carried out at 380-420°C.

Translated from Atomnaya Énergiya, Vol. 38. No. 5, pp. 309-312, May, 1975. Original article submitted July 1, 1974.

TABLE 1. Properties of the Materials Studied

Material	T_{treat} °C	σ_{com}	E, 10^5 kg/cm^2	L_c, Å	Anisotropy index α*
GMZ-1300†	1300	510	1,7	60	0,70
GMZ	2300	300—340	0,9	230	0,70
GMZ-2800†	2800	280	0,6	270	0,70
Experimental‡	2800	295	0,5	250	1,40
KPG	2400	740	1,2	140	1,09

*From the ratio of the electrical resistances in the parallel and perpendicular directions.

†Semifinished material after heat-treatment at 1300 and 2800°C respectively.

‡Different version of GMZ differing from the ordinary form by virtue of the coke in the filler.

TABLE 2. Parameters p and γ from Eqs. (2') and (4) for Various Materials

Material	p	γ	p/γ
GMZ-1300	250	62	4
KPG	225	49	4,3
GMZ	150	31	4,8
GMZ-2800	70	7	10
Exptl.	53	4,5	12

Note. Determined for a time equivalent to an irradiation dose of 1.10^{20} neutrons/cm^2, E > 0.18 MeV, with a single flux intensity of $0.8.10^{13}$ neutrons/cm^2. sec. The parameter γ is given for an irradiation temperature of 380-445°C.

$$\dot{\varepsilon} = \frac{d\varepsilon}{dt} = \frac{A\varphi N \cos^2 \eta}{T\rho_0 + B\varphi t}, \quad (1)$$

where φ is the neutron flux, N is the dislocation density, η is the angle between the Burgers vector and the direction of the applied stress σ; T is the temperature; ρ_0 is the concentration of defect sinks at the initial instant of irradiation, A and B are constants, t is the time taken by the test, equivalent to the time required for the accumulation of a dose D.

It follows from Eq. (1) that the rate of creep falls with advancing time (irradiation dose), obeying a logarithmic law; this was indeed observed experimentally for samples of GMZ graphite. We should accordingly expect that the creep deformation of graphite would be greater in the direction parallel to the easy-slip planes, i.e., the basal planes (00l). However, measurements of the creep deformation of anisotropic graphite samples under neutron irradiation and in the absence of irradiation refuted this

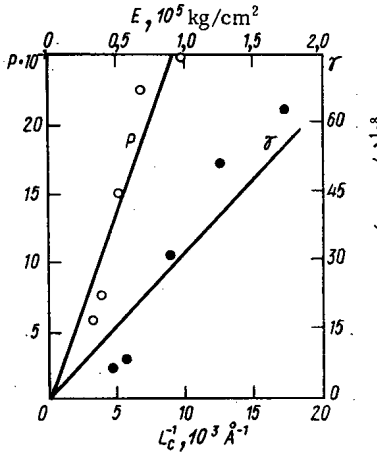

Fig. 3

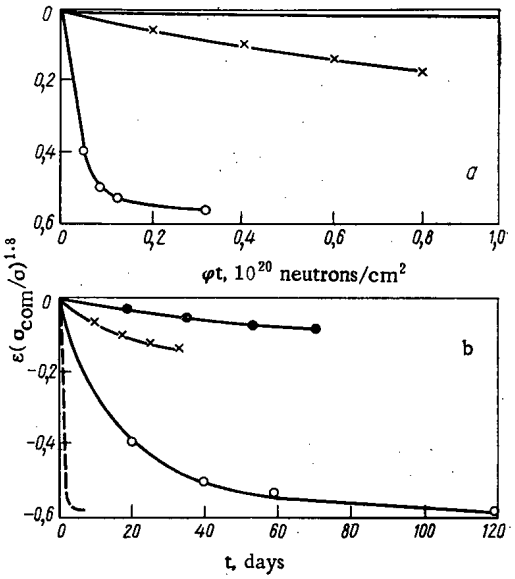

Fig. 4

Fig. 3. Dependence of the parameters p, γ in Eqs. (2') and (4) on the height of the crystal L_c and the elastic modulus E.

Fig. 4. Radiation-induced creep deformation of KPG graphite, reduced to unit strength and load, as a function of accumulated dose (a) and test time (b). Testing carried out at a temperature of 200-250°C for various intensities of the damaging flux (expressed in units of 10^{13} neutrons/cm^2 · sec) for E > 0.18 MeV: 0 (—×—×—), 0.2 (○), 3 (×), and 30 (●).

TABLE 3. Relationship between the Parameters p and γ from Eqs. (2') and (4) and the Intensity of the Damaging Flux φ(E > 0.18 MeV)

φ, 10^{13} neutrons /cm^2·sec	p *	γ †	p/γ †
0	—/70	—	—
0,4	240/0,8	12	20
0,7	150/0,8	10	15
3,1	21/0,5	7	3
30	2/0,5	1,3	1,6

*Numerator—measurement in units of 1.10^{20} neutrons/cm^2; denominator—in days.

†For a temperature of 250°C.

assumption: the creep rate was higher in the direction of the crystallographic C axis, i.e., perpendicular to the easy-slip plane [5]. This might be explained by the creeping (climbing) of dislocations along non-basal (112) planes.

Equation (1) implies a linear increase in the rate of transient creep as the intensity of the damaging flux increases, but experiments fail to confirm this. It might well be considered that the creep rate of material with a less perfect crystal structure would be lower, since the sink concentration in such materials is higher than in graphite. However, this important relationship has also failed to receive any experimental confirmation.

Measurements of creep deformation carried out for a wide range of materials with differing properties [5] revealed a dependence of the rate of transient creep on the strength of the material, the degree of anisotropy of its properties, the applied stress, and the test temperature.

The curves expressing these relationships were satisfactorily approximated by the equation proposed in [6] for describing the creep of metals and alloys

$$\dot{\varepsilon} = a/(1+\gamma t) + v, \tag{2}$$

$$a = \alpha p \left(\frac{\sigma}{\sigma_{com}}\right)^{1.8} \exp\left(-\frac{E}{RT}\right); \tag{2'}$$

γ is a coefficient depending on the material and the temperature, sec^{-1}, α is the anisotropy index determined from the electrical resistance; σ is the applied stress, kg/cm^2; σ_{com} is the (compressive) strength of the material at room temperature, kg/cm, E is the activation energy, cal/g-atom, R is the gas constant, p is a parameter determined by the crystal structure of the material, v is the steady creep rate, sec^{-1}.

The first term in Eq. (2) describes the transient creep, and the second describes the steady creep. For the transient creep deformation Eq. (2) gives

$$\varepsilon = \varepsilon_0 \ln(1+\gamma t), \tag{3}$$

where

$$\varepsilon_0 = a/\gamma.$$

The method usually adopted for measuring creep deformation (periodic unloadings, with the extraction of the test device from the reactor) eliminates the influence of elastic deformation. However, in the investigation under consideration [5] no relationship between the parameters of Eq. (2) and the structural characteristics of the carbon materials or with the intensity of the damaging flux was established.

In view of this we attempted to estimate the influence of the crystal—structural perfection of graphite construction materials and the intensity of the damaging flux on the rate of transient creep. For this purpose we used various materials (Table 1) and tested samples of these by standard methods in irradiation systems providing various intensities of the damaging flux. In addition to this we made use of the results obtained earlier [5].

The experimental data enabled us, first of all, to refine the activation energy of transient radiation-induced creep; this amounted to 6400 cal/g·atom. It is a noteworthy feature that the creep rate increases with irradiation temperature rather than falling, as would be expected from Eq. (1).

The mean of the parameter p for GMZ graphite determined from five different experiments and also graphically (Fig. 1) equalled 145 ±29 (for $\varphi = 0.7 \cdot 10^{13}$ neutrons/cm^2 · sec).

Existing data enabled us to express the temperature dependence of the parameter γ in the form

$$\gamma = \frac{K}{kT} \exp\left(-\frac{6400}{RT}\right), \quad (4)$$

in which the activation energy also equalled 6400 cal/g-atom.

The constant K in Eq. (4) was determined graphically from Fig. 1 for GMZ graphite and an intensity of the damaging flux equal to $\sim 10^{13}$ neutrons/cm^2 . sec; the value so found was $9 \cdot 10^5$.

The lowish value of the activation energy (6400 cal/g-atom) suggests that in transient creep the climbing of the dislocations is due to the motion of displaced atoms and small complexes of these.

On comparing the results obtained for samples of semifinished GMZ treated at various temperatures and tested in a single ampoule device at 380-420°C, we found that the rate of transient creep depended on the perfection of the crystal structure (Fig. 2). For the materials studied the parameters p and γ diminished as the perfection of the crystal structure increased, if this were estimated by reference to the size of the coherent scattering regions determined by the x-ray method, for example, the height of crystallites (Table 2). For different brands of graphite the ratio of the parameters p and γ increases very slightly with increasing perfection of the materials. Thus in materials with a more perfect structure the transient creep deformation is greater than in less perfect materials. However, on considering the inhomogeneity of the materials and the conditions of irradiation, this difference may be regarded as not being very important. The data presented in Table 2 lead (Fig. 3) to the relations

$$p \sim L_c^{-1} \quad (5)$$

and

$$\gamma \sim E.$$

The influence of the intensity of the irradiation may be estimated from the results of tests on KPG and GMZ graphite irradiated at 200-650°C in ampoule systems with different intensities of the damaging flux.

In order to ease comparison, the data obtained for KPG graphite samples were referred to unit strength and unit load by way of Eq. (2'), and to constant temperature (250°C) by virtue of Fig. 1. We then found (Fig. 4a) that an increase in the intensity of the damaging flux reduced the transient creep velocity and deformation. On plotting this "reduced" deformation as a function of the test time rather than the accumulated dose (Fig. 4b), we found that the greatest creep rate and creep deformation occurred in samples tested without irradiation, i.e., with $\varphi = 0$. It was noted earlier [5] that preliminary irradiation completely suppressed transient creep, while annealing the irradiated samples at 2000°C restored this creep.

A calculation of the parameters p and γ from the creep curves of GMZ graphite also revealed a dependence of these parameters on the intensity of the damaging flux (Table 3). The results of Table 3 cannot be used to deduce the corresponding quantitative relationships, since these results were obtained for different temperatures and applied loads. We may nevertheless assert that, the higher the concentration of the irradiation defects formed per unit time, the more difficult is it for the dislocations to climb, this being the process responsible for creep deformation.

Since the treatment of creep based on purely radiative effects [4] fails to explain the experimental data, in order to analyze the foregoing results we may reasonably make use of the general theory of logarithmic creep developed in [7]. This approach would appear quite acceptable, since it implies a dependence of the transient creep rate on the intensity of the damaging flux.

According to this theory the parameters of Eq. (3), reduced to unit load and strength, may be written in the form

$$\varepsilon_0 = kT/hbL^2;$$
$$\gamma = \frac{\nu h b^2 L}{kT} \exp\left(-\frac{E}{RT}\right), \quad (6)$$

where h is a parameter approximately equal to the slope of the stress—strain curve, L is the length of a dislocation section, k is the Boltzmann constant, ν is the frequency, and b is the Burgers vector.

$$a_{red} = \varepsilon_0 \gamma = \frac{\nu b}{L} \exp\left(-\frac{E}{RT}\right).$$

The length of the dislocation section corresponds to the size of the smallest elementary volume which may be subjected to continuous deformation by virtue of the passage of dislocations through it, independently

of the deformation of the neighboring elementary volume. It is reasonable to assume that the quantity L equals the height of the crystallite determined by the x-ray method (or the coherent scattering region L_c).

The foregoing considerations explain the exponential growth of the transient creep rate with temperature, the identical activation energies of the parameters a and γ, and also the dependence of the parameter on the elastic modulus.

The foregoing theoretical arguments make no allowance for the concentration of the dislocations in the material, and cannot explain the influence of the irradiation intensity.

We may thus draw two main conclusions: the deformation of transient creep in carbon material is proportional to the height of the regions of coherent scattering, and the transient creep rate (velocity) falls with increasing intensity of the damaging flux.

LITERATURE CITED

1. O. S. Gurvich and É. N. Marmer, Poroshkovaya Met., No. 2, 77 (1962).
2. N. N. Dergunov and V. N. Barabanov, in: Construction Materials Based on Graphite, No. VI [in Russian]. Metallurgiya, Moscow (1971), p. 63.
3. H. Losty and N. Fiedler, in: Proc. Fifth Conf. on Carbon, Vol. 1, Pergamon Press, New York (1962).
4. P. A. Platonov et al., [2], p. 70.
5. Yu. S. Virgil'ev et al., in: Construction Materials Based on Graphite, No. VII [in Russian], Metallurgizdat, Moscow (1972), p. 73.
6. I. A. Oding, Creep and High-Temperature Strength [in Russian], Mashgiz, Moscow (1962).
7. Physical Metallurgy, Vol. 3 [Russian translation], Mir, Moscow (1968), p. 226.

CREATION OF A STANDARD NEUTRON SOURCE (FIELD) AT THE I. V. KURCHATOV INSTITUTE OF ATOMIC ENERGY

R. D. Vasil'ev, N. B. Galiev, V. P. Yarina, E. N. Babulevich, A. A. Kononovich, M. G. Mitel'man, N. D. Rozenblyum, Yu. M. Shipovskikh, A. G. Inikhov, and V. I. Petrov

UDC 621.384.6

An All-Union calibration scheme for measuring neutron flux density at nuclear physics installations calls for the creation of standard neutron sources (fields) at nuclear reactors for the calibration of in-core detectors.

A standard source is some portion of the neutron field within a reactor which has been studied in detail along with means for monitoring it and which is adapted for metrological work and is verified by the metrological services as a standard.

This paper reports on the creation of a standard neutron source (field) for the calibration of direct charge detectors (DCD) at the materials testing reactor (MR) of the I. V. Kurchatov Institute of Atomic Energy. A vertical channel in the beryllium reflector was used for this purpose. A calibration device consisting of a graphite cylinder 74 mm in diameter was installed in the channel. Eight DPZ-1P detectors were placed on the lateral surface of the cylinder to monitor the neutron field and detectors being calibrated were placed in the center in four channels. The monitors were arranged in staggered fashion above and below the operating portion of the field. With such an arrangement, distortion of the neutron field in the operating portion of the calibration channels introduced by the monitors was insignificant. The operating portion of the field was chosen to be at the level of the center of the core where the neutron flux density gradient vertically along the channel was least.

The direct charge detectors were calibrated with respect to their response to thermal neutrons. To do this, the effective thermal neutron flux density φ_T was determined at a previously selected point of the empty calibrated channel. At the same time, the total monitor current I_M was recorded. A detector being calibrated was then placed in the channel and its current i and the monitor reading I_M^{cal} recorded. Detector response was calculated from

$$\alpha = \frac{\varphi_T^{cal}}{i_T} f[\varphi_T(x)], \quad (1)$$

where φ_T^{cal} is the effective thermal neutron flux density in the reactor channel at the time of calibration, which is determined from

$$\varphi_T^{cal} = (\varphi_T / I_m) I_m^{cal} \quad (2)$$

Here, i_T is the component of the DCD current produced by thermal neutrons; $\varphi_T(x)$ is the distribution of the thermal neutron flux density along the channel length x in relative units; $f[\varphi_T(x)]$ is a correction factor which takes into account the gradient of the effective thermal neutron flux density along the length L of the DCD being calibrated. The value of the factor $f[\varphi_T(x)]$ averaged over the length of a DCD was estimated in the following manner:

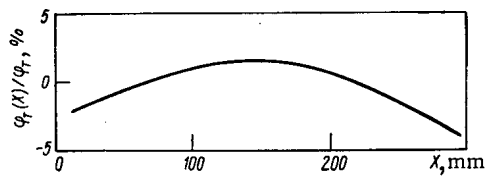

Fig. 1. Distribution of effective thermal neutron flux density over the height of the reactor channel.

Translated from Atomnaya Énergiya, Vol. 38, No. 5, pp. 313-315, May, 1975. Original article submitted August 13, 1974.

TABLE 1. Main Sources of Error in the Determination of φ_T

Quantity	^{60}Co		^{198}Au	
	Error, %			
	random error	unexcluded systematic error	random error	unexcluded systematic error
r_{Cd}	0,42	—	—	—
σ_0	—	0,54	—	0,20
A	0,3	1,5	0,3	0,3
N	—	0,1	—	0,1
λ	—	0,095	—	0,074
t_0	—	0,0001	—	0,001
t_b	—	0,008	—	0,09
R	0,3	1,51	0,3	0,34

TABLE 2. DCD Calibration Errors

Quantity	Determination conditions	Error, %	
		random	unexcluded systematic error
φ_T	During certification of standard source	0,8	2,5
I_M	The same	—	0,5
I_M^{cal}	During calibration of DCD	—	0,5
i	The same	—	0,5
$f[\varphi_T(x)]$	During calibration of DCD (from results of certification of standard source)	0,3	—
r_{Cd}^{DCD}	During calibration of DCD (during manufacture)	0,3	—
f_{Cd}	The same	0,3	—

$$f[\varphi_T(x)] = \frac{\int_{x_1}^{x_2} \varphi_T(x)\,dx}{L}, \tag{3}$$

where x_1 and x_2 are the coordinates of the ends of the emitter of the DCD being calibrated in the channel measured from the bottom of the channel.

To separate out the current component i_T from the total current i, we determined in advance the cadmium ratio (r_{Cd}^{DCD}) of a DCD, which is equal to the ratio between the current from a bare DCD and the current from the same, or an identical, DCD when shielded with cadmium:

$$r_{Cd}^{DCD} = i_{bare}/i_{Cd}. \tag{4}$$

Then

$$i_T = i\left(1 - \frac{1}{r_{Cd}^{DCD} f_{Cd}}\right), \tag{5}$$

where f_{Cd} is a correction factor which takes into account the effect of the cadmium shield on the DCD reading because of attenuation of the epithermal neutron field.

Thus, with Eqs. (2)-(5) taken into consideration, the equation for the determination of α takes the form

$$\alpha = \frac{\varphi_T}{I_M} \frac{I_M^{cal}}{i\left(1 - \frac{1}{r_{Cd}^{DCD} f_{Cd}}\right)} f[\varphi_T(x)]. \tag{6}$$

The quantity φ_T/I_M and the relation $\varphi_T(x)$ appearing in this equation were established during the certification of the standard neutron source (field). The quantities I_M^{cal}, i, and $f[\varphi_T(x)]$ were determined in the calibration of a DCD; r_{Cd}^{DCD} and f_{Cd} are characteristics which were established for specific conditions of DCD use. In addition to φ_T/I_M and $\varphi_T(x)$, the epithermal parameter r, which characterizes the ratio between the thermal and epithermal components of the neutron field, was determined during certification of the source (field).

The effective thermal neutron flux density at the selected point was measured during certification of the standard source by the cadmium difference method and the two-detector method using ^{59}Co and ^{197}Au activation detectors.

Using the cadmium difference method, the thermal neutron flux density was calculated from

$$\varphi_T = \frac{R_b}{\sigma_0 g G_T}\left(1 - \frac{1}{r_{Cd} F_{Cd}}\right), \tag{7}$$

where R_b is the activation integral of the bare detector; σ_0 is the activation cross section at the thermal velocity of 2200 m/sec; g is the Westcott parameter which takes into account the deviation of the energy dependence of the activation cross section from a 1/v law in the thermal region; G_T is a factor which takes into account self-shielding of the detector and perturbation of the neutron field by the detector in the thermal neutron energy region; r_{Cd} is the cadmium ratio, which is the ratio between the activation integrals of the bare and cadmium-shielded detectors; F_{Cd} is a factor which takes into account attenuation of the epithermal neutron field by the cadmium shield.

When using the two-detector method, the thermal neutron flux density was determined from

$$\varphi_T = \varphi_{arb}\left(1-\frac{1}{K_{Cd}}\right) r\sqrt{\frac{T}{T_0}}, \tag{8}$$

where φ_{arb} is an arbitrary (Westcott) thermal neutron flux density; K_{Cd} is a factor which depends on the effective cutoff energy of cadmium and which is 2.29 for the 1-mm-thick cadmium shield used during certification; T_0 and T are the thermal neutron temperatures at the velocity v_0 and at velocities different from v_0.

The arbitrary flux density appearing in Eq. (8) is given by

$$\varphi_{arb} = \frac{R_{Co}}{(\sigma_0 g G_T)_{Co}} \frac{1}{1+\left(\frac{G_p S_0}{G_T g}\right)_{Co} r\sqrt{\frac{T}{T_0}}}, \tag{9}$$

where R_{Co} is the activation integral for the ^{59}Co detector; G_p is a factor which takes into account self-shielding of the detector and perturbation of the neutron field by the detector in the epithermal region; S_0 is the Westcott parameter which takes into account the deviation of the energy dependence of the activation cross section from a 1/v law in the epithermal region.

The epithermal was calculated from

$$r\sqrt{\frac{T}{T_0}} = \left(\frac{G_T g}{G_p S_0}\right)_{Au} \frac{a - R_{Co}/R_{Au}}{R_{Co}/R_{Au} - b}, \tag{10}$$

where

$$a = (\sigma_0 g G_T)_{Co}/(\sigma_0 g G_T)_{Au} \tag{11}$$

and

$$b = (\sigma_0 g G_T)_{Co}/(\sigma_0 g G_p)_{Au} \tag{12}$$

(here, R_{Au} is the activation integral for the ^{197}Au detector).

The activation integral was determined from the measured values of the induced detector activity A, the number N of target isotope nuclei in the detector, and the quantities λ, t_0 and t_b by means of the equation,

$$R = \frac{A}{N(1-e^{-\lambda t_0})e^{-\lambda t_b}}, \tag{13}$$

where λ is the decay constant of the activation reaction product; t_0 is the time of irradiation; t_b is the time from the end of irradiation to the beginning of measurement of activity.

The quantities σ_0, N, and λ appearing in Eqs. (7)-(13) were determined during certification of the activation detectors. The quantities R_b, R_{Co}, R_{Au}, r_{Cd}, A, t_0, and t_b were determined experimentally.

Thermal neutron activation cross section σ_0 was assumed to be 37.3±0.2 and 98.7±0.2 b for ^{59}Co and ^{197}Au respectively.

The number of nuclei N in the ^{59}Co and ^{197}Au detectors were determined by weighing with weights of first class accuracy and by the method of activation weighing of the samples in the neutron field of the thermal column at the heavy water reactor of the Institute of Experimental and Theoretical Physics.

The decay constants for ^{60}Co and ^{198}Au were obtained from the half-lives 5.265±0.005 yr and 2.695±0.002 days respectively.

The induced activity of the detectors was measured using equipment which was part of the State special standard instrument for unit neutron flux density from VNIIFTRI: $4\pi\beta$-γ coincidence equipment, a scintillation γ spectrometer, and scintillation counter with differential discriminator set to the total absorption peak. The equipment was checked with a working standard for unit nuclide activity from VNIIFTRI.

Table 1 gives the errors in the experimental quantities and constants appearing in Eqs. (7)-(13) which were used in the determination of φ_T. The contribution from the errors in the correction factors G_T, G_p, S_0, and F_{Cd} to the error of φ_T was 1%.

The total error of measurement (from the result of a single irradiation) at the 95% confidence level was calculated from

$$\delta_{\varphi_T} = t^{95}\sigma_{\varphi_T} + 1.1\theta_{\varphi_T}, \tag{14}$$

where t^{95} is the Student factor; σ_{φ_T} and θ_{φ_T} are the random and systematic error in the determination of of φ_T. We found $\sigma_{\varphi_T} = 0.8\%$, $\theta\varphi_T = 2.5\%$, and $\delta_{\varphi_T} = 3.6\%$.

The effective thermal neutron flux density at the certification point of the field was determined from the results of numerous measurements. In this case, the error, which was calculated at the root-mean-square deviation for a series of measurements over the course of a year, did not exceed 4%. One should note that the difference between the values of φ_T obtained by the cadmium difference method and by the two-detector method was no more than 0.8%.

The monitor current I_M, as well as I_M^{cal} and i, was measured with a bridge circuit including a P-306 potentiometer with a standard resistor. The error in current measurement did not exceed 0.5%.

The certified quantity φ_T/I_M was determined from measurements of φ_T and I_M with an error of 4.5%.

The distribution of effective thermal neutron flux density over the length of a calibration channel was determined by relative measurements with the ^{59}Co detector. The measurement error at each point was 0.3%. Figure 1 shows the measured distribution $\varphi_T(x)$ in relative units along the reactor channel (the distance x was measured from the bottom of the channel); the values φ_T at the certification point (x = 64 mm) was taken as unity. It is evident from the figure that the gradient of the effective thermal neutron flux density does not exceed 2.5% over the approximately 300 mm length of the operating portion of the field.

The components of the calibration error for certain DCD samples are given in Table 2.

The total error in the determination of DCD response to thermal neutrons was 5%.

RADIOACTIVE CONTAMINATION OF THE WATER ENVIRONMENT AND MEASURES FOR ITS REDUCTION

L. I. Gedeonov, L. M. Ivanova,
B. A. Nelepo, and A. G. Trusov

UDC 551.46:539.16

Recent radioecological studies have made it possible to accumulate a large amount of information in this field of knowledge. Radiation in one form or another and from various sources has had an effect on living matter from the very origin of life on earth. As is well known, it is one of the basic mutagenic factors, if not the principal one, and perhaps the very evolution of forms would have proceeded differently without radiation.

However, the modern formulation of the problem of radioecology, and even the name of this scientific discipline, was defined quite recently. A controversy over the definition of the subject of radioecology and its subdivisions continues as of this moment. Nevertheless, studies are proceeding ever more energetically [1-9] because of the production of artificial radioactivity and the propagation into the environment of radioactive materials not previously present there.

Artificial radioactive materials enter the various portions of the biosphere. Billions of curies of radioactive wastes from the treatment of fuel elements are being stored above ground or underground in extremely concentrated form under the supervision of man. Random or accidental discharge of even a small fraction of the highly active wastes is unacceptable; it would create regions of very hazardous radioactive contamination. Merely the potential possibility of such an event requires well developed knowledge of the environment and of the organisms living in it, i.e., the development of radioecology.

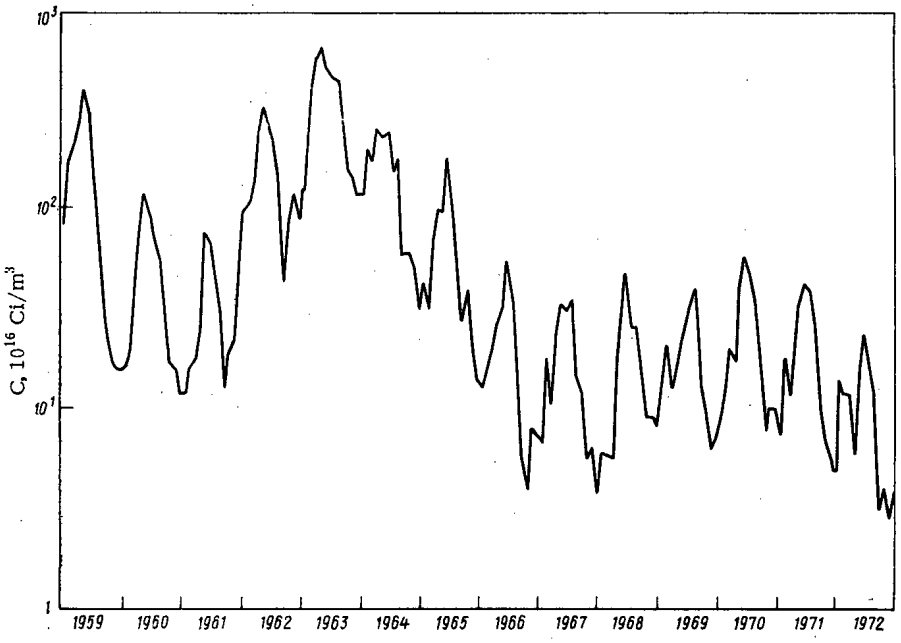

Fig. 1. ^{137}Cs concentration in the surface layer of the atmosphere at Zelenogorsk (near Leningrad).

Translated from Atomnaya Énergiya, Vol. 38, No. 5, pp. 317-323, May, 1975. Original article submitted November 26, 1974; revision submitted January 16, 1975.

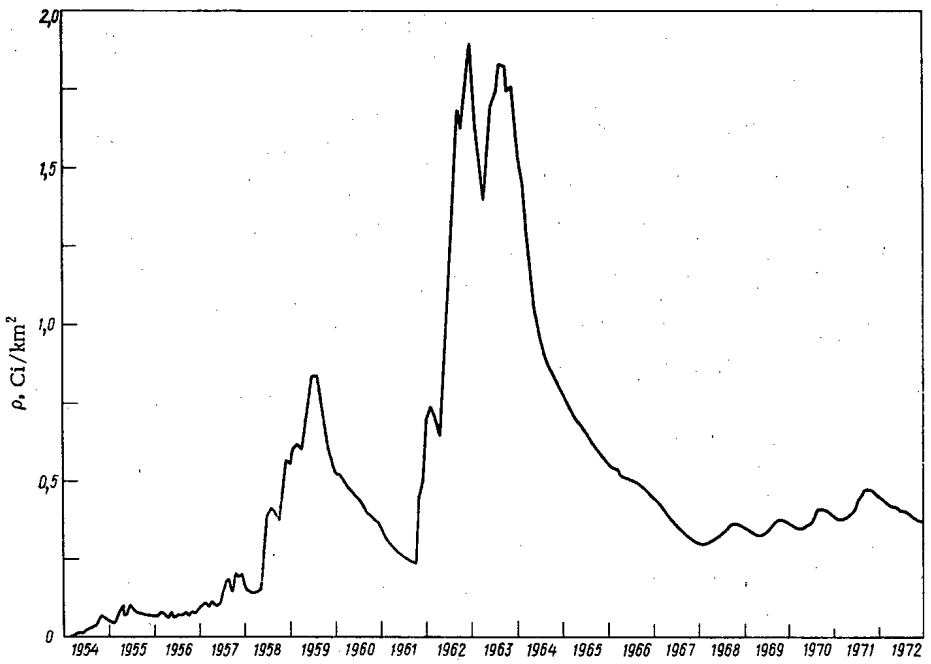

Fig. 2. Buildup and decay at Zelenogorsk of β-active products from nuclear

Tremendous amounts of radioactive fission products were knowingly discharged into the atmosphere during tests of nuclear weapons. The 1963 Moscow agreement prohibiting nuclear testing in three media was a tremendous victory for peace-loving forces and progressive science [10]. Unfortunately not all governments joined in the Moscow agreement, and radioactive products from nuclear explosions are being discharged into the atmosphere even now.

Developing nuclear power and nuclear shipping are also sources for the introduction of artificial radionuclides into the environment. Radioactive materials discharged into the atmosphere, on the soil or into surface layers of the ground, reach the water environment. The oceans are the final collectors for longlived radionuclides. V. M. Klechkovskii [11] made a large contribution to the study of paths of migration for radioactive impurities in soil and water.

As already noted, radioecological investigation begins with an evaluation of the forms and intensities of the radiations acting on organisms under natural conditions. External irradiation can be evaluated by measuring dose rate or absorbed dose with instruments having detectors set up in situ in the environment, and can also be determined by measuring the concentrations of the various emitters. To determine internal irradiation, which often is the main hazard for an organism, it is necessary to know the concentration of emitters, i.e., radionuclides, in environmental objects. It is also necessary to know the pathways by which radionuclides gain entrance into organisms, their migration along the food chain, the coefficients of concentration or discrimination during transfers from one link of the chain to another, the

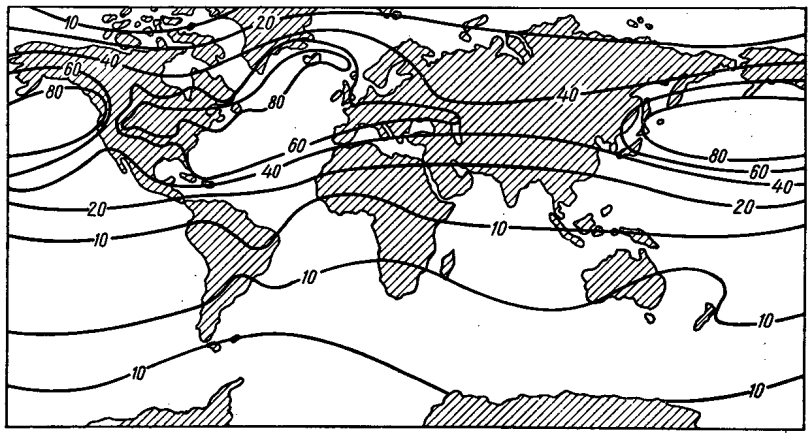

Fig. 3. Global distribution of ^{90}Sr fallout, mCi/km^2

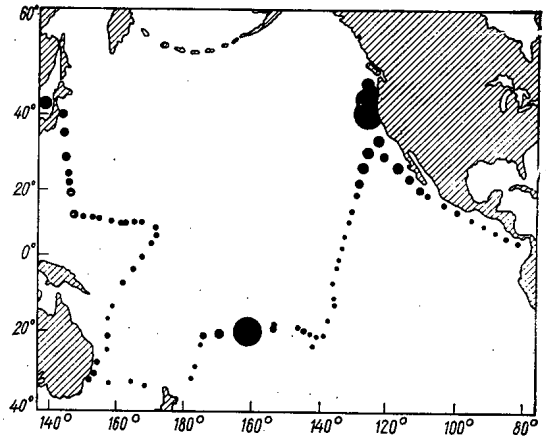

Fig. 4.

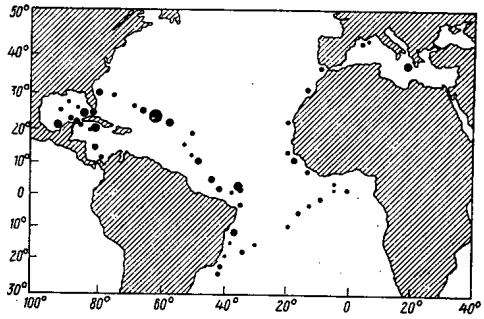

Fig. 5

Fig. 4. ^{90}Sr concentrations in surface waters of the Pacific Ocean. (Diameter of the circles is proportional to the concentration; maximum value is 180 disintegrations/min-100 liters).

Fig. 5. ^{90}Sr concentration in surface waters of the Atlantic Ocean.

nature of organism feeding, etc. Thus a fundamental radioecological study is the determination of the concentrations of radioactive impurities in environmental objects, a study to which this paper is devoted.

On a global scale, the water environment is still being contaminated because of the fallout of radioactive products from nuclear explosions on the surfaces of oceans, seas and reservoirs. The presence of radioactive fission products in the lower layers of the atmosphere is shown in Fig. 1. This data is representative for very large areas of the globe. Thus, a similar picture was observed at Milford Haven (51°30' N, 5° W), Chilton (51°30' N, 1° W), Moosonee (51°16' N, 80°30' W), and New York (40°48' N, 73°58' W).

In the open ocean, as on land, radioactive products from nuclear explosions quickly enter the surface layer of the atmosphere from the troposphere after tests of nuclear weapons but products from the stratospheric reservoir fallout after a longer period of time. The variation of the total amount of β-radioactive products deposited on the surface of the ground at Zelenogorsk in the period from 1952 to 1972 is shown in Fig. 2 [9, 12, 13]. The distribution of the ^{90}Sr accumulation as of 1967 is shown in Fig. 3 [14].

Of course the picture of global radioactive contamination must be supplemented by data on the content of artificial radionuclides in the water environment. A summary of all stages of the studies in this field has been presented [15-17]. The collection of actual data at a few individual points in the Pacific Ocean and its recording was completed by 1967. The application of objective interpolation to the reproduction of

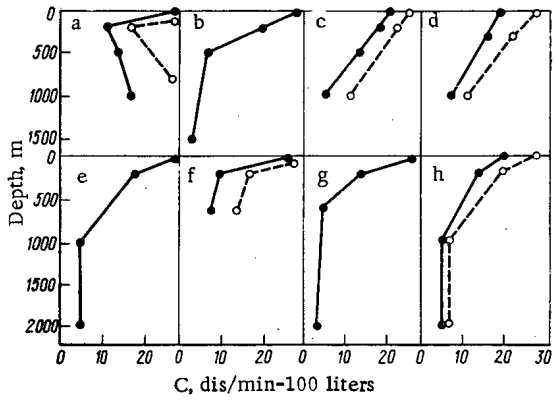

Fig. 6

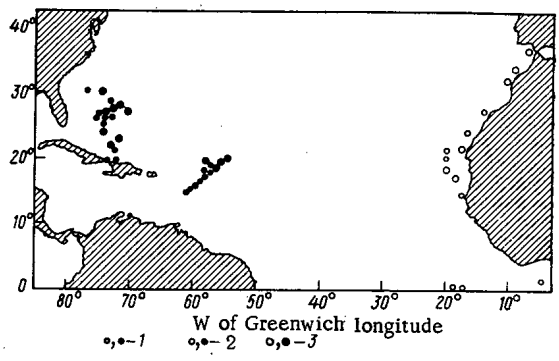

Fig. 7

Fig. 6. Depth distribution of ^{90}Sr (●) and ^{137}Cs (○) in the Atlantic Ocean in 1967: a) 05°57' N, 44°59' W; b) 03°00' N; c) 09°03' S, 32°23' W; d) 10°00' S, 25°00' W; e) 00°03' S, 25°05' W; f) 00°06' S, 39°56' W; g) 06°55' S, 34°13' W; h) 06°53' S, 25°10' W.

Fig. 7. ^{90}Sr concentration in surface waters of the Atlantic Ocean from data of the 12-th trip of the research ship Academician Kurchatov in 1972 (●): 1) 10, 2) 20, 3) 30 disintegrations/min-100 liters.

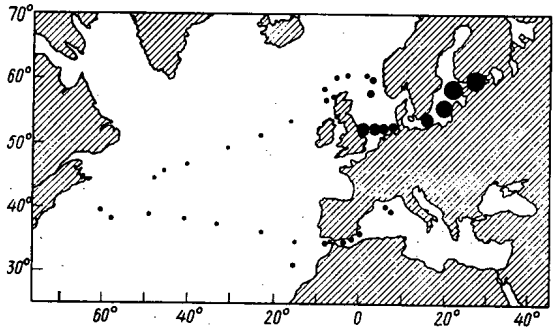

Fig. 8

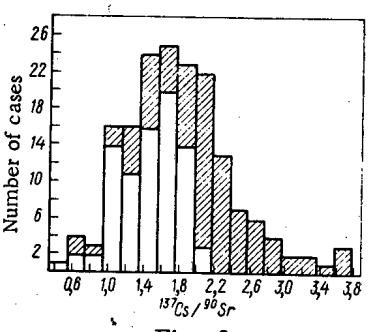

Fig. 9

Fig. 8. ^{90}Sr concentration (in relative units) in the surface waters of the Baltic Sea and Atlantic Ocean in 1970 from data of the 2nd trip of the research ship Academician Vernadskii.

Fig. 9. Distribution of the ratio of ^{137}Cs and ^{90}Sr concentrations: clear area, Pacific Ocean; shaded area, Atlantic Ocean.

the radioactivity field at points not followed experimentally led to the possibility of reconstruction of the total picture of the contamination of surface waters of the Atlantic by radioactive ^{90}Sr [18] as of 1967. It is interesting that data up to the beginning of 1967 is discussed in the main conclusions of the National Academy of Sciences of the US [19].

In the latest stage of the studies to determine the present state of radioactive contamination of the water environment, a special round-the-world expedition of the research ship Mikhail Lomonosov was made in 1966-1967 with the principal purpose being the study of the radioactivity of the Pacific Ocean. (An intensive study was made somewhat earlier of the radioactive contamination of the Irish Sea because of the discharge of liquid radioactive wastes from Great Britain.)

The most important regions of the Pacific and Atlantic Oceans were studied. Not only artificial radioactive contamination was studied on this expedition, but also the natural radioactivity of the water and of the bottom deposits of the ocean [20, 21]. The main data for the distribution of the radioactive contaminants ^{90}Sr and ^{137}Cs (20-th trip of the research ship Mikhail Lomonosov) is shown in Figs. 4 and 5 (see [16]). Figure 4 delineates very vividly the region of radioactive contamination of the Pacific Ocean by discharges of radioactive wastes at the mouth of the Columbia River.

Not only were surface waters studied, but also water from various depths. Integration of depth distribution curves (Fig. 6) made it possible to determine the storage of ^{90}Sr and ^{137}Cs in waters to a depth of 500 m.

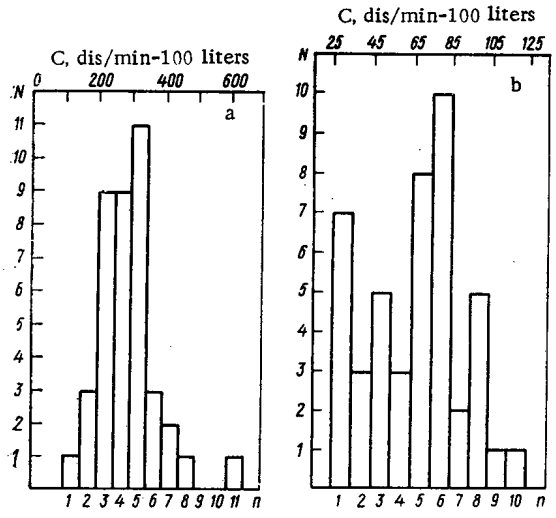

Fig. 10. Distribution of ^{90}Sr (a) and ^{137}Cs (b) concentrations observed in the eastern portion of the Gulf of Finland in 1971. (N is the number of cases and n is the number of the concentration interval).

Generalization of similar data by using optimal interpolation has been performed [22, 23]. Automation of collection and analysis of scientific information from a radiochemical study of the ocean has been reported [24].

The studies in the Atlantic were continued with the research ships Academician Vernadskii, Mikhail Lomonosov, and Academician Kurchatov. The results are given in Fig. 7. We note that despite the decrease in the number of nuclear explosions in the northern hemisphere, practically no reduction was observed in the radioactive contamination of the surface waters of the oceans and seas. The radioactive contamination in the southern hemisphere is increasing. Inflow of water masses into the equatorial flow and partial transport of contaminants in the atmosphere through the equatorial zone leads to penetration of a certain portion of the radioactive contaminants from the southern hemisphere into the northern hemisphere and vice versa. Recent observations have yielded a large amount of experimental material, and analysis of which by optimal interpolation

might reveal stable differences in the distribution of radionuclides between individual regions of the ocean if they exist. It is already clear that, as before, the enclosed seas are distinguished by markedly higher concentration levels of longlived ^{90}Sr and ^{137}Cs than the open oceans.

The increased artificial radioactivity in the area of the Irish Sea and at the mouth of the Columbia River forces one to direct particular attention to the situation in the Baltic and Black Seas. A recent study of the Black Sea (Fig. 8) showed that the ^{90}Sr and ^{137}Cs which is present in it at concentrations exceeding the concentrations in the Atlantic at the same latitude by factors of 6-10 has thus far been made up of global radioactive fallout on water surfaces and drainage of deposited radionuclides with river waters [25]. The effect of discharges of radioactive wastes is small and does not exceed the error in the technique for determining radionuclide content in sea water.

The problems of radioecology do not permit one to record the observed levels of radioactive contamination unconcernedly. One of the modern requirements is the determination of the form of occurrence of radionuclides in water. Information on the ratio of ^{137}Cs and ^{90}Sr concentrations in the waters of the Pacific Ocean was published [26]. On the basis of more than three hundred determinations, it was established that this ratio remains the same both at the surface and in the depths of the ocean and is maintained at a single level in different locations with the exception of those where there is a large amount of fresh water. It is clear from an analysis of histograms (Fig. 9) that both nuclides do not come down with precipitation and are in ionic form.

An entirely different picture is seen in the almost fresh waters of the Neva gulf and the eastern portion of the Gulf of Finland (Fig. 10). The histograms indicate that cesium is predominantly retained in soils and bottom deposits.

The study of the radioactive contaminants of the enclosed seas is inseparably connected with observations on the radioactivity of fresh-water reservoirs. In this connection, attention is directed primarily to the Neve and Volga, and in view of the great interest of member countries of the SEV, a program of joint study of the radioactivity of the Danube water system is being developed [27]. It is clear that the forthcoming development of nuclear power and the potential possibility of the entrance of a number of radionuclides into the water environment demands a search for measures to reduce the radioactive contamination of the water environment. It is necessary that discharged waters do not contain radioactive contaminants in greater amounts than is considered normal for the water of open reservoirs used by the population.

In addition, one should take all measures to prevent the escape of radioactive materials during the operation of nuclear power stations. The Leningrad nuclear power station can serve as an example [28].

Gaseous discharges from the ventilation channels of reactors are undesirable. Falling out on the water surface of reservoirs, they too may be the cause for entrance of radioactive contaminants into the water. In order to reduce discharges, filtration and other forms of purification of the discharge air are used as well as storage in tanks for the elimination of shortlived radioactive components through decay. Meteorologic and hydrologic conditions should be studied in detail along with their possible effect on the dissipation of discharges from a nuclear power station. It is necessary to select the most advantageous hydrometeorological conditions for the discharge of gases.

Attention must be devoted to the problem of trapping inert gases and highly volatile materials, particularly iodine and ruthenium. It is imperative that the rise in ^{85}Kr content in the planetary atmosphere be halted in time. Also in line is a detailed study of tritium in ecologic systems and a search for technical solutions to the problem of preventing the escape of tritium into the environment. At the present time, the tritium content in the waters of rivers, lakes, and sources of water supply is continually increasing. The tritium problem may become very serious in the near future if the required measures are not developed and put into practice.

The difficulty of solving these problems is obvious. In one case, it is necessary to separate inert gas from tremendous masses of air and to store it for a decade. In the other case, it is necessary to separate tritium from hundreds and thousands of cubic meters of water or from ventilation air. In this instance, it is necessary to separate one isotope of hydrogen from another; vaporization or chemical procedures are ineffective and the output of electrolysis is low. Undoubtedly these difficulties will be overcome like many others facing science and technology. Radioecology should help in the solution of the problem by presenting as detailed and precise information as is possible about radionuclides in the environment.

At the present time, radiation conditions in the environment are satisfactory on the whole. Although observed levels of radionuclide concentration in water and air are $\sim 10^{-3}$ of the level of natural radioactivity in these media, the very entrance into the biosphere of artificial radioactive isotopes leads, as a rule, to the breakdown of historically accumulated levels of radioactivity in its corresponding substrates. Migrating in the biosphere along the same paths as the natural isotopes, artificial radioactive materials increase the radioactivity of the corresponding components of the biosphere and thereby increase the intensity of radiation effects on living organisms.

There are local patches of radioactive contamination of the water environment which have a noticeable effect in particular regions of the Pacific Ocean. Measures to control discharges are being undertaken through IAEA on the basis of ICRP standards which ensure the safety of the population.

Vigorous growth of nuclear power at the end of the twentieth century is assumed and, as a consequence, the location of a large number of nuclear power stations and installations on the shores of rivers and seas leading to a tremendous amount of radioactive wastes, the "isolation" of which from the environment is a great scientific and technical problem. Furthermore, the entrance of any amounts of radionuclides into the hydrosphere is obviously undesirable.

Further ecologic studies of the behavior of radionuclides in various objects in the hydrosphere will be of great interest for science and practice.

LITERATURE CITED

1. Radioactive Contamination of the Environment [in Russian], V. P. Shvedov and S. I. Shirokov, eds., Gosatomizdat, Moscow (1962).
2. L. A. Pertsov, Natural Radioactivity of the Biosphere [in Russian], Atomizdat, Moscow (1968).
3. Investigation of Radioactive Contamination of the Water of the Pacific Ocean [in Russian], a compilation, N. I. Popov, ed., Vol. 82, Nauka, Moscow (1966).
4. V. P. Shvedov and S. A. Patin, Radioactivity of Oceans and Seas [in Russian], Atomizdat, Moscow (1968).
5. G. G. Polikarpov, Radioecology of Marine Organisms [in Russian], Atomizdat, Moscow (1966).
6. G. G. Polikarpov, Marine Radioecology [in Russian], Naukova Dumka, Kiev (1970).
7. B. A. Nelepo, Nuclear Hydrophysics [in Russian], Atomizdat, Moscow (1970).
8. I. L. Karol'et al., in: Trudy Instituta Okeanologii [in Russian], Vol. 82, Nauka, Moscow (1966).
9. L. I. Gedeonov, At. Énerg., 33, 650 (1972).
10. Soviet Scientists on the Hazards of Nuclear Weapons Tests [in Russian], I. V. Kurchatov, ed., Atomizdat, Moscow (1959).
11. V. M. Klechkovskii and I. V. Gulyakin, Pochvovedenie, No. 3, 1 (1958).
12. Z. G. Gritchenko et al., Ékspress-informatsiya, MGI, Akad. Nauk Ukranian SSR, No. 9, Izd. MGI Akad. Nauk Ukranian SSR, Sevastopol' (1967).
13. N. V. Vasil'eva et al., in: Nuclear Meteorology [in Russian], No. 25, Gidrometeoizdat, Moscow (1972), p. 166.
14. Document Un A/AC, 82/R/241, 1069.
15. V. I. Baranov et al., III Geneva Conference (1964), USSR Paper 28/P/384.
16. V. M. Vlovenko et al., At. Énerg., 31, 409 (1971).
17. V. M. Vlovenko et al., in: Proc. IAEA Symp. on Disposal of Radioactive Wastes into Seas, Oceans, and Surface Waters, Vienna, 16-20 May, 1966, p. 425.
18. V. I. Belyaev et al., Izv. Akad. Nauk SSSR, Ser. Fizika Atmosphery i Okeana, 5, 381 (1969).
19. Radioactivity in the Marine Environment, National Academy of Sciences, Washington (1970).
20. D. S. Mikolaev et al., in: Radioactive Elements in Rocks [in Russian], Abstracts of papers at All-Union meeting in Novosibirsk, Novosibirsk (1972), p. 69.
21. E. M. Emel'yanov et al., Litologiya i Polezne Iskopaemye, No. 4, 28 (1973).
22. K. G. Vinogradova et al., At. Énerg., 35, 136 (1973).
23. O. S. Zudin et al., At. Énerg., 32, 347 (1972).
24. O. S. Zudin and B. A. Nelepo, in: Trudy AANII [in Russian], Vol. 301, Gidrometeoizdat, Leningrad (1972), p. 80.
25. L. I. Gedeonov et al., At. Énerg., 33, 835 (1972).
26. A. G. Trusov, L. M. Ivanova, and L. I. Gedeonov, At. Énerg., 34, 394 (1973).
27. Radioactive Contamination of the Danube and Evaluation of Radiation Conditions [in Russian], Fourth session of KNTS on Radioactive Wastes and Decontamination, Pk IAE SEV, Moscow (1973).
28. A. M. Petros'yants et al., At. Énerg., 31, 333 (1971).

R. E. Uhrig

RANDOM NOISE TECHNIQUES IN NUCLEAR REACTOR SYSTEMS*

Reviewed by L. V. Konstantinov

The book by R. Uhrig that is being reviewed is the first monograph translated into Russian that is devoted to the experimental applications of methods of investigation of reactor noise. In the book the methodological bases of the theory of statistical processes in nuclear reactors are discussed, and various methods of recording and processing random processes are given, with the use of the mathematical apparatus of probability theory and modern computational technology.

The first chapter gives the general characteristics of random processes in nuclear reactors and draws attention to microscopic (discrete) and macroscopic levels in the study of noise.

The short second chapter presents basic concepts in the theory of noise (mean values, characteristic and correlation functions, etc.).

In the third chapter there is an analysis of statistical discrete methods of measurements in reactor systems, where it is assumed that the systems can be satisfactorily represented by a model having lumped parameters. The material of the chapter can serve as a different type of reference book, in which the experimentors find not only a systematized catalog of basic methods of discrete measurements of reactor noise, but also recommendations on their use.

The fourth chapter gives basic relations of random noise theory. This chapter is actually an expansion of the questions discussed in the second chapter, and the material from these chapters should have been combined.

In the fifth chapter, the elementary theory of macroscopic reactor noise is considered, and models are presented for a reactor with lumped and spatially dependent parameters.

A great deal of the book is occupied with a description of methods of measurement and analysis of noise. Problems of selecting the measurement method and estimating the accuracy of statistical measurements using specialized devices are successfully extended in the sixth and seventh chapters.

The eighth and ninth chapters are devoted to the application of numerical techniques to the acquisition, transmission, recording, and processing of data. The tenth chapter also touches upon these subjects. Chap. 10 considers methods of generation of pseudorandom noise and their application for reactor investigations. Here we should note the description of important details of the synthesis and analysis of a different series of pseudorandom sequences, which finds practical application. Unfortunately, the most promising direction in the technique of processing of random processes, connected with the use of a rapid Fourier transformation making use of computers, is given only a sketchy discussion in the book.

A systematization of the numerous noise measurements carried out in nuclear reactors is given in Chap. 11. Besides a description of the measurement methods and experimental results, the chapter also contains recommendations of the author concerning the conditions of applicability of methods of investigation of reactor noise.

In the final chapter (Chap. 12) the application of special statistical methods in reactor research is considered. The material that is discussed attests to the promise of the treatment of random-noise

* Atomizdat, Moscow (1974); [Russian translation edited by A. I. Mogil'ner from English Edition] Ronald Press, New York (1970).

Translated from Atomnaya Énergiya, Vol. 38, No. 5, p. 323, May, 1975.

methods of measurement of technological characteristics of nuclear reactors, coolant velocity, level of vibration of elements of the core, boiling of the coolant, etc.

The book contains an extensive bibliography on the subject of reactor noise.

A shortcoming of the book is the overabundance of general data on the theory of random processes for a relatively small amount of experimental material on noise measurements in power reactors.

In conclusion we note that the book will be useful both for specialists occupied with experiments in the field of reactor physics and also for students and graduate students in the corresponding disciplines.

SOME REGIMES OF HYDRAULIC INSTABILITY IN THE FIRST CIRCUIT OF A FAST REACTOR

I. A. Kuznetsov

UDC 621.039.526.53

We consider the effects of a hydraulic instability in the first circuit of a multi-loop nuclear power plant. The instability is initiated by displacements of the check valves located in each circulation loop of the circuit. All the loops are connected in parallel to the pressure and output collectors of the reactor. For deviations from some stationary state, the motion of the check valve and the motion of the coolant in the loops are described by the equations:

$$\frac{d^2\varphi}{d\tau^2}=k_\varphi\varphi+k_G G_i+k_T\frac{d\varphi}{d\tau}+\frac{M_p}{J_v}, \quad (1)$$

$$\frac{d\bar{G}_i}{d\tau}=R\bar{G}_i-k_{p\varphi}\varphi, \quad (2)$$

where φ is the opening angle of the valve; $\bar{G}_i$ is the flow rate of the coolant in the i-th loop, referred to nominal values; M_p is the perturbing moment; and J_v is the moment of inertia of the valve about the rotation axis.

The characteristic equation of the system has the form

$$(s^2-k_T\cdot s-k_\varphi)(s+R)+k_G k_{p\varphi}=0. \quad (3)$$

In agreement with the Routh—Hurwitz criterion on the basis of this equation we write three inequalities, whose satisfaction is necessary and sufficient to ensure stability of motions of the valve. Considering these inequalities, connecting the parameters of the circuit and the check valve, we can conclude that the breakdown of stability of the motions of the check valve and the coolant in the first circuit of the nuclear power plant for normal direction of circulation can be caused by the breakdown of stability of operation of the pumps or distortions of the valves of the field by the velocity of the coolant, leading to an increase (in certain ranges of angles of opening) of the hydraulic resistance of the valve, the drag of the plate, and their ratio.

We consider regimes with opposite direction of circulation of the coolant in the loops; as a result, we obtain criteria for the closing of the check valve. It is shown that closing of the valve is connected with breakdown of the stability of its position in the coolant flow. This breakdown arises for some critical flow rate of the coolant. The angle of deviation of the normally open valve from the equilibrium position for critical flow rate of coolant is connected with the resistance of the valve and of the circuit by the relation

$$\operatorname{ctg}(\varphi_*-\varphi_R)=\frac{\xi_k}{\xi+\xi_k}\cdot\frac{d(\ln\xi)}{d\varphi}, \quad (4)$$

where φ_R is the angle of opening of the valve at the equilibrium position; ξ_k and ξ are coefficients of hydraulic resistance of the circuit and of the valve, respectively; τ is the time; φ_* is the angle of opening of the valve for the critical flow rate. From this expression it follows that the angle of deviation from equilibrium and, hence, the magnitude of the critical flow rate, decrease with increasing hydraulic resistance of the loop of the first circuit in comparison with the resistance of the valve alone. On the basis of this relation with the use of measurement results for the critical flow rate of coolant under natural conditions we can determine the hydraulic resistance of the valve for small opening angles. The results obtained can be used in the design and interpretation of experimental results.

Original article submitted May 31, 1974.

Translated from Atomnaya Énergiya, Vol. 38, No. 5, pp. 325-330, May, 1975.

DETERMINATION OF THE NONHERMETICITY OF A TYPE IRT-M FUEL ASSEMBLY IN THE CORE OF A REACTOR

O. F. Gusarov

UDC 621.039

On an IRT-2000 research nuclear reactor of Tomsk Polytechnic Institute an experiment was conducted on the detection of a nonhermetic type IRT-M fuel assembly (FA) based on the Xe^{135} concentration in samples of water withdrawn from the FA directly in the core for a shut-down reactor.

The water samples were analyzed on an AI-100 analyzer with a USD-1 detector having a NaI crystal of dimensions 40 × 40 mm in the 80-500 keV energy range. We used a conical collimator having a 20° field of view of the USD-1 device. As a result of checking all 26 FA's of the active core we detected a FA in which calculation of the pulses in the Xe^{135} photopeak (E_γ = 250 keV) was 13.3 times greater than the background value. For the remaining FA's, the value of the pulses in the Xe^{135} photopeak varied in the limits of ±7% of the background value: for the background value we took into account the pulses in the Xe^{135} photopeak from the sample of water taken 1.5 m above the core.

The FA in the channel of the safety rod proved to be nonhermetic. After it was replaced, the specific activity of the gas decreased by a factor of 10 in the above-reactor space, the γ-background in the upper area decreased by a factor of 4, and that of the pump of the first circuit decreased by a factor of 3.

Before selecting the water samples from the FA, the reactor was operated at a power of 2 MW for 4 days. After the reactor had been shut down for 30 min, the pumps of the first circuit were disconnected. Samples were taken 2 h after the pumps had been disconnected.

The sampler was a tube made of the alloy SAV-1, 23 mm in diameter, and 7.2 m long. On the upper end of the tube, a rubber hose 30 cm long was slipped on and pinched by a clamp. On the lower end a centering washer made of Teflon was fastened, which allowed us to place the tube exactly on the FA, covering the FA from above in order to reduce the inflow of water from the resorvoir tank.

Sampling of the water tubes from the FA is carried out in the following manner: the empty tube with pinched hose is lowered into the reactor tank and the centering washer is placed on the FA. After the clamp is removed, the water from the FA and from the space between the given FA and the neighboring FA's fills the tube up to the water level in the tank, the hose is pinched by the clamp, after which the sampler is removed from the tank. To reduce the outflow of water from the tube when it is raised, its lower internal diameter is reduced by means of a section of vacuum hose with interior diameter 5 mm and length 15 cm, embedded in the lower end of the tube. A sample of water in the amount of 2.5 liters is poured off into the prepared vessel after the clamp is removed. We used 30 mm of H_2O for the analysis. For the sampling of the water from the FA, in which the control-rod channel was located, the centering washer was not used. It was moved along the tube into the upper part and tightened. The tube was located directly on the tip of the FA close to the control and saftey rod channel. The check of the 26 FA's consumed 4 h.

Original article submitted July 1. 1974.

DETERMINATION OF "SYNTHETIC" SCATTERING CROSS SECTIONS OF SLOW NEUTRONS FOR APPROXIMATE EQUATIONS OF THERMALIZATION

N. I. Laletin

UDC 621.039.51.12

The energy distribution of slow neutrons ($E \lesssim 1$ eV) is frequently described by approximate equations, differential with respect to the energy [1-5]. It is shown in [6] how the approximate neutron-thermalization equations can be obtained from the exact transport equation. In the present study we solve a problem that in a certain sense is the inverse of the problem considered in [6]. Based on the given functions $\xi\Sigma_s(\varepsilon)$ and $\gamma(\varepsilon)$, which enter into the approximate equations, we establish an approximate formula for the differential scattering cross section $\Sigma_s(\varepsilon' \to \varepsilon)$ ["synthetic" cross section].

The most general form of the cross section for which the integral equation will reduce to a differential equation has the form

$$\Sigma_s(\varepsilon' \to \varepsilon) = \widetilde{\Sigma}_s(\varepsilon' \to \varepsilon) + \alpha(\varepsilon)\,\delta(\varepsilon - \varepsilon');$$

$$\widetilde{\Sigma}_s(\varepsilon' \to \varepsilon) = \varepsilon e^{-\varepsilon} \begin{cases} v(\varepsilon')\,p(\varepsilon), & \varepsilon' \geqslant \varepsilon; \\ p(\varepsilon')\,v(\varepsilon), & \varepsilon' \leqslant \varepsilon. \end{cases} \tag{1}$$

Here $\varepsilon = E/kT$ is the neutron energy in units of kT (T is the temperature of the medium, and k is the Boltzmann constant). We take into account that the cross section should satisfy the condition of detailed balance.

For the function $\alpha(\varepsilon)$, $p(\varepsilon)$ and $v(\varepsilon)$ in the work we obtain the following relations:

$$\alpha(\varepsilon) = \Sigma_s(\varepsilon) - \frac{\xi\Sigma_s(\varepsilon)}{\gamma(\varepsilon)};$$

$$v(\varepsilon) = \widetilde{\Sigma}_s(\varepsilon) \int_{\infty}^{\varepsilon} \left\{ e^{\varepsilon'} \frac{d}{d\varepsilon'} \left[\frac{1}{\xi\Sigma_s(\varepsilon')\,\varepsilon'} \right] \times \int_{\varepsilon'}^{\infty} v(\varepsilon'')\,\varepsilon'' e^{-\varepsilon''}\,d\varepsilon'' \right\} d\varepsilon'; \tag{2}$$

$$p(\varepsilon) = v(\varepsilon) \int_{0}^{\varepsilon} \frac{1}{v^2(\varepsilon') \int_{\varepsilon'}^{\infty} \varepsilon'' e^{-\varepsilon''} v(\varepsilon'')\,d\varepsilon''} \times \left[v(\varepsilon') \frac{d\widetilde{\Sigma}_s(\varepsilon')}{d\varepsilon'} - \widetilde{\Sigma}_s(\varepsilon') \frac{dv(\varepsilon')}{d\varepsilon'} \right] d\varepsilon'. \tag{3}$$

Here

$$\widetilde{\Sigma}_s(\varepsilon) = \int_0^{\infty} \widetilde{\Sigma}_s(\varepsilon \to \varepsilon')\,d\varepsilon' = \frac{\xi\Sigma_s(\varepsilon)}{\gamma(\varepsilon)}$$

and $$\Sigma_s(\varepsilon) = \int_0^{\infty} \Sigma_s(\varepsilon \to \varepsilon')\,d\varepsilon'.$$

Equations (3) can be simply solved for the model of a gas with m = 1, which can be used to control the accuracy of the transformations that are carried out. For this case $v(\varepsilon) = 1/\varepsilon$ and $p(\varepsilon) = \operatorname{erf}\sqrt{\varepsilon}/\,\varepsilon e^{-\varepsilon}$.

It turns out that Eqs. (3) give simple analytical solutions in one important particular case, namely, for the 2K-model. In [5] it was shown that the spectra of slow neutrons in water with various absorbers at room temperature are well described by a differential equation if we assume

$$\xi\Sigma_s(\varepsilon) = \text{const} = \xi_0\Sigma_0, \quad \gamma(\varepsilon) = \text{const} = 1.$$

Here $\xi_0\Sigma_0$ is the moderating power of water at energies $E \approx 10\text{-}10^4$ eV. Such a two-constant model is also convenient because it admits a simple analytical investigation [7, 8]. For this model, Eqs. (3) yield $v(\varepsilon) = 1/\varepsilon$ and $p(\varepsilon) = (1 - e^{-\varepsilon})/\varepsilon e^{-\varepsilon}$. Thus, the scattering cross section for the 2K-model has the form

$$\Sigma_s(\varepsilon' \to \varepsilon) = [\Sigma_s(\varepsilon) - \xi_0\Sigma_0]\,\delta(\varepsilon - \varepsilon') + \xi_0\Sigma_0 \begin{cases} \dfrac{1 - e^{-\varepsilon}}{\varepsilon'}, & \varepsilon' \geqslant \varepsilon; \\ \dfrac{1 - e^{-\varepsilon'}}{\varepsilon'} e^{(\varepsilon' - \varepsilon)}, & \varepsilon' \leqslant \varepsilon. \end{cases}$$

LITERATURE CITED

1. M. Cadihac et al., BNL-719 (c-32), (1962), Vol. 2, p. 439. M. V. Kazarnovski and V. I. Mostovoi (editors), Thermalization of Neutrons [in Russian], Atomizdat, Moscow (1964).
2. M. Cadihac et al., III Intern. Conf. Geneva, 1964, Rep. 73.
3. H. Pitcher, AEEW-M-350 (1963).
4. N. I. Laletin, At. Énerg., 14, No. 5, 458 (1963).
5. N. I. Laletin, At. Énerg., 16, No. 5, 402 (1964).
6. N. I. Laletin, At. Énerg., 34, No. 6, 445 (1973).
7. M. Williams, Brit. J. Appl. Phys., D, 1, 957 (1968).
8. P. Jauho, I. Pitkaranta, and P. Silvennoinen, J. Nucl. Sci., 6, 287 (1972).

Original article submitted July, 15, 1974;
abstract submitted November 26, 1974.

RADIAL DISTRIBUTION OF AN ELECTRON STREAM FROM A MONODIRECTIONAL POINT SOURCE

A. M. Kol'chuzhkin and A. V. Plyasheshnikov

UDC 539.121.72

The linear functionals of transport theory are usually expressed in terms of the differential flux Φ or the adjoint function Φ^+:

$$I=(\Phi, D)=(\Phi^+, S),$$

where D(x) is a function of the detector sensitivity; S(x) is the density of sources in the phase space of the coordinates r, the directions Ω, and the energies E. If the symmetry of the detector is higher than the symmetry of the source, a second method proves to be preferable [1]. We use it to determine the total flux of electrons from a monodirectional point source.

By virtue of the symmetry of the problem, the adjoint function will depend only on the distance r and the angle ϑ (Fig. 1). The adjoint equation in the approximation of small angles and constant cross sections can be written in the form

$$\frac{\partial\Phi^+}{\partial r}(r, \vartheta)-\frac{\vartheta}{r}\frac{\partial\Phi^+}{\partial\vartheta}(r, \vartheta)+\Sigma_s\Phi^+(r, \vartheta)$$
$$-\int d\varphi'\int d\vartheta'\Sigma_s(\theta)\Phi^+(r, \vartheta)=\frac{\delta(r)\delta(\vartheta)}{2\pi r^2\vartheta} \quad (1)$$

and can be solved uding the Fourier—Bessel transformation:

$$\Phi^+(r, \vartheta)=\int_0^\infty d\eta\eta J_0(\vartheta\eta)\Phi^+(r, \eta);$$

$$\Phi^+(r, \eta)=\int_0^\infty d\vartheta\vartheta J_0(\vartheta\eta)\Phi^+(r, \vartheta),$$

which leads to the equations

$$\Phi^+(r, \eta)=\frac{1}{2\pi r^2}\exp\left[-r\int_0^1 d\xi F(\xi\eta)\right]; \quad (2)$$

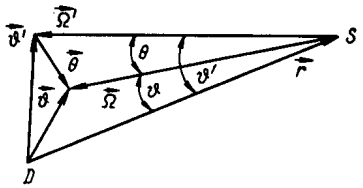

Fig. 1. Diagram illustrating the derivation of Eq. (1).

$$\Phi^+(r,\vartheta)=\frac{1}{2\pi r^2}\int_0^\infty d\eta\eta J_0(\vartheta\eta)\exp\left[-r\int_0^1 d\xi F(\xi\eta)\right], \tag{3}$$

where

$$F(\eta)=2\pi\int_0^\infty d\theta\theta\Sigma_s(\theta)[1-J_0(\theta\eta)]. \tag{4}$$

Using the value of $F(\eta)$ calculated in [2] for the Rutherford small-angle screened cross section, we can write the radial distribution of the total flux of electrons from a monodirectional point source in the form

$$\Phi(\rho,z)\,2\pi\rho\,d\rho=\psi\,d\psi\sum_{n=0}^{\infty}f^n(\psi)/B^n,$$

$$f^n(\psi)=\frac{1}{n!}\int_0^\infty duuJ_0(\psi u)\left(\frac{u^2}{4}\ln\frac{u^2}{4}\right)^n \times\exp\left[-\frac{u^2}{4}\right], \tag{5}$$

where ρ and z are cylindrical coordinates, determining the relative position of the source and the detector.

$$\psi^2=3\rho^2/\chi_c^2z^2B,\quad B-\ln B=\frac{5}{3}-1n3-2C+\ln(\chi_c^2/\chi_a^2), \tag{6}$$

where χ_c, χ_a are the parameters in Moliere's theory.

Equations (5) are identical in form to the Moliere distribution describing the angular distribution of electrons in plane geometry [2]. They differ only in the form of the auxiliary variables (6).

For small values of ψ in the expansion (5), the first term is the principal term:

$$\Phi(\rho,z)\,2\pi\rho\,d\rho\approx 2\exp[-\psi^2]\,\psi\,d\psi,$$

i.e., the radial distribution is close to a normal distribution. For large ψ the following asymptotic form is valid:

$$\Phi(\rho,z)\,2\pi\rho\,d\rho=\frac{2\psi\,d\psi}{B\left\{\psi^4-4\psi^2\left[1+\frac{2}{B}\ln\frac{2\psi}{5}\right]\right\}}.$$

The radial distribution that is presented was calculated without using the Fokker–Planck approximation; therefore, it is more exact than the well-known Fermi distribution.

LITERATURE CITED

1. A. P. Suvorov, E. B. Breshenkova, and V. V. Orlov, in: Questions in the Physics of Reactor Shielding [in Russian], Gosatomizdat, Moscow (1963), p. 30.
2. H. Bethe, Phys. Rev., 89, 1256 (1953).

Original article submitted July 19, 1973;
revision submitted December 9, 1974.

OUTPUT CURRENT OF AN EVACUATED DIRECT-CHARGING DETECTOR

G. V. Kul'akov

UDC 539.1.074

The evacuated direct-charging detector is a system of spatially separated electrodes of various materials in vacuum which are charged by γ rays without an external power supply. We divide the spectrum of electrons produced by γ rays at the electrodes into two groups: "slow" electrons, at energies below 50 eV, and "fast" electrons, with energies above 50 eV. The fast electrons are produced directly by γ rays in the photoelectric and Compton effects, while the slow electrons are produced through an interaction of the fast electrons with the electrode surfaces. Below we outline mathematical models for the sensitivity of evacuated direct-charging γ detectors; these models can be used to optimize the detector parameters.

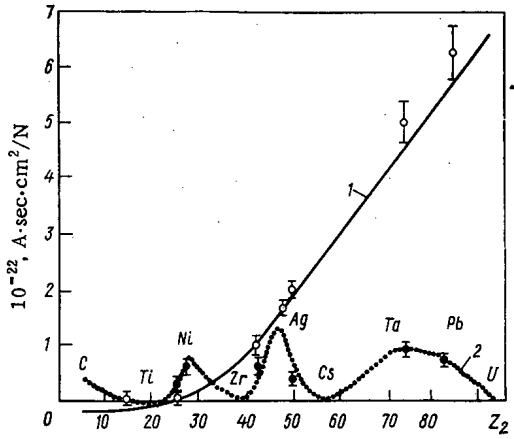

Fig. 1. Sensitivity of a direct-charging γ detector. 1) Sensitivity due to fast electrons; 2) sensitivity due to slow electrons. E_γ = 1.25 MeV, Z_1 = 13. The curves are calculated from Eqs. (1) and (3) (curves 1 and 2, respectively); the points are experimental.

We describe the sensitivity due to fast electrons as follows (in units of amperes × seconds × square centimeter per γ ray):

$$W_f = \int_{E_\gamma} \Phi(E_\gamma)\, dE_\gamma \frac{e}{2} (F_1 S_1 A_{12} - F_2 S_2 A_{21}), \tag{1}$$

where $\Phi(E_\gamma)$ is the γ spectrum (reciprocal megelectron volts), normalized to one; e is the electronic charge (coulombs); F is the probability of the emission of a fast electron (electrons per γ ray); and S is the surface area of the outer (S_1) or inner (S_2) electrode (in square centimeters). The probability for the absorption of an electron from electrode i by electrode j is

$$A_{ij} = \frac{\int_0^{\theta_{ij}} d\theta \int_{50}^{E_{max}} dE f(\theta, Z_i, E)\{1-\eta[\varphi_j(\theta), Z_j, E]\}}{\int_0^{\pi/2} d\theta \int_{50}^{E_{max}} dE f(\theta, Z_i, E)}, \tag{2}$$

where θ is the emission angle (degrees), $\theta_{ij} = \arcsin r_j/r_i$, (degrees), r is the electrode radius (centimeters), Z is the atomic number of the electrode material, f is the spectral-angular distribution (electrons per megelectron volt per radian), η is the differential coefficient of inelastic electron reflection, and $\varphi_j(\theta) = \arcsin(r_j \sin\theta/r_i)$ is the angle of incidence of the electron (degrees).

The mathematical model for the sensitivity due to "slow" electrons is

$$W_f = 3.48\cdot 10^{-21}\left\{2 - A_{12} + \frac{F_2}{F_1}[2 - A_{21} - a_{12}(1 - A_{21})] \times k_1 S_1 M_{12} a_{12} - \left[1 + a_{12}\left(1 - A_{21} + \frac{F_1}{F_2}\right)\right] k_2 S_2 M_{21}\right\}, \tag{3}$$

where

$$a_{12} = \int_0^{\arcsin r_2/r_1} \psi\, d\theta \Big/ \int_0^{\pi/2} \psi\, d\theta$$

is the probability for a fast electron from the first electrode to be incident on the second electrode; M_{ij} is a function of the potential difference between the electrodes, which takes into account the attenuation of the slow-electron flux during the charging of the detector; and $k = \delta_0 E_0^{0.35}/720$, g/(MeV·cm^2) [here δ_0 is the maximum probability for slow-electron emission for the given material, and E_0 (electron volts) is the corresponding energy of the fast electron]. The analytic form of M_{ij} is quite complicated and is given in the article proper for plane and cylindrical electrodes. The article proper also gives data on all the quantities which appear in Eqs. (1)-(3). Figure 1 shows the results calculated on the basis of these mathematical models along with the corresponding experimental results. We see that these models give an adequate description of the sensitivity.

The author thanks V. I. Ivanov for interest in this study.

Original article submitted February 15, 1974;
abstract submitted December 30, 1974.

CHLORINATION OF URANIUM AND PLUTONIUM OXIDES IN MOLTEN CHLORIDES OF THE ALKALI AND ALKALINE EARTH ELEMENTS

M. P. Vorobei, A. S. Bevz, and O. V. Skiba

UDC 541.661:621.039.59

Processes of chlorination of UO_2, U_3O_8, UO_3, and PuO_2 with gaseous chlorine in molten chlorides of magnesium, calcium, and the eutectic mixture of sodium (34 mole %) and cesium chlorides in a temperature interval 500-800°C were studied by the methods of chemical spectrophotometric, and x-ray diffraction studies. It was shown that at 800°C in air, uranium oxides interact with molten magnesium chloride with the formation of the uranates MgU_3O_{10} and $MgUO_4$, which precipitate; no interaction is observed with molten calcium chloride under these conditions. The pumping of chlorine through the melt leads to an intensive dissolution of the oxides and uranates formed. According to the data of chemical analysis, uranium exists in solution in penta- and hexavalent states. The formation of U(V) occurs as a result of the equilibrium reaction:

$$Cl^- + UO_2^{2+} \rightleftarrows 1/2Cl_2 + UO_2^+, \quad (1)$$

for which the equilibrium constants were calculated [for the system with magnesium chloride $(350 \pm 0.3)\cdot 10^{-1}$ atm, for the system with calcium chloride $(1.20 \pm 0.3)\cdot 10^{-2}$ atm].

An analysis of the reaction products of uranium oxides with a molten salt solvent and the absence of a chlorinating agent, as well as an analysis of the products formed during the passage of chlorine through the melt, have made it possible to suggest a scheme of the reaction of chlorination in molten magnesium chloride:

$$MgUO_4 + nCl_2 \rightarrow MgUO_{4-n}Cl_{2n} + \frac{n}{2}O_2 \quad (2)$$

and in molten calcium chloride:

$$U_3O_8 + nCl_2 \rightarrow CaUO_{4-n}Cl_{2n} + \frac{n}{2}O_2. \quad (3)$$

Subsequently there is a gradual replacement of oxygen by chlorine in $MeUO_4{-}nCl_{2n}$ with the formation of a series of intermediate chlorouranates. The end products of this process (by analogy with the chlorination of uranium oxides in molten alkali metal chlorides) are the complexes $MeUO_2Cl_4$, where Me is magnesium or calcium.

In the absence of a chlorinating agent, PuO_2 is practically insoluble in molten magnesium and calcium chlorides. It dissolves extremely slowly during the process of chlorination. Thus, after 12 h of continuous pumping of chlorine through the melt, the plutonium content (in the tri- and tetravalent states in a ratio of ~10:1) in melts of the investigated salts did not exceed 0.15-0.25% by weight. Chlorination of PuO_2 in a molten eutectic mixture of NaCl—CsCl was studied in the temperature interval 500-850°C (see Table 1). The appearance of Pu(II) is due to the equilibrium reaction

$$Pu^{4+} + Cl^- \rightleftarrows Pu^{3+} + 1/2Cl_2, \quad (4)$$

for which the temperature dependence of the equilibrium constant was obtained in the interval 700-850°C. The mechanism of the chlorination of PuO_2 in molten NaCl—CsCl in analogous to that cited earlier [1].

TABLE 1. Results of the Chlorination of PuO_2 in Molten NaCl-CsCl

Plutonium content in the system before chlorination, % by weight	Plutonium concentration in the melt after chlorination, % by weight	Temperature of chlorination, °C	Time of complete dissolution of PuO_2, hours	Valence states of plutonium in solution, %		
				III	IV	VI
0,5	0,47	500	2,5	—	90	10
1,75	1,70	550	3,2	≤ 5	≥ 95	—
1,86	1,82	600	2,7	≤ 5	≥ 95	—
2,2	2,14	650	2,2	≤ 5	≥ 95	—
1,9	1,84	700	2,0	5	95	—
2,5	2,47	750	2,0	14	86	—
2,65	2,58	800	1,6	26	74	—
5,0	4,88	850	1,9	38	62	—

LITERATURE CITED

1. M. I. Vorobei, et al., At. Énerg., 33, 553 (1972).

Original article submitted July 15, 1974;
abstract submitted December 9, 1974.

THERMAL STABILITY OF CESIUM URANYL TETRACHLORIDE ON HEATING IN AIR TO 1000°C

M. P. Vorobei, A. S. Bevz, and O. V. Skiba

UDC 541.11:546.791.06+548.734

The thermal stability of the compound $Cs_2UO_2Cl_4$ on heating in air in the temperature interval 20-1000°C was studied by thermogravimetric, x-ray diffraction, and chemical methods of analysis. The derivatogram of $Cs_2UO_2Cl_4$ is characterized by six endothermic effects: 415, 460, 620, 660, 675, and 850°C (see Fig. 1).

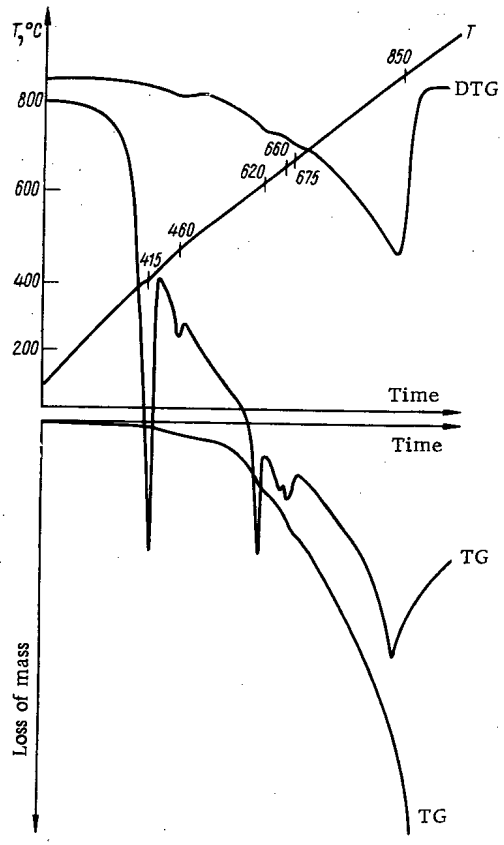

Fig. 1. Thermogravigram of $Cs_2UO_2Cl_4$ in an atmosphere of air in the temperature interval 20-1000°C at a rate of heating 2 deg/min.

An analysis of the integral curve of the loss of mass (TG) gives evidence of the stability of $Cs_2UO_2Cl_4$ in the temperature region up to 415 ± 3°C (the melting point of $Cs_2UO_2Cl_4$). With the passage of $Cs_2UO_2Cl_4$ into the liquid state in a melt in air, thread-like crystals with an orange color begin to appear: gradually the entire mass of the melt is converted to a homogeneous solid phase product. The nature of this conversion is determined by the oxidation of the uranyl chloride complex $[UO_2Cl_4]^{-2}$ in the melt by atmospheric oxygen to a chlorouranate with liberation of free chlorine into the atmosphere. The effects at 620, 660, 675, and 850°C correspond to conversions in the solid phase products, leading to the formation of four stable intermediate phases. For x-ray diffraction identification and determination of the chemical composition of the intermediate phase of the thermal decomposition of $Cs_2UO_2Cl_4$ we conducted isothermal exposures of the starting material at the corresponding temperatures until the establishment of a constant weight of the sample. On the basis of the results of the analysis we proposed a scheme of thermal conversions of $Cs_2UO_2Cl_4$ in heating in air to 1000°C:

$$Cs_2UO_2Cl_4\ sol \xrightarrow{415^\circ C} Cs_2UO_2Cl_4\ liq \xrightarrow{460^\circ C}$$

$$\rightarrow Cs_2UO_3Cl_2\ sol \xrightarrow{620^\circ C} Cs_2UO_{3,5}Cl_{(TD)} \xrightarrow{660-675^\circ C}$$

$$\rightarrow Cs_2U_3O_{10}\ sol \xrightarrow{850^\circ C} Cs_2U_4O_{13}\ sol.$$

The heat of melting of $CsUO_2Cl_4$ (ΔH_m = 3.90 kcal/mole) was determined according to the data of differential thermal analysis, and the entropy change (ΔS_m = 5.8 cal/mole·deg) was calculated.

Original article submitted July 15, 1974.

LETTERS TO THE EDITOR

GAS CLEANING TEST USING A CERAMET FILTER IN FLUIDIZED BED DEWATERING AND CALCINING WASTE SOLUTIONS

N. S. Lokotanov and O. A. Nosyrev

UDC 621.928.9

Waste gases from drying and dehydration processes in fluidized bed apparatus contain suspended particles. Concentration (by weight) of these can be as high as 50 g/m^3 [1]. Product loss reduction and atmospheric pollution prevention are the most common reasons for removing the suspended particles. Dewatering and calcining of nuclear power industry waste solutions requires special attention to the second objective [2, 3]. Equipment widely used in drying installations (cyclones, scrubbers, electrostatic precipitators, and bag filters) do not meet the special conditions of these processes and do not provide the required level of contaminant removal. Research and investigation of gas cleaning methods, which meet the more stringent process requirements and conditions, is one of the most important problems in the reprocessing of liquid wastes.

This article presents test results* of an experimental 26 m^2 effective surface ceramet filter. These tests lasted for 1000 h at a dewatering and calcination fluidized bed unit for nitrate—phosphate solutions. Solution composition was: 125 g/liter $NaNO_3$, 240 g/liter $Al(NO_3)_3$, 120 g/liter H_3PO_4, and 90 g/liter residue.

Filter construction is shown in Fig. 1. The filter is a cylindrical apparatus 2 m in diameter × 4 m height. The bottom section is a offset cone shaped hopper. An internal baffle divides the filter into two zones forming the cyclone section with tangential gas inlet. The filter has three separate sections each with 72 filter cartridges. The cartridges consist of an assembly of 111 ceramet porous elements 40 mm diameter (3 mm thick walls) × 80 mm long. These are sintered stainless steel (Kh18N9T) powder with 0.1-0.2 mm size granules. The elements are welded together.

Each cartridge is equipped with a blowback device at the top end (Fig. 2). The device consists of a nozzle, diffuser, and connecting coupling with side openings for clean gas outlet. All the cartridges in a section are connected and are attached to a hollow tube sheet whose inner volume is piped to the clean gas line. The volume above the tube sheet is connected to the blowback compressed air line through an interconnecting pipe.

The ceramet filter was equipped with monitoring—measuring instruments and automatic controls. Gas temperatures at the filter inlet and outlet, and pressure drop could be monitored continuously. Automatic filter regeneration could be initiated when a certain pressure drop was reached and/or after fixed time intervals.

The waste gas impurity removal efficiency was evaluated based on analysis of aerosol weight samples before and after the filter. The removal coefficient was calculated as the ratio of solid phase concentrations before and after the filter. Samples were taken by external filtration on a fiberglass filled glass cartridge (before upstream of the filter) and on flat basalt fiber filters (after the filter). The samples were gravimetrically analyzed by universally accepted methods [4].

Particle size analysis of the solids entrained by the gases was simultaneously carried out using a MBI-6 microscope.

* A. K. Petrov participated in these tests.

Translated from Atomnaya Énergiya, Vol. 38, No. 5, pp. 331-332, May, 1975. Original article submitted September 19, 1973; revision submitted December 16, 1974.

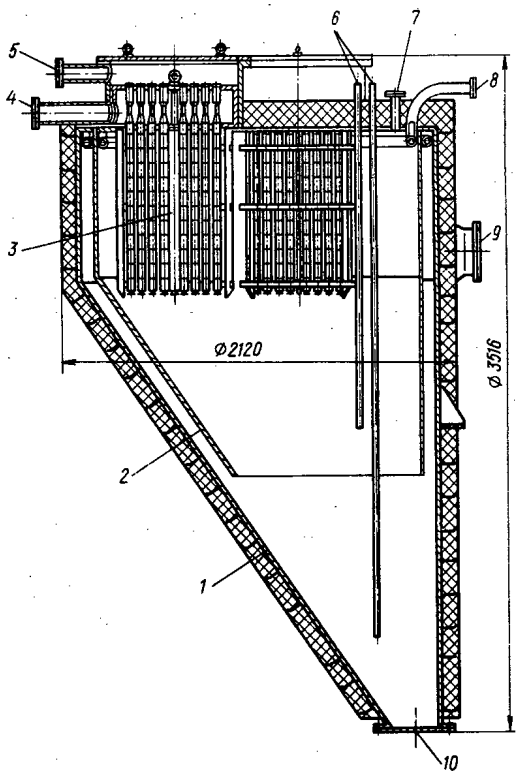

Fig. 1

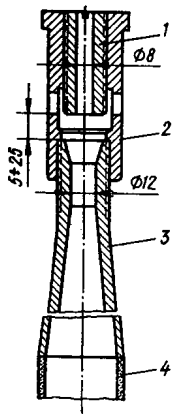

Fig. 2

Fig. 1. Ceramet filter: 1) housing. 2) internal baffle, 3) filtering section, 4) gas outlet, 5) compressed air inlet for blowback, 6) separated material level sensors in the hopper, 7) temperature sensor connection, 8) inlet for filter surface wash water, 9) gas inlet, and 10) recovered product discharge.

Fig. 2. Device for filter cartridge blowback: 1) nozzle, 2) connecting coupling, 3) diffuser, and 4) ceramet filtering element.

The ceramet filter was tested during operation of a 70-95 liter/h capacity dewatering and calcination unit. The weight composition of the gases formed was: 92% air, 6.3% water vapor, 1.1% NO+ NO_2, < 0.6% $H_2 + CO_2$. The entire volume of produced gas (670-680 m^3 at STP), at 300°C, was passed through the filter using a VVN-12 pump.

Solid particle concentration in the waste gas varied from 22 to 74 g/m^3. This variation is related mainly to changes in the process conditions of drying apparatus operation. However these concentration variations had no significant effect on filter operation, except for some change in the rate of pressure drop increase between regenerations.

The particles carried by the gases corresponded (in chemical composition) to $n_1Al_2O_3 \cdot n_2Na_2O \cdot n_3P_2O_5$ polyphosphates with $NaNO_3$ as an impurity (up to 2 wt %). The particle size analysis of the solid particles was: 43% < 1 μm, 28% 1-2 μm, 15.4% 2-3.5 μm, 7.0% 3.5-5 μm, 6.6% 5-10 μm. The chemical composition of the gas stream solid phase and the operating temperature conditions of the filter ruled out the possibility of condensation and compounds melting on the filtering surface. This was of deciding importance in filter operation.

Filter pressure drop was 150-160 mm H_2O at the start of operation. It gradually increased as cake built up on the filtering surface. The first experiments with regeneration were carried out when

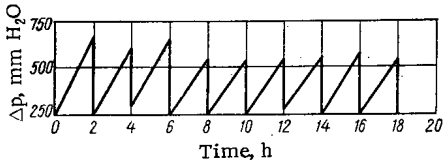

Fig. 3. Filter pressure drop variation with periodic regeneration.

pressure drop reached 700-800 mm H_2O. After the optimum blowback compressed air pressure (3 kg/cm^2) was selected, regeneration was carried out every two hours. The volume of compressed air supplied for blowback is equal to the volume of filter elements being regenerated in one cycle. Figure 3 shows a curve of pressure drop variation in steady state operation of the filter. It shows that blowback can reliably reduce filter pressure drop to less than half, i.e. from 550-600 mm H_2O to 250 mm H_2O.

Stabilization of the initial (after regeneration) pressure drop (250 mm H_2O) indicates that the cake layer in the filtering element pores is not destroyed during regeneration but is in dynamic equilibrium due to the adhesive forces between the particles and the filtering membrane. Filter pressure, therefore, increased only as a result of cake layer buildup on the filter element surface during operation and is a linear function of operating time (see Fig. 3).

The tests showed that solid particle concentration after the filter did not exceed $9 \cdot 10^{-3}$ g/m^3 at STP. Average was $5 \cdot 10^{-3}$ g/m^3. The calculated coefficient of solid particle removal from waste gases on the ceramet filters was 10^3-10^4.

LITERATURE CITED

1. M. V. Lykov, Drying in the Chemical Industry [in Russian], Khimiya, Moscow (1970).
2. K. P. Zakharova, et. al., in: Transaction of the II Congress of the Council of Economic Cooperation, "Investigations in the Field of Reprocessing Irradiated Fuel" [in Russian], KAE Czechoslovak SSR, Prague (1973), p. 182.
3. Londing, et. al., in: Transaction of the II Geneva Conference [Russian translation], Vol. 5, Atomizdat (1959), p. 463.
4. G. M. Gordov and I. L. Peisakhov, Monitoring of Dust-removal Units [in Russian], Metallurgizdat, Moscow (1964).

PROTECTION OF STAINLESS STEEL AGAINST INTERACTION WITH BERYLLIUM

R. M. Al'tovskii and E. A. Vasina

UDC 621.039.531:621.039.532.5

Even at relatively low temperatures, beryllium interacts with many metals in contact with it. This results in the formation of a brittle beryllide of the respective metal and a solid solution of beryllium in the metal. At 550-600°C beryllium reacts intensively with stainless steels, copper, nickel, iron, zirconium, and alloys of the Alumel and Chromel type [1, 2]. Beryllium reacts strongly with stainless steel 1Kh18N9T, commercial iron, alloy ZhS6-K, and molybdenum [3]. Layers of interaction 50-100 μ thick are formed on steel and commercial iron in tests at 800° for 6 h.

Protection of metals against interaction with beryllium requires the use of diffusion barriers, one of which may be BeO, since the diffusion coefficient of beryllium in BeO is smaller than in iron and other components of the steel [4, 5]. Beryllium oxide is one of the most inert materials with respect to various metals. It does not interact with molybdenum, tantalum, tungsten, or tungsten—rhenium alloys at temperatures of 2200, 2550, 2300, and 2250° respectively [6].

A coating of BeO on beryllium is most conveniently obtained by means of anodic oxidation. The kinetics of anodic oxidation of beryllium was investigated earlier [7, 8], and it was found [9] that anodic oxidation substantially improves the corrosion resistance of beryllium in gases.

This work is a continuation of [7] on the development of methods of anodic oxidation of beryllium in chromic acid and the interaction of anodized beryllium with stainless steel 1Kh18N9T.

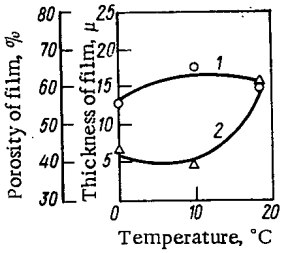

Fig. 1

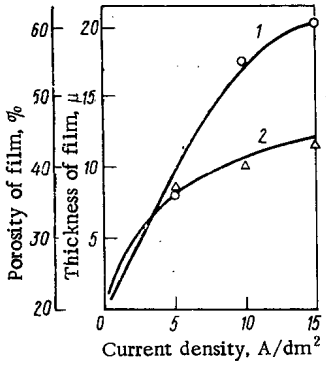

Fig. 2

Fig. 1. Thickness (1) and porosity (2) of anodic film on beryllium in relation to electrolyte temperature (20% H_2CrO_4, 10 A/dm^2, 1 h).

Fig. 2. Thickness (1) and porosity (2) of anodic film in relation to current density (20% H_2CrO_4, 10°C, 1 h). 10^{-3}-10^{-4} mm.

Translated from Atomnaya Énergiya, Vol. 38, No. 5, pp. 333-334, May, 1975. Original article submitted February 4, 1974.

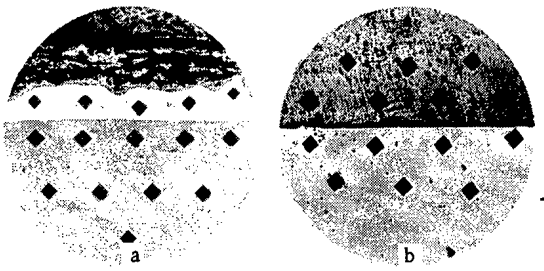

Fig. 3. Micrographs of the zone of contact between diffusion pairs of steel 1Kh18N9T and beryllium. a) Untreated beryllium; b) anodized beryllium.

EXPERIMENTAL METHOD

The samples of distilled beryllium (99.7% Be) were cut from beryllium bars produced by hot pressing and extrusion. Anodizing was conducted in solutions of chromic acid. The thickness of the film was determined by the optical method in a binary Linnik microscope (MIS-11) by the usual method [10], and the porosity of the outer layer by filling with spindle oil [11]. The compatibility was investigated by the method of diffusion pairs. The samples of beryllium and steel were ground and loaded in a molybdenum container with a stopper. The samples of anodized beryllium were tested without grinding. In the container the samples were subjected to a pressure of 2-3 tons/cm^2, which ensured complete contact. The containers were annealed at 700° in a vacuum muffle furnace with a molybdenum heating element. The vacuum was maintained within limits of 10^{-3}-10^{-4} mm Hg. The temperature was measured by means of a Chromel—Alumel thermocouple with an accuracy of ± 1-2%. After diffusion annealing, the container was cut in two along the generatrix by means of spark machining, and microsections were prepared. Each section was examined in the MIM-7 microscope. The microhardness was measured in the PMT-3 apparatus under a load of 100 g.

EXPERIMENTAL RESULTS

The most important parameters determining the quality of the anodic film are the temperature of the bath and the current density at which anodizing was conducted. Figure 1 shows the variation in the thickness of the film and its porosity with the electrolyte temperature. It can be seen that the thickest film is obtained at 10°C. The porosity of the outer layer is almost identical at anodizing temperatures of 0 and 10°C, but it increases ~ 50% at 18°C, evidently due to more intensive solution of this layer by the electrolyte. Figure 2 shows the variation of the thickness and porosity of the anodic film with current density at identical anodizing times. It can be seen from Fig. 2 that the thickness and porosity of the film increase with increasing amounts of electricity. With the same amount of electricity passing through, the thickness and porosity of the film are independent of the current density. Changes in the concentration of chromic acid within the limits investigated (2-20%) have no substantial effect on the quality of the film. Thus, by changing the anodizing conditions (time, current density, temperature) one can change the thickness and porosity of the anodic film within wide limits.

For practical use we recommend the following conditions for anodizing beryllium in 20% chromic acid (temperature of the electrolyte 10°C):

Current density, A/dm^2	Anodizing time, h
10	1
10	2
7	3
5	4

A continuous high-quality coating 15-20 μ thick (porosity of the outer layer not over 40%) is obtained with 10-20 A-h/dm^2.

It was shown previously [7] that the anodic film consists of a thin barrier layer directly adjacent to the metal and a porous outer layer. Electrochemical and electron microscopic investigations showed that the thickness of the barrier layer varies with the forming voltage and amounts to 30-40 Å; the thickness of the porous layer depends on the amount of electricity passing through. The porous outer layer is permeated with randomly arranged pores 200-400 Å in diameter. According to x-ray analysis, the anodic film consists of amorphous beryllium oxide, which crystallizes after annealing at 700°C.

In the investigation of the compatibility of unprotected beryllium with steel 1Kh18N9T in vacuum at 700°C for 1000 h the formation of a diffusion zone 100-110 μ thick was observed (Fig. 3a).

X-ray diffraction analysis with the URS-50I apparatus showed that the diffusion zone consists of a layer of $FeBe_2$ (hexagonal lattice of the $MgZn_2$ type, $a = 4.213$ Å, $c = 6.833$ Å) with a thickness of 68 μ and a solid solution of beryllium in the steel with a thickness of 48-50 μ. The microhardness of the beryllide was 1290 kg/mm^2. It is not excluded that chromium and nickel may be dissolved in $FeBe_2$, in very small concentrations that do not affect the lattice constant of the intermetallic compound. The microhardness of the solid solution of beryllium in the steel varied from 398 to 240 kg/mm^2, i.e., down to the microhardness of the original steel. The results obtained are in good agreement with the data in [3], a study of the interaction of commercial iron and stainless steel with beryllium; a layer of $FeBe_2$ with the same microhardness was formed, and a solid solution. Tests of stainless steel with beryllium anodized under the conditions recommended showed that annealing in vacuum at 700°C for 40 days does not change the structure or microhardness of the steel in the boundary zone (Fig. 3b). The anodic film does not dissolve and prevents interaction of the steel with beryllium. It was found by metallographic and x-ray analysis in the course of a year that an anodic film with a thickness of at least 10 μ is a reliable protection for stainless steel at temperatures up to 700°C. At 800°C compatibility is ensured only for 160 days. At 850-900°C a diffusion zone is formed within 40 days. Under these conditions beryllium evidently diffuses into BeO and $FeBe_2$ and the film of BeO becomes "transparent" to beryllium.

Thus, anodizing of beryllium in 20% chromic acid at 10°C ensures its compatibility with stainless steel for 1 year at 700° in vacuum.

LITERATURE CITED

1. W. Vickers, Metallurgy of Beryllium, Chapmans and Hall Ltd., London (1963), p. 335.
2. A. Knapton and K. West, J. Nucl. Materials, 3, 2, 239 (1961).
3. G. V. Zemskov and N. I. Mel'nik, Metal. i Term. Obrabotka Metal., 62, 4, 3 (1966).
4. G. Grigor'ev and L. V. Pavlinov, Fiz. Metal. Metalloved., 25, 2, 5 (1968).
5. B. Seddon and J. Miss, Reactor Group. Rep. UKAEA, 842 (R) (1965).
6. R. Fries et al., J. Nucl. Materials, 32, 171 (1969).
7. R. M. Al'tovskii et al., Zashchita Metal., 5, 2, 206 (1969).
8. Z. Whitby et al., Techn. Proceed. 48th Ann. Convent. Amer. Electroplat. Soc. (Boston, 1961), New York (1961), p. 106.
9. J. Vachon, J. Nucl. Materials., 6, 1, 139 (1952).
10. A. F. Bogoyavlenskii, Zavod. Lab., 1, 64 (1956).
11. N. D. Tomashov and A. V. Byalobzheskii, Zavod. Lab., 3, 307 (1951).

VALIDITY OF THE HYPOTHESIS OF HARDENING IN CALCULATIONS OF CREEP OF IRRADIATED STRUCTURES

V. N. Kiselevskii, B. D. Kosov, N. P. Losev, D. V. Polevoi, B. V. Samsonov, and N. Yudino

UDC 620.172.2

A substantial increase in the reliability of nuclear reactors requires the development of scientifically valid methods of calculating their structural elements. In the first place, this refers to structures subject to the action of irradiation, high temperatures, and loads, which lead to the development of creep. At present for the calculation of the kinetics of deformation during the creep of structural elements of the usual aggregates, depending on the type of material being used, well-known hypotheses (or theories) are used, which, as a rule, in some measure correspond to the actual behavior of the material. In particular, for structures made of structurally stable stainless steels of austenitic class, equations are used that proceed from a hardening hypothesis [1], which generally can be represented in the form

$$\dot{p} = f(\sigma, T, p), \tag{1}$$

where p and $\dot{p}$ are the values of the creep and its rate at the given time; σ and T are the stress and the temperature.

The creep rate depends on the parameters of the temperature—force interaction and the structural state, which in Eq. (1) is characterized by the magnitude of the creep itself. Reactor irradiation is a powerful factor in the action on the structural state of the material and, therefore even for structurally stable materials, Eq. (1) can prove to be unsuitable.

In connection with this, we formulated the following problem: to verify the applicability of the hardening hypothesis, i.e., Eq. (1), for irradiated austenitic steel of type Kh16N15M3B.

From the structure of Eq. (1), it follows that such a confirmation can easily be accomplished for stepwise variation of σ or T. In the present study we apply the method of stepwise variation of the stress at constant temperature, equal to 650°C.

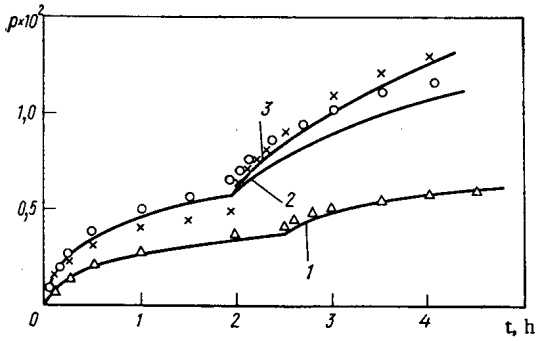

Fig. 1. Curves of unsteady creep of steel Kh16N15M3B for a one-step increase in stress. Experimental conditions for all the figures are: T = 560°; $\Phi = 5.3 \cdot 10$ neutrons/(cm^{-2}·sec^{-1}); 1) $\sigma = 20 \rightarrow 22$; 2) $22 \rightarrow 24$; 3) $22 \rightarrow 25$ kg/mm^2.

First we studied the creep of the indicated steel in the stress range 20-26 kg/mm^2 [2], where the investigation method was also described. Under ordinary conditions and under conditions of inside-reactor loading, the increase in creep satisfies the equation

$$p = A\sigma^n t^m$$

with t given in hours. The corresponding values of the coefficients A, m, and n are given in Table 1.

TABLE 1. Values of Coefficients in the Equation of the Initial Sections of the Creep Curves

Intensity of neutron flux (E ≥ 0.85 MeV), neutrons /(cm^{-2}·sec^{-1})	A	n	m
0	$7{,}64 \cdot 10^{-11}$	5,8	0,4
$5{,}3 \cdot 10^{12}$	$1{,}09 \cdot 10^{-12}$	7,3	0,6

Translated from Atomnaya Énergiya, Vol. 38, No. 5, pp. 335-336, May, 1975. Original article submitted February 11, 1974.

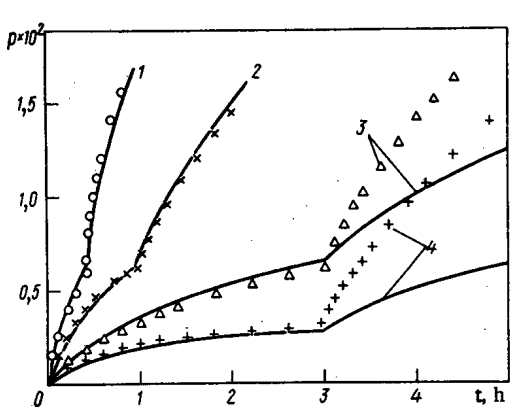

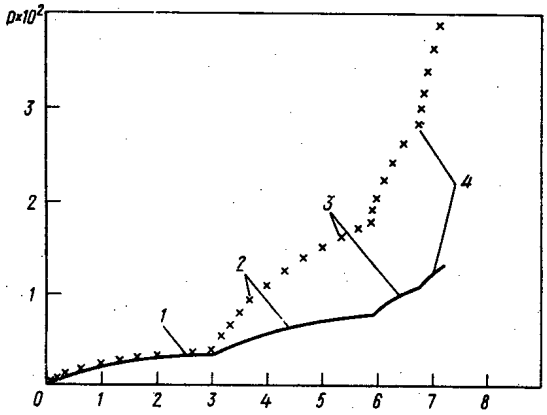

Fig. 3

Fig. 2. Curves of unsteady creep of steel Kh16N15M3B irradiated in the reactor for a one-step increase in stress: 1) $\sigma = 21 \rightarrow 26$; 2) $22 \rightarrow 24$; 3) $20 \rightarrow 22$; 4) $18 \rightarrow 20$ kg/mm^2.

Fig. 3. Curves of unsteady creep of steel Kh16N15M3B irradiated in the reactor for multiple stepwise increase in stress: 1) $\sigma = 18$; 2) 20; 3) 22; 4) 24 kg/mm^2.

Investigations for the stepwise increase in stress ($\Delta\sigma = 2$ kg/mm^2) showed that the initial sections of the creep curves after loading are well approximated by Eq. (2) with appropriate coefficients. The control experiments (without irradiation) showed that the hardening hypothesis in the first approximation can serve as a basis for calculations on the creep of structural elements of steel Kh16N15M3B (Fig. 1). If we take into account the natural spread in the experimental results, which is especially appreciable for the investigation of the creep of materials, then we can recognize that the agreement between the calculated curves and the experimental data is fully satisfactory.

Figure 2 shows the initial curves of creep for stepwise loading of irradiated steel (separate points) and the calculated curves (solid lines), corresponding to the hardening hypothesis. For large values of the stress and small irradiation times, when the radiation effects of the variation of structure do not affect the kinetics of the deformation we note agreement between the experimental and calculated data, which once again attests to the validity of the hardening hypothesis for unirradiated steel Kh16N15M3B. However, in proportion to the increase in irradiation time, the difference between the actually observed creep and that predicted from the hardening hypothesis increases, and for an integral flux of about 10^{17} neutrons/cm^2 attains an appreciable value, which indicates the unsuitability of the hardening hypothesis for determining the creep of irradiated steel under the investigated conditions of loading.

To confirm this conclusion we carried out a special experiment, in which the stress in a single sample was varied in steps of 2 kg/mm^2 in the range 18-24 kg/mm^2 (Fig. 3). Just as in the preceding experiments, for small deformation times we obtained agreement between the calculated and experimental values of the creep deformation. With increasing time of creep deformation of the irradiated steel there is a considerable increase in the values found on the basis of the hardening hypothesis.

Thus, it has been shown that in the case of the investigated loading conditions, the hardening hypothesis is not applicable for the calculation of creep deformation for neutron irradiation even for structurally stable materials.

LITERATURE CITED

1. Yu. N. Rabotnov, Creep of Structural Elements [in Russian], Nauka, Moscow (1966).
2. G. S. Pisarenko et al., Probl. Prochnosti, No. 4, 3 (1974).

EFFECT OF REACTOR RADIATION ON THE THERMOEMF OF CHROMEL—ALUMEL AND CHROMEL—COPEL THERMOCOUPLES

M. N. Korotenko, S. O. Slesarevskii, and S. S. Stel'makh

UDC 621.039.531

The accumulation of radiation-induced defects in thermocouple materials standing in the radiation field of a nuclear reactor can lead to an alteration in the physical properties of the materials themselves. These alterations ensure that the readings given by the thermocouples do not correspond to the actual temperatures they are supposed to be measuring.

In the present work we examine the way in which reactor radiation alters the thermoemf of a chromel—alumel thermocouple (diameters of electrodes 0.2 and 0.5 mm) and a chromel—copel thermocouple (diameter of electrodes 0.5 mm), an aluminum oxide ceramic being used for insulation. A qualitative assessment of the change in the thermoemf was arrived at by comparing the reading of the test thermocouple with those of a standard thermocouple and a control thermocouple made of the same materials and of the same dimensions as the test thermocouple, but which was not itself irradiated. Individual calibration graphs were drawn up for all the thermocouples over the temperature range 20 to 300°C; the errors did not exceed ± 0.2% of the measured temperature. The thermocouple was calibrated in a specially designed thermostat both before and after irradiation. During calibration, conditions such as the arrangement of the thermocouples and the heat losses were held constant.

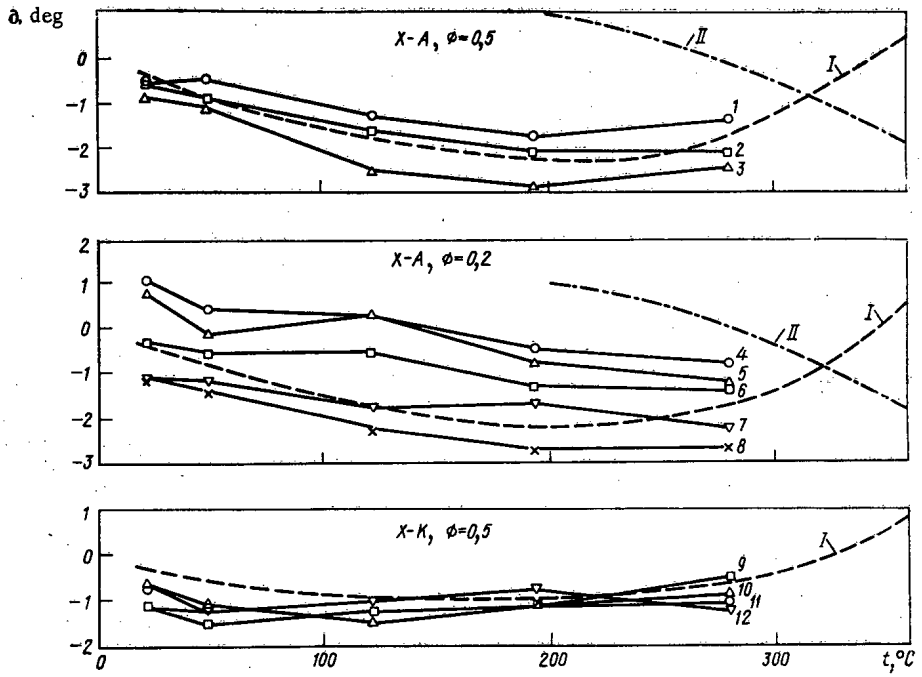

Fig. 1. Deviations of second calibrations (after irradiation) from first calibrations (I, II are the averaged data given in [2] and [3] respectively).

Translated from Atomnaya Énergiya, Vol. 38, No. 5, pp. 336-337 May, 1975. Original article submitted May 16, 1974.

TABLE 1. Neutron Flux in the Vertical Channel of the Reactor

Parameter	nV_0 ($e = 0{,}025$)	$\int_{1,3}^{\infty} \Phi(E)\,dE$
Neutron flux density at 10 MW, neutrons/(cm^2 sec)	$1{,}2 \cdot 10^{14}$	$4{,}9 \cdot 10^{13}$
Intergral neutron flux, neutrons/cm^2	$3{,}6 \cdot 10^{20}$	$1{,}5 \cdot 10^{20}$

The thermoemf was measured by the compensation method. An automatic potentiometer type P-365 of accuracy class 0.005 was used as the second instrument. The thermocouple under test was irradiated at about 130°C in air in a dry vertical channel within the active zone of a type VVR-M reactor. The spectral characteristics and neutron flux density were measured along the height of the channel by means of activation detectors, for various reactor power levels [1]. The values of both thermal and fast neutrons are given in Table 1.

The deviations of the second calibrations from the first for 12 test thermocouples are shown in Fig. 1 over their normal range of operating temperatures. This shows clearly that chromel—alumel and chromel—copel thermocouples, when subjected to intensive ionizing radiation, can give readings 1.5 to 3.0°lower over a period of time, this tendency being the more marked in the case of chromel—alumel. Certain correlations were observed between the diameters of the electrodes and the spread of the deviations between individual couples, a wider spread being noted with the thinner thermocouples.

Figure 1 also shows the results of the work described in [2] and [3]. These show us that our results are qualitatively similar to the data given in [2]. Some quantitative differences appear at our higher levels of integral neutron flux.

It is difficult to explain the divergences between our results and those given in [3], insofar as the authors of the latter do not give any information about the levels of neutron flux during irradiation, about the type of thermocouple insulation, or about various other important factors.

LITERATURE CITED

1. V. M. Pasechnik et al., At. Énerg., 35, No. 5, 315 (1973).
2. N. F. Pravdyuk et al., At. Énerg., 25, No. 3, 233 (1968).
3. G. Bianchi and S. Moretti, Energia Nucleare, 11, No. 8, 426 (1964).

CATHODE SPUTTERING OF NIOBIUM AND ITS ALLOYS IN A HELIUM GLOW DISCHARGE

D. M. Skorov, B. A. Kalin, V. B. Volkov, P. I. Kartsev, and N. M. Kirilin

UDC 621.039.54.2

Niobium and its alloys are regarded as possible materials for the first wall in thermonuclear reactors. This is, in particular, because it combines good physical properties, high heat resistance, and suitability for industrial production. However, niobium is subject to considerable ion sputtering. Over a year of thermonuclear reactor operation more than 1 mm of the first wall might be sputtered away from a wall of niobium alloyed with 1% zirconium [1]. The maximum wall sputtering would be due to interaction of the material with light ions, such as the fusion reaction products deuterium and helium. This means that a study of the possibility of protecting niobium from sputtering due to light ions is of current interest.

In the present work we have studied the effect of alloying, surface smoothness classification, and coatings on sputtering of niobium samples by helium ions. The experiments were conducted in a glow discharge on a VUP-2K device at pressures of $(1\text{-}2)\cdot10^{-4}$ Torr, with an accelerating voltage of 9.0 kV and a current of 1.4-3.0 mA/cm^2. The sample was held at a temperature of 20-50°C. The cavity of this device has been described previously [3]. To estimate the relative amount of sputtered material the optical thickness of the material deposited on a collector was measured [3]. Four glass plates were used as collectors, and were located on the periphery parallel to the generatrix of the cylindrical chamber at different distances from the sputtering target.

The optical density of the material deposited on the collectors was measured with a type MF-4 microphotometer. The compositions of the sputtering materials are given in the table. The niobium and alloys underwent recrystallization annealing at 1100-1250°C for 3 hours in vacuum.

Samples with various degrees of surface smoothness (▽2-▽8)were prepared by grinding and polishing. The degree of surface smoothness was estimated using a model 201 profilograph—profilometer with a chart recording of the surface relief.

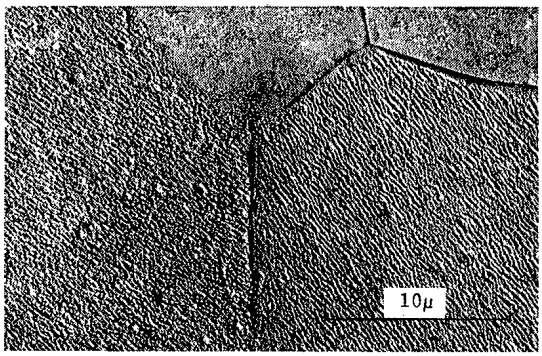

Fig. 1

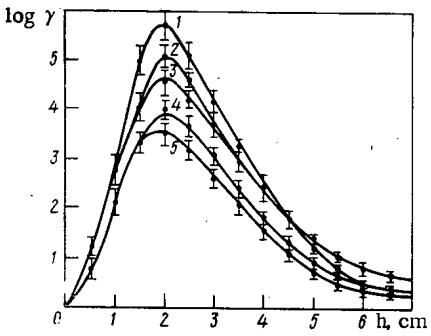

Fig. 2

Fig. 1. Electron microscope picture of a replica with a niobium surface after sputtering.

Fig. 2. The distribution of the density of sputtered material according to the height of the collector for niobium and its alloys. Labelling is given in the table.

Translated from Atomnaya Énergiya, Vol. 38, No. 5, pp. 338-339, May, 1975. Original article submitted May 17, 1974; revision submitted November 18, 1974.

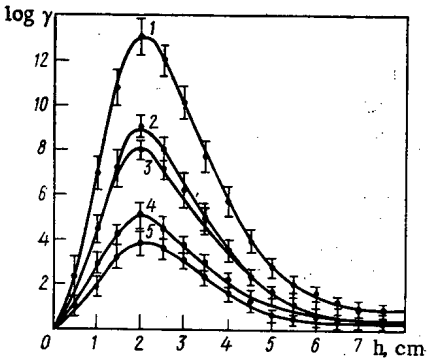

Fig. 3. The distribution of the density of sputtered material for niobium samples with different surface smoothness classifications: (1) fourth smoothness class; (2) fifth; (3) third; (4) seventh (electrolytic polishing); (5) sixth (mechanical polishing).

TABLE 1. Composition of the Alloys Studied, wt. %

Material	Labelling	C	Fe	Ni	Ta	Ti	Zr	Mo	W
Nb	1*	0,01	0,005	—	0,29	0,01	—	0,005	0,005
NVCh alloy	5	0,09	—	—	—	—	1,10	—	—
BN-2AE alloy	4	0,015	0,1	0,1	0,2	—	0,80	4,2	—
	3	0,021	0,1	0,1	0,4	0,2	0,76	4,1	—
	2	0,015	0,1	0,1	0,4	0,2	0,72	4,05	—

*These labels are used in Fig. 2.

The fine structure of the sample surfaces before and after sputtering was studied by electron microscopic examination of carbon replicas. The samples were calorized by hot dipping at the melting temperature (720°C) for 20 minutes. A niobium coating was sputtered onto the samples to be studied in a glow discharge in the same apparatus. The structure of the metal exposed during bombardment of the surface by helium ions is shown in Fig. 1. The results of measurements of the sputtering of the materials studied are given in Fig. 2, where γ is the root mean square optical density of the sputtered material on the collector plates determined from the data of four measurements, and h is the height of the collector. The sputtering coefficients of the alloys relative to the initial niobium were determined as the ratio of these root mean square quantities for a fixed angle (the maximum) of sputtering to the value obtained for sputtered niobium. These ratios form the following proportion

$$\gamma_1 : \gamma_2 : \gamma_3 : \gamma_4 : \gamma_5 = 1 : 0.9 : 0.88 : 0.72 : 0.66.$$

It is clear that the alloys sputter somewhat less than unalloyed niobium. Sputtering decreases as the zirconium content of the alloy increases. This agrees with the published results [1], but nevertheless alloying does not significantly decrease the sputtering of niobium.

The results of measurements of the effect surface smoothness on the sputtering rate are shown in Fig. 3. Minimum sputtering is observed on mechanically polished surfaces (curve 5). During sputtering of samples with developed surfaces smoothing of nonuniformities and the appearance of microstructure were observed. Preliminary sputtering of a layer of niobium onto the sample reduced sputtering of the sample by helium ions by a factor of two.

A substantial increase in the resistance to sputtering was achieved by calorizing the samples, which did not undergo noticeable sputtering when the sputtering time was increased by about 10 times. Measurements of the microhardness showed that the protective layer has a very high hardness (H_V = 1100 kg/mm^2). X-ray phase analysis on a type URS-50-I diffractometer showed that the compounds Nb_2O_5, $NbAl_3$, and Al_2O_3 exist in the zone between the coating and the matrix. The high sputtering resistance of the surface layer is apparently due to the presence of these compounds. This is in agreement both with experiment [1] and with the physical ideal of the dependence of cathode sputtering on the interatomic binding energy [3].

LITERATURE CITED

1. R. Behrisch, Nuclear Fusion, 12, 695 (1972).
2. D. M. Skorov, et. al., Atomnaya Énergiya, 32, 319 (1972).
3. N. V. Pleshivtsev, Cathode Sputtering [in Russian], Atomizdat, Moscow (1968).

RADIOACTIVE IMPURITIES IN SEMICONDUCTING GERMANIUM

A. A. Pomanskii and S. A. Severnyi

UDC 621.039.58

Success in various experiments to distinguish rare events depends largely on the use of detectors consiting of substances with very low levels of intrinsic radioactive contamination. Some experiments demand the use of detectors containing less than 10^{-9}% of radioactive uranium and thorium.

One of the most popular semiconducting metals is germanium. Very stringent requirements are imposed on the purity of germanium: the permitted amounts of some impurity elements are less than 10^{-9}% [1]. High-purity single crystals of germanium can also be used as cathodes in proportional counters, e.g., to register very rare decays of ^{37}Ar and ^{7}Be which are the products of the interaction of solar neutrinos with a target [2], or as semiconductive Ge(Li) detectors, e.g., in seeking the double β^- decay of ^{76}Ge [3]. However, for this purpose we must know how much radioactive impurity is present in the substance.

One of the simplest and most sensitive methods of determining radioactive contaminants in metals is to measure their surface alpha activity. For this purpose, from various specimens of monocrystalline germanium manufactured by various plants we prepared proportional counters. Since single crystals of germanium are hard to work mechanically, the cylindrical holes in the specimens were made by means of ultrasound, thus avoiding the possibility that foreign radioactive impurities could reach the counter wall. The counters were of various sizes: ϕ = 3.3 mm, l = 25 mm; ϕ = 11 mm, l = 80 mm. Through the Plexiglas stoppers we inserted gold-plated tungsten filaments 8 μ thick. The counters were fitted with a mica calibration window 0.8 mm in diameter and filled with a working mixture of 90% Xe plus 10% CH_4 to a pressure of 1 atm; they were tested with the aid of an external alpha-particle source of ^{239}Pu. The remaining counters were calibrated with an internal gamma-ray source. The total measurement time was 700 h. The results revealed that the alpha activity of all the counters was the same 0.1 pulses/h·cm^2. Since the Plexiglas and tungsten filament had very low contamination [4, 5], they could not have made an appreciable contribution to the observed activity. The appearance of powerful pulses in the counter might have been due to the nucleon component of the cosmic rays. However, this was probably not the case, because analysis of the time distribution of the events revealed the presence of a corresponding number of correlated pulses from decay of ^{222}Rn and ^{218}Po ($T_{1/2}$ = 3.05 min) in the uranium series.

We checked the possibility that a contribution was made to the overall background count from atmospheric radon diffusing through the single crystal, by placing the counter in an atmosphere enriched with radon. We observed no increase in the total alpha-activity count. This suggests that all the alpha activity of the counters is due to the presence of radioactive elements of the uranium and thorium series in the germanium. The relative uranium and thorium content is about 10^{-6}%.

Although the surface alpha activity of monocrystalline semiconductor germanium is no higher than that of the best specimens of steel and copper [5], its use for low-background experiments requires special purification from the radioactive impurities uranium and thorium. This is clearly possible in practice. For example, Fiorini [3] used semiconducting germanium with about 10^{-9}% of uranium and thorium.

To check the validity of the identification of the "high" pulses with alpha particles, we prepared counters with cathodes made of metals which, owing to their high melting points, should have been fairly free from impurities, namely, molybdenum (ϕ = 7 mm, l = 66 mm) and tantalum (ϕ = 10 mm, l = 97 mm).

Translated from Atomnaya Énergiya, Vol. 38, No. 5, pp. 339-340, May, 1975. Original article submitted July 1, 1974.

(This applies particularly well to tantalum obtained by vacuum remelting.) The intensity of the "high" pulses in the molybdenum counters was higher (0.02 pulses/h·cm^2) than in the large germanium ones, and that in the tantalum counters (0.003 pulses/h.cm^2) lower, although the germanium counters had a volume intermediate between the molybdenum and tantalum counters. Of the metals and semiconductors examined by us, tantalum is the purest with respect to alpha activity.

In tantalum and molybdenum counters we also clearly see paired pulses which we identified with decays of radon present in equilibrium with ^{226}Ra in the counter walls. In particular, in one tantalum counter, of 26 pulses occurring at a mean rate of 1 pulse in 12 h, four were in the form of two distinct pairs in which the time interval between the pulses was less than 5 min. This enables us to accurately determine the ^{226}Ra content of the materials, to which it is difficult to apply the previously-developed method [6].

The authors thank G. T. Zatsepin, who suggested that the contamination of metals could be determined from their surface alpha activities.

LITERATURE CITED

1. Methods of Determination and Analysis of Rare Elements [in Russian], Izd-vo AN SSSR, Moscow (1961).
2. G. T. Zatsepin and V. A. Kuz'min, in: Proceedings of International Seminar on the Physics of the Neutrino and Neutrino Astrophysics [in Russian], Izd. FIAN, Moscow (1969), p. 156.
3. F. Fiorini et al., Nuovo Cimento, 13A, 747 (1973).
4. I. R. Barabanov, V. B. Veshnikov, and A. A. Pomanskii, At. Énerg., 26, No. 3, 299 (1969).
5. G. E. Kocharov and V. O. Naidenov, Pribory i Tekhnika Éksperimenta, No. 3, 5 (1966).
6. A. A. Pomanskii, S. A. Severnyi, and E. P. Trifonov, At. Énerg., 27, No. 1, 36 (1969).

DETERMINATION OF EPITHERMAL NEUTRON SPECTRA FOR RESONANCE DETECTORS BY THE CADMIUM RATIO

R. D. Vasil'ev and V. P. Yaryna

UDC 621.039.5

The cadmium ratio is the ratio of the activation reaction rates in a test neutron field for one and the same sample (or identical samples) in bare form and when shielded by cadmium.

Neglecting thermal and resonance self-shielding and the attenuation of resonance neutrons by cadmium, we obtain the following obvious relation between the cadmium ratio $r_{Cd}^{1/v}$ for a 1/v detector and the cadmium ratio r_{Cd} for a resonance detector:

$$r_{Cd}^{1/v} = r_{Cd} + \frac{I'}{I^{1/v}}(r_{Cd} - 1), \tag{1}$$

where $I^{1/v}$ is the resonance integral of the portion of the activation cross section which is proportional to 1/v and I' is the excess resonance integral above this portion of the cross section. This relation is valid for any neutron spectrum if the resonance integrals I' and $I^{1/v}$ are determined for the given spectrum and a given effective cutoff energy E_{Cd}.

A relation similar to Eq. (1) can be written in the Westcott representation. Including all corrections we obtain

$$r_{Cd}^{1/v} = r_{Cd}\frac{1 - wk_{Cd}}{G_T} + \frac{G_r S_0}{G_T g} k_{Cd}(F_{Cd} r_{Cd} - 1), \tag{2}$$

where $s_0 = 2I'/(\sqrt{\pi}\sigma_0)$ and g are Westcott parameters; σ_0 is the activation cross section at the neutron velocity $v_0 = 2.2 \cdot 10^3$ m/sec; $k_{Cd} = (\sqrt{\pi}/4)\sqrt{E_{Cd}/E_0}$ (here, $E_0 = 0.0253$ eV is the neutron energy corresponding to the velocity v_0); G_T and G_r are the self-shielding coefficients in the thermal and resonance regions respectively; w is a small correction factor (0.024 for gold) which takes into account the deviation from the 1/v law for the activation cross section in the region of the cadmium cutoff energy. The parameter s_0 in Eq. (2) was determined under the assumption of a 1/E spectrum for the epithermal neutrons. We note in passing that

$$s_0 k_{Cd} = I'/I^{1/v}. \tag{3}$$

We further consider epithermal neutron spectra which are proportional to $E^{-(1-\alpha)}$ where α is a positive or negative number. We assume the resonance detector has a single resonance at the energy E_R. We then have for a $E^{-(1-\alpha)}$ spectrum

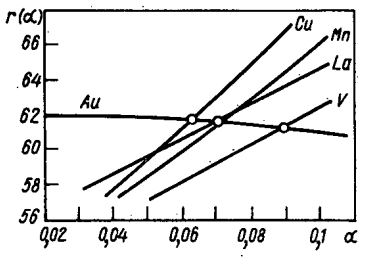

Fig. 1. Measurement of epithermal neutron spectrum by the cadmium ratio method.

TABLE 1. Detector Characteristics

Target isotope	d, mg/cm²	E_R, eV	G_T	G_r	s_0	r_{Cd}
^{197}Au	21,6	5,35	0,979	0,507	17,3	3,89
^{139}La	16	72,4	0,995	$G_r S_0 = 0,933$		
^{55}Mn	51	402	0,977	0,825	0,666	22,9
^{63}Cu	20	638	0,995	0,920	0,730	20,7
^{51}V	85	4160	0,981	$G_r S_0 = 0,107$		

Translated from Atomnaya Énergiya, Vol. 38, No. 5, pp. 340-341, May,1975. Original article submitted August 19, 1974.

$$I'/I^{1/v} = (I'/I^{1/v})\,(E_R/E_{Cd})^{\alpha}\,(1-2\alpha). \quad (4)$$

In this case, Eq. (2) takes the form

$$r_{Cd}^{1/v} = r_{Cd}\frac{1-wk_{Cd}}{G_r} + \frac{G_r S_0}{G_{rg}}\,k_{Cd}\,(F_{Cd}r_{Cd}-1) \times (1-2\alpha)\left(\frac{E_R}{E_{Cd}}\right)^{\alpha}. \quad (5)$$

The relation obtained offers an opportunity to determine the coefficient α from cadmium ratio measurements for a 1/v detector and a resonance detector. One can also use two resonance detectors. In this case, α is determined from the equation which is obtained by equating the right sides of Eq. (5) for two resonance detectors.

The proposed method was tested by estimating the eqithermal neutron spectrum in a thermal neutron source from VNIIFTRI [1]. Some of the characteristics of the resonance detectors used in the measurements are given in Table 1. An effective energy value $\bar{E}_R$ [2] was used in place of the true values of the main resonance energies in the activation reaction. The contributions of the most important secondary resonances to activation of the samples was taken into account in this way.

The values $G_r s_0$ for lanthanum and vanadium were obtained from an analysis of experimental results [2, 3]. In the measurements, cadmium shields 1 mm thick, for which $k_{Cd} = 2.293$, were used in an isotropic neutron field. A graphic determination of the coefficient α by the method described is shown in Fig. 1.

The result of this experiment ($\alpha = 0.06$-0.07) is in satisfactory agreement with determinations of α by subtraction of the contribution of the portion of the activation cross section proportional to 1/v[3] ($\alpha = 0.06$) and by comparison of the test spectrum with a known spectrum [4] ($\alpha = 0.065$). The latter method also confirms the rise in α in the neutron energy region above 1 keV obtained by the present method (see Fig. 1, $\alpha = 0.09$ for vanadium).

LITERATURE CITED

1. V. P. Yaryna, Dissertation, VNIIFTRI, Moscow (1973).
2. T. Ryves and E. Paul, J. Nucl. Energy, 22, 759 (1968).
3. Operating Instructions for Reconstruction of the Differential Energy Spectrum of Epithermal Neutrons by Subtraction of the 1/v Contribution [in Russian], Izdvo Standartov (1973).
4. K. Geiger and L. Van der Zwan, Metrologia, 2, 1 (1966).

INTERNATIONAL CONFERENCE: "ADVANCED REACTORS: PHYSICS, ECONOMICS AND DESIGN"

L. A. Kochetkov

This conference was held at Atlanta, Georgia (USA) on September 8-11, 1974 and was sponsored by the American Nuclear Society jointly with the Technological Institute and Southern Interstate Nuclear Association. Sixty-three papers were given from the USA, England, Italy, USSR, Federal Republic of Germany, France, Japan, and other countries. The extensive range of subjects covered included an account of national programs in advanced atomic energy power plants, experiences in building and operating advanced prototypes of installations, problems of economics, physical calculations, physical experimentation, and activities related to preparing constants.

The first and part of the seventh sessions were devoted to achievements and tasks in the field of advanced reactors.

A paper by Namsek and Cunningham, "Current State of Fast Breeder Development Programs in the USA," was of interest for the following aspects and considerations. The present US program gives priority to fast breeder reactors (FBR) with oxide fuel and sodium coolants. It has set itself the goal of doubling within a short time — "10 years or less." Despite the fact that current designs being worked out for oxide fuel-burning reactor cores which estimate the breeding factor (conversion ratio) at 1.20-1.25 (the doubling time is approx. 30 years), there is confidence in the possibility of improving it (by improving the oxide fuel) so much that the doubling time will be shortened to 15 or even 10 years. The need of developing carbide and nitride fuels as reserve varieties was noted. The calculated breeding factors at present precondition levels for oxide, carbide, and nitride fuels stand at 1.25, 1.40, and 1.30, respectively.

Attention was drawn to the fact that the program does not at present assign a place to metal fuel, although it allows in principle the highest breeding factor yield to be obtained, and the US AEC has spent huge amounts of resources on its development.

Besides the reduction in doubling time, the tasks to be undertaken are the attainment of maximum burnup (15%), development of improved materials for fuel element and container sheathing, which would

TABLE 1. Several Parameters of French Reactors

Parameters	Phenix	Commercial Phenix	Super-Phenix
Power output (electric) MW	250	450	1 200
Maximum Fuel Burnup (MW · days/tons)	50 000	70 000	70 000 *
Temperature of fuel element sheathing (no. deviations/deviations), °C	650/700	630/700	620/700
Linear capacity (W/cm)	430	430	430
Number of loops in the secondary circuit	3	4	4

* It is planned in future to boost burnup to 150,000 (MW · day)/ton.

Translated from Atomnaya Énergiya, Vol. 38, No. 5, pp. 342-344, May, 1975.

have at integrated fluxes of $2.5 \cdot 10^{23}$ neutrons/cm^2, a volume expansion not greater than 5%, and greater creep resistance within the reactor. Fuel reprocessing requires a shorter external cycling — with reduced exposure time of up to 30-120 days, improvement in the technology of more thorough extraction of fissile isotopes in reprocessing, and fuel element manufacturing from secondary fuels with high ^{240}Pu content.

A great amount of attention was given to safety problems.

Among the closest landmarks of this program are the construction of the experimental FFTF reactor (1976) and the CRFR loop-type demonstration reactor (1982) with the following parameters: power output (heat and electric) 975 and 350 MW; sodium temperature at reactor input and output 390° and 535°C; steam temperature and pressure 480°C and 100 atm; and average fuel burnup depth 100,000 MWh/ton.

As an alternative, a gas-cooled fast reactor and a fused-salt thermal breeder were considered possibilities. The work on the fast gas-cooled reactor was successfully combined with the development of gas-cooled thermal reactors and was based on them. The positive experience gained in using the Peach Bottom Atomic Power Station and in developing the Fort St. Vrain gas-cooled reactor with an output power of 330 MW(e) has made it possible for the General Atomic Corporation to obtain authorization to put into commercial use power plants with an output of 770-1200 MW(e) by the 1980's. It is planned in the future to boost the power output to 1500 MW(e) and raise the gas (helium) temperature to 1000°C and convert to a direct cycle with a net efficiency of over 50%.

It was noted in the paper by C. d'Orval, et al. "The French Advanced Reactor Program" that at the present time the French Atomic Energy Commissariat is concentrating its attention on fast sodium, high-temperature gas-cooled thermal reactors and light-water thermal reactors. Much success was achieved in France in the development of fast sodium reactors: the Phénix reactor was put into operation at the end of 1973. For some time past it has been run at full capacity. The net power utilization factor has been 0.6 (since start-up). The steam generators work well enough. In recent months the plants were tied up with breakdowns in their steam fittings, in the control systems for pump rotation and with disruptions in reliable power supply; there was one instance of a complete cutoff from the outside mains, which served as a serious check on the emergency cooling system based on natural circulation in all three circuits (the third circuit has air cooling).

In France there are two fast breeder programs under development: the commercial model of the Phénix and the Superphénix, in the development of which the Federal Republic of Germany and Italy are participating. Several parameters of these reactors are shown in Table 1.

An integrated grouping is adopted for all reactors. Fuel exposure takes six months until processing.

In the development of high-temperature gas-cooled reactors, progress has been associated with the recent construction of an experimental reactor with a gas output temperature of 750°C. It is thought possible in the future to raise the output gas temperature to ~1000°C without changing the fuel particle temperature limit of 1350°C. Only thermal gas reactors were taken into account. The necessity of increasing the gas temperature is connected with the future use of reactors in chemistry and metallurgy.

The program paper from the Federal Republic of Germany was delivered by Wirtz (Karlsruhe). In 1973, the Federal government adopted its "Fourth Atomic Energy Program" for 1973-1976, which provided for the study of two types of future reactors: a helium-cooled thermal reactor and FBR.

Efforts have been concentrated in the gas-cooled reactor development program on working out a high-temperature gas-cooled reactor with a capacity of 300 MW(e) that uses thorium oxide fuel pellets; a high-temperature (helium) gas-cooled direct-cycle reactor that uses a gas turbine; the use of a high-temperature heat-transfer gas in industrial processes; and the development of fuel elements for high-temperature gas-cooled reactors.

Joint work is being conducted with the USA in fuel elements for high-temperature gas-cooled reactors (HTGR) aside from the development of their own concept of fuel element pellets. It was maintained that the present HTGR reactor core with the same fuel temperature limits, specific heat release, fuel elements, and rod controls can heat helium up to 940°C. By using a more ramified and smaller-sized rod control system and by reducing the power intensity from 8.4 to 7 kW/liter the temperature of the helium can be increased to 990°C. Control of the improved core and an axially adjustable core allow the helium to be heated up to ~1100°C. Specific efforts are being undertaken to shorten the fuel cycle time from four to three years.

The FBR program has concentrated on developing sodium-cooled fast reactors. The first stage in implementing this program will be to build the SNR reactor with a power output of 300 MW(e). Construction of the reactor was begun in 1973. After its completion in 1980, it is planned to build a power unit producing ~2000 MW(e). At this moment, development work is underway on a unique kind of reactor that produces ~1000 MW(e), having the following basic parameters: specific load 380 kW/liter; average burnup 67,000 (MW·day)/ton; breeding factor 1.27; steam parameters 538°C, 169 atm; and net efficiency 42%.

The advanced reactor development program in Japan was described in the paper of Takeda, "Progress in Fast Reactors and Development of Heavy-Water Reactors in Japan." The paper related that in 1968 the government adopted an advanced program which focussed its resources on fast sodium-cooled and thermal heavy-water reactors. In accordance with this program, 1975 is the date planned for introducing the Fugen heavy-water (retardant) reactor with boiling light-water heat exchanger and thermal power of 557 MW, and the Joyo experimental fast reactor. An important feature of the Fugen reactor is its negative vacuum effect, which is important from the standpoint of safety.

At the same time as the Joyo is being built, the Monju demonstration plant is planned, whose construction is scheduled to start in 1976. Its basic parameters are: thermal power 714 MW; average burnup 80,000 (MW·day)/ton; temperature of the heat exchanger at reactor imput and output, respectively, 390°C and 540°C.

No program paper was forthcoming from England.

The paper of the Soviet delegation related about the state-of-the-art, achievements, and difficulties encountered in the BR-10, BOR-60, BN-350 and BN-600 fast reactors, and stressed the expediency of bringing into a specific coordination in the future the FBR and high-temperature gas-cooled thermal reactors which have the best economic and dynamic characteristics. Besides this, special attention was drawn to the breeding factor and doubling time.

It may be said, in summing up, that in all countries at present the oxide-fuel and liquid-sodium heat exchanger FBR are regarded as the principal future energy-producing reactor type. In England, USSR, and France the first prototypes of such a model have already been built. In USA, Federal Republic of Germany, and Japan they are intensively under development. In many countries the development of more powerful (~1000 MW(e)) reactors has been started.

The high-temperature helium-cooled thermal reactor is regarded as the most preferable "partner" to the FBR. The successfully operation of the experimental reactors in the USA and Federal Republic of Germany are a strong stimulus to development in this direction. The economies, high efficiency (over 50%), safety features, excellent fuel cycle characteristics, and enormous future potentialities of use for these reactors in the metallurgical and chemical industries, all favor their development.

Previously, a certain interest was evinced in heavy-water thermal reactors.

The problem of breeding was considered in one way or the other in all the panels. The increased interest in it might possibly be explained by the question which has been sharply raised in the USA concerning the independent supply of its energy by fuels. It was maintained in the Taylor-Bethe report published in the USA prior to this conference that on the one hand the future is for fast reactors, and on the other that current fast reactors can yield an efficiency of ~1.20-1.25 and the doubling time of the system is 30 years, and consequently one is faced with the development of some sort of completely new fast reactor. The very fact that the problem of breeding has been considered in so many papers attests to a new, no longer ignorable relation to this question now prevalent abroad. The idea which is quite remarkable and enunciated in the program paper of the USA is that a doubling time of 15 or even 10 years can possibly be attained in improved oxide cores, despite the fact that there is no greater efficiency than 1.25 in present developments of breeder reactor cores. A further boost in efficiency is linked with the use of carbide and nitride fuel.

It was stressed in the paper of the Soviet delegation, "Current State and Development of Fast Reactors in the USSR," that the problem of breeding in FBR has been given top-priority attention in the Soviet Union ever since the first development of fast reactors began. It was maintained that the core of the BN-350 reactor (with plutonium fueling) produces a yield of $kV \approx 1.40\text{-}1.50$. This became the subject of a lively discussion. The conclusion may be drawn from the exchange of views at the conference and subsequent study of the foreign papers that the significantly better breeding ratios of the Soviet BN-350 and BN-600 reactors are explainable by the larger volumetric fuel proportions (40-43% against

30-33% abroad); greater thickness of shields (40-60 against 25-30 cm); the use of fuel compensators in place of boron; and the use of high ^{240}Pu, ^{241}Pu, and ^{242}Pu content fuel (in rated prerequisite amounts).

It stands to reason that the economics, the selection of optimum parameters for fast reactors, was also given attention.

It was particularly noted in the Soviet paper that in fast reactors, in contradistinction to thermal reactors, a definite boosting of parameters that does not lead to a reduction in power intensity does influence both the reduction in fuel and capital components of energy-production costs. This notion was well demonstrated by the example of designing the BN-350 and BN-600 reactors.

A detailed analysis of the nuclear fuel resources as a function of fuel cost was given in the US paper. It was shown that the fuel cost will rise in the near future, while the competitiveness of fast reactors in comparison with thermal reactors will increase. It is therefore expected that in 1985 the competitiveness of fast reactors will be 71-91 dollars/kW.

The basic problem was most probably considered in the third to the sixth panels, that of the accuracy of calculating the neutron–physical parameters for fast reactors and the role of physical experimentation in solving these problems. The accuracy reached in calculating the neutron–physical characteristics was, according to the data of the foreign authors, ± 1% for the multiplication factor, ~3-5% for energy emission distribution and ~8-10% for the breeding factor. To increase the accuracy of calculation, it was thought necessary to considerably improve the accuracy of cross-section determinations, especially in the 1-200 keV region.

The discussion on methods of physical calculations and physical experimentation were interesting, although this is the subject of another report.

In conclusion, I express my gratitude to my colleagues at the conference: V. N. Rumyantsev, A. V. Kamaev, N. I. Ermakov, as well as to my comrades at work: V. V. Orlov, V. B. Lytkin, and M. F. Troyanov, who to a great extent helped to make this review appear.

SOVIET—AMERICAN SEMINAR ON STEAM GENERATORS FOR FAST REACTORS

P. L. Kirillov

The Seminar was held in Los Angeles, California (USA) on December 2-4, 1974. It was conducted on behalf of the US Atomic Energy Commission by a division of Atomics International Corporation in California, in accordance with the Agreement between the USSR and USA on Scientific and Technical Cooperation in the Peaceful Uses of Atomic Energy. Representatives of a number of institutes and the State Institute for the Control of Atomic Energy made up the Soviet delegation. Staff members of the Reactor Research and Development Division of the Atomic Energy Commission, Argonne and Oak Ridge National Laboratories participated from the United States, together with employees from leading US industrial companies, such as Babcock-Wilcox, Combustion Engineering, Foster Wheeler, General Atomic, General Electric, Westinghouse, Atomics International, and others.

Each side presented 10 reports. The Soviet reports were:

1) Basic principles of sodium-water steam generator construction.
2) Experience in starting-up and tune-up work in the BN-350 reactor steam generator.
3) Steam generator construction and design for the BN-600 Atomic Electric Power Plant and its foundation.
4) Heat exchange in direct-flow steam generators heated by sodium.
5) Stall in the sodium-water type steam generators and heat exchange in the stall zone.
6) Development of water leaks into the sodium by defects in the pipe walls and at the sealing joints in the pipe panels.

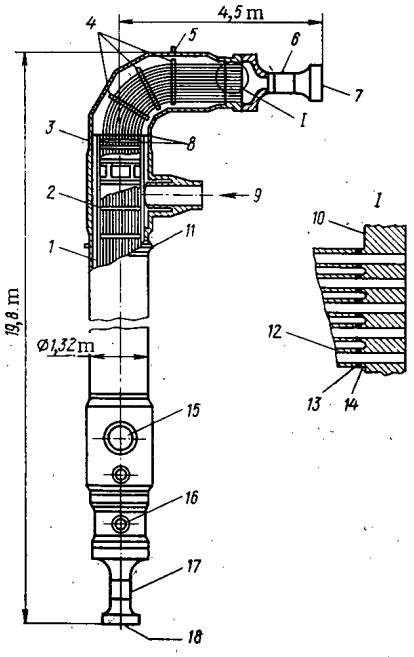

Fig. 1. Single-walled pipe and multiple forced circulation steam generator manufactured by Atomics International: 1) frame; 2) pipe grid; 3) heat shield; 4) vibration guards; 5) ventilation hole; 6) 17) steam escape adapter; 7) steam outlet; 8) disc and thick sleeve baffles; 9) sodium inlet; 10) pipe panel; 11) compensator; 12) pipe (15.87 × 2.78 mm); 13) butt weld; 14) machine finish; 15) sodium outlet (two openings); 16) drain hole; 18) steam inlet (water).

Translated from Atomnaya Énergiya, Vol. 38, No. 5 pp. 344-347, May, 1975.

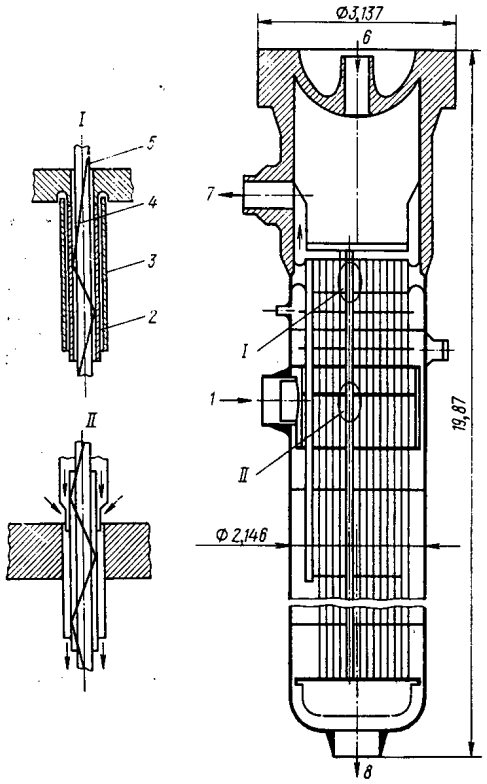

Fig. 2. Steam generator with protected bayonet direct-flow type pipes made by Foster-Wheeler. 1) Sodium inlet; 2) heat transfer pipe; 3) protective pipe; 4) whirler; 5) bayonet pipe; 6) water inlet; 7) steam outlet; 8) sodium outlet.

7) Investigation of the breakdown of different steels used in control jets.

8) Leakage detection of steam generators in fast reactor plants.

9) Steam generator emergency safety systems.

10) Computational research in temperature and concentration fields in the sodium-water interaction zone.

The American reports were:

1) Historical review of steam generator development in the USA, including the problems involved in developing and testing the operation of the EBR-II and Enrico Fermi reactor steam generators.

2) Research and development program on steam generators for liquid-metal-cooled fast reactors.

3) Description of steam generators and other assemblies for the Clinch River first demonstration atomic electric power station.

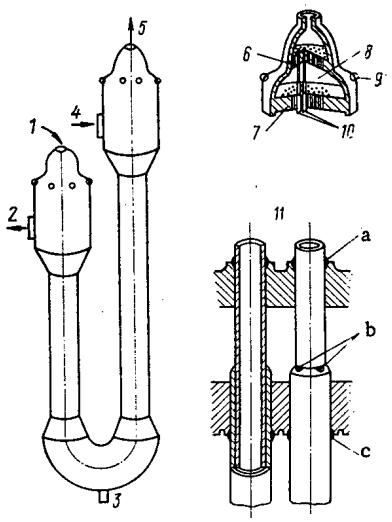

Fig. 3. Steam generator with U-shaped two-layered pipes and multiple forced circulation manufactured by Westinghouse: 1) water inlet; 2) sodium outlet; 3) drainage; 4) sodium inlet 5) steam outlet; 6) pipe mounting panel from the water side; 7) pipe panel from the sodium side; 8) helium (stagnant) 9) inspection window; 10) double pipes (≈ 24 m);11) overall view of the connections between the double pipes and the pipe panels a) top weld; b) longitudinal grooves for leakage detection; c) bottom weld).

4) Development and test results of the evaporator (steam superheater) with single pipes made by Atomic International. including experiments with the 30 MW power model.

5) Development and test results of the evaporator (steam superheater) using Field pipes on the 1.5 MW power model.

6) Development and test results of the steam generator using Westinghouse double-walled pipes.

7) Materials selection for the steam generator.

8) Danger of small leaks and results of experiments with them.

9) Small leakage detection, description and characteristics of experimental plants.

10) Methods of analyzing large leaks in steam generators, including a description of tests on a large leakage test stand.

Steam Generator Construction

About 20 different steam generator designs were described in the reports of the USA, two of which were used at the EBR-II and Enrico Fermi power stations. During operation of the steam generator at the Enrico Fermi plant where coiled pipes are used, leaks were detected that were caused by corrosion and vibration, as well as by inadequate welding at the pipe panel. The steam generators of the EBR-II reactor have been running since 1964, up to now satisfactorily (40,000 h in the steam system, and 88,000 h total). Two-ply pipes made of 1X2M steel and double-pipe panels with air in the intermediate spaces are used in them. Periodic spot inspections of the surfaces showed the wall material to be in good condition.

The American experts have been enabled by their experience in developing and testing both these steam generators at the installations and many models to work out the basic principles of designing and constructing steam generators, envisioning:

1) as high a reliability in the heat-transfer surface as possible (pipes without butt welding, two-ply pipes, double-pipe panels, etc.);

2) high-grade welding;

3) use of perlitic steel of $2^1/_4$Cr1M, obtained in the USA;

4) supply of reliable hydrodynamic steam and water flow (greater preference is given to vertical steam generators with straight pipes);

5) elimination of vibrations;

6) use of protective membranes located in the sodium;

7) use of modularity (one module has a capacity of about 100 MW); joining modules together in sections;

8) shutting off the steam generator when any leakage is detected;

9) safety features for rupture in the one to six pipes of the steam generator.

For the 350 MW Clinch River demonstration station project operations are planned to begin in the middle of 1982), three possible steam generator designs are taken into account: with the hockey stick type single-walled pipes and multiple forced circulation (Fig. 1); with protected bayonet pipes (Field) of the direct-flow type (Fig. 2); and with U-shaped two-layered pipes and multiple forced circulation (Fig. 3).

Materials and Control

Independently of the construction of steam generators, there is a clearly discernible attempt to use high-purity materials (electric arc vacuum smelting). It is considered expedient to carefully test the pipes before use in production (quality control testing with ultrasound, eddy currents, etc.). X-ray control is used on all welded seams. Pores up to 0.05 mm are detected in this process. Vacuum inspection (10^{-5}-10^{-6} mm Hg) is made only when the apparatus is in a cold condition.

The basic material which is taken for granted in all projects is unstabilized perlitic steel of $2^1/_4$Cr1M. Its application is possible for evaporators and steam superheaters up to temperatures of 510°C. It is assumed there is 50% decarbonization of the walls at a depth up to 2 mm; the use of austenitic steel is considered expedient because of possible bursting when moisture falls on them. Several companies consider it possible to use Incaloy-800 and high-chromium steel (13% Cr). American experts are of the

opinion that stabilization of the $2\frac{1}{4}$ Cr1M steel with niobium leads to technological difficulties and does not provide the required durability of mechanical properties at high operating temperatures.

The water cycle of the steam generator receives a great deal of attention. Systematic investigation with different qualities of water has been contemplated for a special circuit at one of the power stations in Florida.

Steam Generator Calculations

The surface of steam generators in the USA is calculated by formulas that are different than those used in the USSR. This is true both for calculating the heat emission coefficient in the boiling and stall zones and for calculating the position of the stall section. All of the formulas are empirical and will be refined in later experiments. It would be proper to compare the methods of calculation used in the USSR with those of the USA. Since the American experts calculate the steam generators for extensive service times without washing, their interest in every kind of pipe surface deposit (fouling) is very understandable, as is therefore the concern with modifying the heat exchange. Naturally, special attention is given to the water composition.

A research cycle on heat exchange in steam generators is planned at Argonne National Laboratories. Steam generator stability calculations are based on the American Society of Mechanical Engineers (ASME) boiler codes (Code Section III) with certain additions related to the effects of sodium.

Technology of Sodium

The sodium is purified from impurities by cold traps, which are able to accumulate impurities up to 15% by weight. A cold trap with a volume of 2 m^3 is changed once in 2-5 yr. The cold traps also clean the sodium in the second circuit of tritium, which makes it possible to reduce the tritium concentration in the turbine system at the same time. Experts working on the EBR-II think that tritium in the sodium is not dangerous. In the opinion of some experts, special latticed filters to hold back corrosion products from the building materials and hot traps to control the thermodynamic activity of carbon in the sodium are necessary. Nevertheless, besides the cold traps, no other cleaning devices are provided at the Clinch River plant.

Besides the plug indicator to control impurities in the sodium, it is proposed that other devices be used. Oxygen content is controlled by an electrochemical mesh with hard ceramic electrolyte, consisting of thorium oxide and yttrium oxide. A basic problem is considered to be the stability of the indicators in time. Carbon is proposed to control the device with a diffusive nickel membrane. To control the hydrogen content in the sodium a device consisting of a nickel membrane and an ion-discharge pump are used. The sensitivity of the instrument is 3-30 ppm. This unit is widely distributed in testing benches.

All instruments are calibrated by standard methods: wires made of special materials are held in the sodium at 750°C and then chemically analyzed. For oxygen, vanadium is used, for carbon a special stainless steel is used, and for hydrogen scandium is used. An electrochemical honeycomb and a diffusive nickel membrane are proposed to be used to control water precipitation into the sodium. In addition, the control of hydrogen in an inert gas is provided by a chromatograph. An acoustic method developed by American specialists to trace leaks only after the steam generator is stopped is considered promising, because a transmitter made of lithium niobate lying in an oxygen atmosphere is used in the device.

It is suggested that alcohol be used to wash sodium residues out the equipment, although washing with water vapor is not excluded in principle. The latter method is considered to be dangerous because of subsequent alkaline decomposition of the steel, especially if the surface temperature exceeds 150°C. At present, the use of debanol ($C_4H_{10}O_2$) is planned, which is capable of multiple applications, because its regeneration is possible.

Processes with Water Leakage into the Sodium

To study the processes that occur when water leaks into the sodium and the behavior of the construction materials in the reaction zone, a large number of experiments were made at sodium temperature up to 500°C, flow deliveries up to 45 g/sec, and sodium velocities up to 3 m/sec. No effect on deterioration was noticed by the velocity of the sodium. The protective pipes in the steam generators (see Fig. 2) help to increase the operation time up to the bursting of the adjacent tube with water, which was experimentally confirmed.

Experiments are being set up to investigate large leaks in a steam generator model (see Fig. 1). The purpose of these intended experiments is the confirmation and improvement of computational programs as well as laying the experimental foundation for protective systems in the steam generator for the Clinch River Reactor.

The TRANSWRAP-II program has been worked out to calculate the transient processes in the second circuit when large leakage appears. It assumes the bursting of one pipe with subsequent bursting of six pipes. The maximum water discharge (41 kg/sec) is reached in 0.1 sec after the initial rupture. A refined SWAAM program is being written which will make it possible to define the extent of the danger of dynamic loading on the frame of the steam generator from the interaction of sodium with the water and to predict the behavior of the membrane.

Steam Generator Protection Systems

Three systems are provided to protect steam generators from excess pressure. The functioning of each of the systems is determined by the magnitude of the leakage: in flows up to 45 g/sec detected by one of the hydrogen detectors the steam generator can be stopped either manually or automatically; in flows of 45-900 g/sec the loop is automatically stopped by the operation of a protective explosive membrane in a gas cavity with expandable capacity; and in flows greater than 900 g/sec there is an automatic stopping by the operation of a protective explosive membrane in the sodium.

A pressure transmitter behind the explosive membrane gives a signal to indicate the automatic stoppage. At this time a reverse type membrane made of Incoloy-800 is assumed to be used. The pressure scattering of the break is 2%. The membranes are arranged at distances of ~600 mm from the inlet to the superheater and outlet from the evaporator.

After the Seminar, our delegation visited the research center of Atomics International at Santa Susana (near Los Angeles), the General Electric Company in Sunnyvale (near San Francisco), Westinghouse in Madison (near Pittsburgh), the Argonne National Laboratory and its affiliate at the National Reactor Testing Station in Idaho Falls (the EBR-II reactor). The Soviet experts acquainted themselves with the laboratories at these centers; it was here that discussions were held on problems of mutual interest.

FOURTH SYMPOSIUM OF THE INTERNATIONAL AGENCY ON ATOMIC ENERGY ON THERMODYNAMICS OF NUCLEAR MATERIALS

O. S. Ivanov and A. S. Panov

The symposium was held in October, 1974, in Vienna. The program was far broader than that announced and also included problems of diffusion, chemical interactions, and safety in emergency situations. The principal topics were the thermodynamics and processes of diffusion in oxide and carbide fuels under operating conditions. Some 67 reports were presented.

Rend (England) presented some results and mentioned prospective uses of thermodynamics in predicting and understanding the behavior of nuclear fuels under operating conditions. He discussed uranium and uranium–plutonium oxide and carbide fuel, its interaction with the jacket, decomposition products, and the heat transfer agent; considerable attention in relation to the problem of safety was given to the behavior of the fuel and the active zone of the reactor during hypothetical emergency situations. The scantiness of the thermodynamic data on the two main types of fuel for fast reactors was indicated (uranium–plutonium oxides and carbides) and the contribution of the symposium in clearing up this problem, for example, the thermodynamic potential of oxygen in oxide fuel in relation to its nonstoichiometry and also at high temperatures. Rend stated that thermodynamics can be used to solve existing problems in the atomic industry and thought conditions good for international cooperation in the study of the behavior of stainless steels in fast reactors.

In the section devoted to phase equilibrium of irradiated fuel we should mention the reports of Potter (England) and Hollek (Federal Republic of Germany) concerning the analysis of ternary carbides and nitrides of the system of actinide metals (U, Th, Pu) with participation of fission products (rare earth metals, platinide metals, etc.). Common to all systems investigated is limited solubility in dicarbides and sesquicarbides and the continuous solubility in most monocarbides. Voluminous data were presented. In only one report Hollek presented data on 54 ternary phase diagrams. The report by O. S. Ivanov and coworkers (USSR) gave data on phase equilibria in ternary systems, U–C–Mo (W, Cr, Re) and U–Th–Mn (Fe, Ni). Raduleck (Rumania) discussed the change in phase equilibrium in UO_2–SiO_2 fuel under the influence of irradiation.

Vestrum (USA), Flotou (USA), O'Hair (USA), and Akhachinskii and coworkers (USSR) presented data from calorimetric studies of heat capacity and the enthalpy of uranium and thorium pnictides, plutonium fluorides and oxides, complex ternary oxides of uranium with lithium, potassium, rubidium, and cesium, and several compounds of lithium and titanium. Almost all the data presented are new. Especially valuable are the results of Flotou's experiments on hard-to-obtain plutonium isotopes. Takahashi and coworkers (Japan) gave additional data on the heat capacity of uranium monophosphide at temperatures down to 1080°K. O. S. Ivanov and coworkers and G. B. Fedorov and coworkers (USSR) gave the results from experiments and calculations of thermodynamic properties of binary and ternary solid solutions based on uranium. Tetenbaun (USA) presented interesting data on changes in the thermodynamic properties and characteristics of the vaporization of uranium dioxide with the addition of plutonium and neodymium oxides to it. Ackerman and coworkers (USA) systemized the thermodynamic properties of the actinide–oxygen system. The relationships established made it possible to calculate previously unknown constants for AmO_2 and other oxides.

Translated from Atomnaya Énergiya, Vol. 38, No. 5, pp. 347-348, May, 1975.

In the section on mass transfer and redistribution of components in irradiated fuel there were interesting reports by Matska and coworkers (Federal Republic of Germany), who gave data on selfdiffusion of uranium in uranium monocarbide and discussed the effect of impurities, nonstoichiometry, and reactor irradiation. R. A. Andrievskii and coworkers (USSR) discussed partial thermodynamic and diffusion characteristics of nonstoichiometric carbides of transition metals. Data were also presented on the effective diffusion coefficients obtained in creep tests.

Naomides and coworkers (Federal Republic of Germany) and Lindmeyer (USA) presented interesting data on migration of the fuel nucleus in the field of a temperature gradient in coated particles of fuel in high-temperature gas-cooled reactors. The mechanism of the movement was presented and the relative advantages of carbonitride fuel were discussed. The type of coating was discussed from the viewpoint of more effective detention of fission products.

In the section concerning interactions of fuel with fission products, the jacket, and the heat transfer agent an interesting and detailed report was given by Kordfunk (Netherlands) on the interaction of uranium dioxide with cesium. He reported that the most stable compound at 600-1000° is $Cs_2U_4O_{12}$, with a relatively low density as compared with UO_{2+x}. This leads to additional swelling of the fuel. The temperature and concentration regions of UO_{2+x} at which this compound does not occur were reported.

In connection with the problem of safety, there were several reports on experimental and theoretical studies of the equation of state and vapor pressure of uranium dioxide, uranium—plutonium, and sodium at temperatures up to 7000°K, making it possible to determine the behavior of these materials at high temperatures under emergency conditions.

On the whole, the symposium demonstrated the substantial development of studies concerning the thermodynamics of nuclear materials, characterized by studies of the effect of operating conditions (reactor irradiation, high temperature gradients, fission products, etc.) on the condition of nuclear fuel and construction materials (including redistribution of oxygen and plutonium), the ameba effect, swelling, diffusion mobility of uranium and its high-melting compounds with carbon and oxygen, and chemical interaction of the fuel with fission products and the jacket. The characteristics of phase equilibrium in numerous systems of the original nuclear fuel were given (high-melting oxides, carbides, nitrides, metallic in the solid and liquid states), and also irradiated fuel, taking into account numerous components — fission products. General data were given characterizing the basic thermodynamic parameters of nuclear materials, including nuclear fuel for fast breeder reactors.

The International Agency on Atomic Energy will publish the proceedings of the symposium in the second quarter of 1975. A set of reports has been published in TsNIIAtominform.

INTENSE FLUXES OF FAST PARTICLES FOR THERMONUCLEAR DEVICES

N. N. Semashko

During October and November of 1974 N. N. Semashko and V. V. Kuznetsov of the I. V. Kurchatov Institute of Atomic Energy (IAE) visited scientific laboratories at Berkeley, Livermore, and Oak Ridge, where they became familiar with research and development of intense ion sources and fast atom injectors in the Program on Controlled Thermonuclear Fission, and also took part in the work of the Second International Symposium on Ion Sources and the Formation of Ion Beams held in Berkeley.

Research and development efforts on powerful injectors and high-current ion sources are concentrated in the Lawrence Berkeley Laboratory (LBL), the Lawrence Livermore Laboratory (LLL), and the Oak Ridge National Laboratory (ORNL). The injectors are designed for the supplementary heating of plasma in closed systems of the tokamak type or the buildup of plasma in open ended traps. The work on ion sources is directed mainly toward the development of modules furnishing currents of 50-100 A with pulse lengths of a few seconds and particle energies up to 150-200 keV, the production of ion sources hundreds of square centimeters in area, the extraction of an ion beam with moderate current densities (0.5 A/cm^2), and its shaping by a multiaperture ion-optical system. The parameters of the gas-discharge plasma as an ion emitter and the electrostatic acceleration system are carefully adjusted to obtain beams with an angular divergence as small as 2-3°. The stability of the plasma emitter parameters over the surface and in time ensures identical characteristics of all the apertures during a pulse and makes it possible to obtain beams with minimum angular divergences.

The main effort in the development of injectors is directed toward the production of systems for obtaining atom fluxes of 1-2 MW per module with a high energy efficiency. The problem is being attacked from several directions: recovery of the energy of ions not used in neutralization, recirculation of ion beams through the neutralizer using a magnetic field, obtaining beams of negative ions which are efficiently transformed into neutrals at high energies.

To investigate intense sources and to develop elements of injectors of future devices such as the large PLT, TCT, D-III and other tokamaks at ORNL and LLL, test units are being built with high-power electrical supply systems which will be started up in stages during 1975-1977.

At LBL and LLL the injectors use a magnetic-field-free ion source. In its present form it has a 120 × 400 mm rectangular discharge chamber around the periphery of which are 86 hairpin-shaped tungsten filaments forming a filamentary cathode. The anode is a rectangular frame of rather large area to avoid the formation of anode sheaths which can lead to the production of noise in the discharge and a loss of power. Ions are emitted over an area of 70 × 350 mm with a current density up to 0.5 A/cm^2 which is uniform to ±6%.

The ion beam is extracted and shaped with a three-electrode ion-optical system which contains over 180 slots positioned with an accuracy of ±10μ. The beam is focused in one direction by the curvature of the electrode surfaces and in the other direction by a programmed displacement of the relative positions of the slots in the emission and accelerating electrodes. At the present time beam currents of ~80A are obtained with a pulse duration up to 10 msec for ion energies of 20 keV. The beam is well shaped. More than 80% of the beam is contained in a solid angle of ±4° in the direction across the slots, and more than 50% in an angle of ±2°. A serious fault of the source is the small ratio (1/80-1/50) of the beam current to the arc current.

Translated from Atomnaya Énergiya, Vol. 38, No. 5, pp. 348-350, May, 1975.

The modular principle of source construction has certain advantages: the possibility of producing an emission surface of any reasonable size and shape; an increased over-all reliability of a system of self-contained elements. The magnetic-field-free source permits dense packing of the modules, and this increases the average density of the ion-emission current. Two injectors containing up to six modular sources of the type described were constructed for the 2XIIB open ended trap. It is proposed to introduce an atom flux of ~600 A equivalent with an energy of 20 keV into the trap in the course of 10-20 msec. The experiment is designed to confine a dense hot plasma ($n \approx 10^{13}$ cm^{-3}; $T \approx 10$ keV, $\tau \sim 10$ msec) and to demonstrate the possibility of maintaining such a state by the external injection of fast atoms.

Work is being carried on at LBL on the physical problems arising in the development of sources as well as on the solution of technological problems. The magnetic-field-free ion source is being modified by improving the gas efficiency, controlling the component composition of the ion beam, increasing the ion energy (to 120 keV by 1976) by using two- or three stage acceleration systems, and by increasing the pulse duration to 1 sec. A means for producing the ion optics for stationary beams has still not been found. For existing models of sources there has been developed an original technology for manufacturing electrodes of a multiaperture ion-optical system with a provision for protecting the electrodes against high-voltage breakdowns by using electron tubes (tetrodes). This significantly lengthens the operating time of the sources.

At ORNL the injectors use an ion source of the duoPIGatron type, a modification of the well-known duoplasmatron source developed over a period of years. An oscillating discharge with a plasma source from a duoplasmatron heats up in a magnetic field diminishing practically to zero where an ion-emission surface several tens of cm^2 in area is formed. A three-electrode ion-optical system of the axial type contains several hundred very accurately positioned openings 3.8 mm in diameter. The inhomogeneity in the density of the gas-discharge plasma along the radius (up to 30%) is compensated by using a variable length of the acceleration gap along the radius, and a programmed shift of the centers of the openings in the emission and acceleration electrodes is used to focus the peripheral beams. For an ion-optical system 7 cm in diameter the beam current is ~5A and the pulse duration is 0.3 sec for ion energies up to 40 keV and a small angular divergence (up to $\pm 1.2°$). The sources are used in two injectors for the ORMAK device. The available focusing of the beam permits an increase in the power density of an atomic beam at the entrance to the ORMAK chamber from 2.4 to 5.5 kW/cm^2. Although the beam currents obtained so far have been smaller than those from magnetic-field-free sources, the duoPIGatron has a number of advantages. The ratio of the beam current to the discharge current is higher and reaches values of 1/15-1/10; beams are obtained with smaller angular divergences ($\sim \pm 1°$), and this in conjunction with water-cooling of the electrodes of the ion-optical system permits lengthening the current pulse to 0.3 sec. In principle this source construction leads to high gas efficiency, the ratio of the current of the accelerated beam to the flow of gas entering the source. A module 10 cm in diameter giving a current of 15A and a power up to 150 kW was been developed for two new injectors of the ORMAK device. It is proposed that later the diameter be increased to 20 cm to obtain an ion beam of up to 40A and a pulse duration of 1 sec for energies up to 160 keV for injectors of the TCT and other devices. Data exist showing that the radial inhomogeneity in the density is not increased for larger source diameters.

The Second Symposium on Ion Sources and the Formation of Ion Beams held October 22-25, 1974 at Berkeley was attended by more than 130 scientists from the United States and about 30 from England, Canada, the USSR, France, West Germany, Japan, and other countries. Eleven summary reports and and more than 50 papers were presented in the following divisions: discharges in ion sources, extraction and formation of beams, new types of ion sources, sources of negative and polarized ions, and the application of ion sources (beams) in technology.

In the session on discharges a great deal of attention was paid to the analysis of oscillations in discharges of various types of ion sources, possible methods of suppressing them, and the characteristics of oscillating discharges in uniform and nonuniform magnetic fields. A paper on oscillations in the oscillating discharge of a source and their effect on the transverse divergence of an accelerated ion beam (IAE, USSR) aroused definite interest. Interesting reports were heard on the use of a hollow cathode in the discharge of an ion source of the duoplasmatron type (Stanford) and the effect of sources with an oscillating discharge where the magnetic field is produced by a "helical" anode or cathode (Kyoto University).

A large fraction of the papers on the extraction and formation of beams was devoted to computer calculations of the motion of particles in ion-optical systems of various types for the analysis of the focusing of beams, the optimization of the characteristics of multielectrode accelerating systems, and the achivement of the required densities of the ion-emission currents (LBL, Sandia Laboratories (SL), LLL, and

Culham, England). Results of numerical experiments on computers were compared with experimental data obtained in actual multiaperture ion-optical systems (IAE, USSR). Systems with preacceleration of ions (Culham) were discussed. The use of such systems enables the current density of emitted ions to be maintained independently of the final energy of the beam ions. Interest was shown in the analysis of characteristics of the secondary plasma formed by an intense beam of fast ions in a charge-exchange target of an injector in view of the effect of the plasma on the beam transport (IAE, USSR).

In the session on new types of ion sources papers were presented on three methods for the collective acceleration of ions using relativistic electron beams (SL). The moving potential relief produced by them ensures the acceleration and focusing of an ion beam of more than 100 A with a pulse duration of 1 nsec. A beam of ions up to 100 A was obtained on the six-stage Hall accelerator (Culham) for an accelerating potential of 20 kV. This is significantly higher then in a two-stage system. About 70% of the power of the emerging beam in concentrated in a solid angle of $\pm 10°$, which is appreciably worse than the results obtained with modern ion sources.

In the session devoted to high-current ion sources papers were presented on sources without an external magnetic field (LBL, LLL), the duoPIGatron (ORNL), and the development of similar sources in Europe for injection into devices of the tokamak type (France, England), and the stellarator (West Germany). The annular duoPIGatron developed in Fontenay-aux-Roses (France) has certain merits including a high degree of uniformity of the ion-emission current. Attention was drawn to sources with a radial discharge (IAE, USSR) operating in a cusped magnetic field and having a large ion-emission surface with a system for accelerating ions across the magnetic field.

Among the papers on sources of negative ions the greatest interest was aroused by a communication on a surface-plasma source of negative hydrogen ions (IYaF, SOAN, USSR). A current of 0.88 A and a pulse duration of 1 msec at an energy of 15-20 keV were achieved by using this source.

A certain interest was shown in an injector of polarized H^- ions for LAMF (Los Alamos). The H^- ion current, obtained by charge exchange of positive ions on a cesium target, reached 0.1 mA for an energy of 750 keV.

In the technology session papers were presented on the production of high-intensity ion beams of micron diameters for analysing surfaces, treating them, producing semiconductor devices (ion energies 25-200 keV, intensities to 10^6 A/cm^2 sr keV) and producing beams with large cross sections for ion etching, obtaining coatings by cathode sputtering, changing the physical properties of surfaces (ion energies 1-5 keV, beam currents tenths of an ampere). A cluster ion source with the evaporation of metals, in particular copper and lead, was discussed for the production or application of films. Certain technological aspects of ion engines (Lewis Research Center) with diameters up to 30 cm and a lifetime up to ten thousand hours were discussed. A neutron generator consisting of two ion sources of the duoplasmatron type was described. Two beams of mixed deuterium and tritium ions are incident on a chromium covered copper target (ion energy 170 keV, total current to 300 mA, neutron yield to $6 \cdot 10^{12}$ sec^{-1}).

CONFERENCE ON APPLIED SUPERCONDUCTIVITY

E. Yu. Klimenko

The Fifth United States National Conference on Applied Superconductivity was held in Oakbrook between September 30 and October 2, 1974. More than 650 scientists, engineers, and industrialists took part in the Conference, including 67 scientists from other countries. The Soviet delegation numbered nine.

The papers presented to the Conference may be roughly divided into the following categories: superconducting materials; superconducting magnetic systems; superconducting electrical machines; superconducting electrical transmission lines; "magnetic-cushion" transportation; applied aspects of weak-current superconductivity (instruments based on Josephson contacts, superconducting radiation detectors, memory devices, microcircuits, and superconducting resonators). In addition to the traditional review articles and communications regarding specific developments, programs relating to individual aspects of applied superconductivity now being developed in the United States were outlined and questions of financing these programs were considered.

The latest views of business circles as to the role of applied superconductivity were set out in the most outspoken manner by the Director of the Electrical-Energy Institute M. Rabinowicz, who considered that applied superconductivity had already become a commercial proposition. In view of this the Institute had decided to finance projects for the industrial use of superconducting devices, not envisaging competition between individual companies but rather uniting their efforts to secure the cheapest and most speedy solution to the problem. It is proposed for example that the now-competing Westinghouse and General Electric companies should jointly erect a 100 MVA superconducting electrical generator designed to work as a synchronous compensator in the power system. After this the Institute may start financing 500 MVA generators rivalling traditional electrical machines. The new relationship to applied superconductivity furthermore appears in the fact that the Electrical Energy Institute and industrial companies have started financing scientific investigations and expanding the financing of industrial projects on the assumption that superconductivity is already capable of showing a profit.

This rather narrow practical approach was opposed by the United States Atomic Energy Commission, which proposed extremely broad scientific programs for the development of superconducting materials and the use of superconducting devices in atomic science and technology. The Atomic Energy Commission has financed the creation of new superconductors, a study of the tunnel effect and the thermal conductivity of layer-like superconductors based on molybdenum and sulfur compounds, neutron, Mössbauer, and NMR investigations into the properties of superconductors, research into the exciton mechanism of superconductivity, and a study of electron–phonon interactions. These investigations will have cost $3 million in the 1974-1975 financial year. Detailed programs have been set up for the use of superconducting magnet systems in producing a controlled thermonuclear reaction and in high-energy physics.

The use of superconducting magnet systems in connection with possible industrial applications of thermonuclear energy in the 1990's is being planned in three directions: in installations of the Tokamak type, in θ pinches, and in open traps. Regarding superconducting magnetic systems as one of the decisive components of industrial thermonuclear reactors, the Atomic Energy Commission has assigned some $100 million to their development. The aim of the six-year program (July 1973 to June 1979) is to solve the basic material-science and constructional problems involved in large superconducting magnet systems by the year 1980, i.e., the time proposed for a final determination of the type of installation which will subsequently be developed as a demonstration thermonuclear reactor. This program will make wide use of existing scientific groups as well as the industrial sector, without actually organizing any new center.

Translated from Atomnaya Énergiya, Vol. 38, No. 5, pp. 350-353, May, 1975.

It is intended to spend some $5 million in 1974 on the application of superconductivity in high-energy physics. Work on superconducting elementary-particle accelerators is being conducted very intensively. In addition to the development of accelerators, plans are in hand for replacing ordinary magnets by superconducting versions in beam-separating systems and deflecting, focusing, and analyzing devices. This change should create a substantial economy in electrical power and enable a large number of experiments to be carried out on existing sites.

Superconducting materials occupied a considerable part of the conference program. Members of the Massachusetts Institute of Technology reported some new achievements in the synthesis of ternary molybdenum sulfides. These are layer-like compounds possessing extremely high critical fields, for example $Pb_{0.9}Mo_{5.1}S_6$ has a critical field of 38 T. One new result was also discussed in the corridors: a sample of $PbMo_5S_6$ with a critical field of 60 T in a field directed along the layers, and 40 T in one perpendicular to the layers.

A new technological achievement is the possibility of obtaining layers of niobium carbonitride up to 2 μ thick on carbon filaments 7 μ in diamter. This material is obtained in a form suitable for winding solenoids. A stabilizing copper layer may be deposited on the filament. The critical current density in the intrinsic field reaches $2 \cdot 10^6$ A/cm^2; by treatment with silicon tetrachloride fairly high current densities may be obtained even in magnetic fields up to 5 T (10^5 A/cm^2).

In the year which has elapsed since a record critical temperature was achieved in the compound Nb_3Ge, considerable advances have been made in developing a technology for obtaining coil-winding materials based on this compound. Although not a single meter of such a material has in fact yet been produced, the basic conditions for the development of a high-temperature superconductor have been established, and technological methods (cathodic sputtering, deposition from a mixture of niobium and germanium chloride vapor) have been developed for producing material with a fairly high critical temperature and high critical currents. The current densities in these materials at liquid helium temperature reach values similar to those characteristic of the best niobium—tin samples. An extra advantage of the new material appears at higher temperatures, since at 15°K individual samples possess critical characteristics similar to the characteristics of niobium—titanium materials in liquid helium. A wide variety of methods have been devised to obtain coil wires from other new intermetallic compounds of the niobium—aluminum and niobium—gallium systems; however, some research workers regard these achievements as simply a useful technological experiment to be used in developing a more promising niobium—germanium winding material.

A great deal of attention is being directed at the effect of nuclear irradiation on the winding material; these investigations are directed at establishing the possibility of using superconductor windings in thermonuclear reactors. The results of measurements carried out in industrial niobium—titanium conductors at 330, 37, and 5°K under doses of up to 10^{20} neutrons/cm^2 indicate that the critical current of these materials diminishes with increasing dose, but this effect exhibits a saturation state corresponding to a 15-30% fall in critical current. At the same time as the fall in the critical current, owing to the increase in copper resistance the stability of the conductors is impaired, and so is the insulation. Many research workers consider that it is the resistance of the insulation to irradiation which determines the possibility of using niobium—titanium magnetic systems in a field of irradiation. Intermetallic compounds behave differently under irradiation. Workers in the Brookhaven National Laboratory have studied the effect of irradiation dose on the critical temperatures of practically all known superconductors of this group. The critical temperature and field in all the intermetallic compounds fall after irradiation; there is universal relationship between the dose and the ratio of the critical temperature before and after irradiation: The critical temperature falls by 5% for a dose of 10^{18} neutrons/cm^2 and by 80% for a dose of $5 \cdot 10^{19}$. The critical current also falls rapidly for doses exceeding 10^{18} neutrons/cm^2. This relationship between the critical parameters and the dose may be associated with the disordering of the structure of the intermetallic compounds. The properties of the latter are restored after brief high-temperature annealing.

In many countries multicored cables are being developed from niobium—tin and vanadium—gallium compounds in a bronze matrix. The main problem to be solved in the development of these cables lie in ensuring the flexibility of the conductor, increasing the occupation factor (the proportion of the cross section of the conductor occupied by the intermetallic compound), and stabilizing the conductor. One of the best ways of solving these problems lies in making fairly thin (0.1-0.15 mm) multicore wires and twisting them into a cable suitable for winding solenoids, with the subsequent addition of stabilizing copper wires and impregnation with indium. Intermagnetic General proposes using this technology for the winding

material in the magnetic systems of thermonuclear installations and the inductors of electrical machines. In large magnetic systems in which the wire does not have to be bent sharply, cables of considerable cross section may be employed; for example, Erco has developed a coil cable about 10 mm^2 in cross section and this is being tested in the Lawrence Laboratory, Livermore, California. Difficulties encountered in increasing the occupation factor largely arise from the fact that bronze only deforms satisfactorily if it contains no more than 10-14% tin; hence the occupation factor of the cable cross section by the intermetallic compound cannot be more than 20%. In order to increase the amount of intermetallic compound in the cable, methods are being sought for introducing an additional amount of lead into the cable cross section in such a way as to exert no serious harmful effect on the deformation capacity. For example, tin-rich bronze may be placed inside tubular niobium filaments, the thin outer layer of the incompletely-transformed niobium then acting as a diffusion barrier with respect to the tin, preventing it from poisoning the copper matrix of the cable, which acts as stabilizer. It is also quite possible to use filaments made, not of pure niobium, but of a quenched alloy of niobium with 4% tin, or to place the core of tin-rich bronze on the axis of the cable, where the conditions for its deformation are the most favorable. The method proposed by M. Suenaga in the Brookhaven National Laboratory is also continuing to be developed; it is based on the fact that the cable is first prepared with niobium filaments in a copper matrix after which it is tinned and subjected to homogenizing and reactive annealing. The cable is stabilized by the copper, which is either protected from tin contamination by means of tantalum diffusion barriers or else soldered to the finished cable. However, neither of these means of production has been adopted by industry. Up to the present time less than ten small laboratory solenoids have been made from these multicore materials; in the majority of cases the reactive annealing of the material has been carried out after winding the solenoid. The best result so far has been obtained by the Rutherford High-Energy Laboratory: a solenoid with an internal diameter of 30 mm and an external niobium—titanium section creating a field of 6.5 T has enabled a total field of 12.2 T to be obtained.

There was considerable interest in some Soviet reports relating to a record combined magnetic system (providing for the steady generation of a magnetic field of 25 T), and also, an electrolytic method of manufacturing stabilized superconducting cables now being used in Soviet industry (this contribution was of further interest in that the method so outlined was suitable, without any material changes, for the stabilization of intermetallic multicored cables), as well as in the Soviet program regarding superconductor engineering and the screening of magnetic fields by niobium—tin plates.

The attention of the conference was drawn to the many unsuccessful attempts at creating unstabilized stationary—magnetic systems of the saddle-shaped variety, mainly designed for use in superconducting particle accelerators. It has so far proved impossible to introduce a current exceeding 60-80% of the calculated value into such magnetic systems (as recently produced in the USA and various parts of Europe). This new manifestation of the degradation effect is associated with random heat evolution of a mechanical nature in the winding, capable of converting it into the normal state. The reason for these evolutions of heat has not been uniquely established; they may be due to the cracking of the compound impregnating the winding or the plastic deformation of copper under the action of ponderomotive forces. So far neither quantitative measurements nor even estimates of these evolutions of heat have been made. Proposed methods of combating degradation lie either in strengthening the winding with external bandages or in improving the heat release from the winding. Experimental models have shown that a winding preliminarily compressed with a force exceeding the maximum ponderomotive forces suffers no degradation. The most disappointing results were clearly those obtained in the Enrico Fermi Laboratory, in which this phenomenon necessitated the reconsideration of an already-started program of erecting superconducting dipoles, intended for doubling the energy of the existing accelerator in Batavia, and a return to research with small experimental magnets. Nevertheless this laboratory has serious plans for overcoming the difficulties arising, as confirmed by the tempo of present investigations: in only six months (March-September 1974) it has made and tested a dozen model superconducting dipoles.

In the last year there have been two accidents with stationary-stabilized magnetic systems; one of these put the magnetic system of the large European bubble chamber out of action for a year. The reason for these misfortunes (in which the busbar carrying the magnetic system bent in an unexpected direction, or whole sections of the winding became detached) apparently lay in the screening currents existing in busbars containing parallel filaments. In a magnetic field a busbar of this kind behaves as a strongly diamagnetic material, and this must be remembered when designing the magnet systems. A radical method of combating this phenomenon lies in the use of winding bars with transposed superconducting filaments.

Serious consideration is being given in the USA to the use of superconducting energy-storage devices in power systems in order to even out fluctuations in energy demands. The superconducting storage devices, furnished with a converter—inverter system, should be considerably more effective than the presently-used hydraulic-pump power stations the efficiency of which is no greater than 67%; they should have an advantage over the latter in their rapidity of action, and would not require vast areas for water storage. An investigation into this problem is being conducted by the Los Alamos Laboratory and a group of scientists in Wisconsin University headed by Professor R. Buhm, which has developed a detailed preliminary design for a storage system with a capacity of 10^4 MW·h. It is hoped that 1975 will see a solution to the problem of financing the construction.

The conference also discussed United States, Japanese, West German, and Canadian programs for the development of transport on magnetic cushions, together with problems of superconducting electrical transmission lines and superconducting electrical engineering.

Considerable time was devoted to superconducting instrument making based on the Josephson effect, superconducting memory devices, and microcircuits. The detection of ionizing radiation with superconducting film detectors was described. One of these detectors was formed by an indium—tin film deposited on a glass substrate, 500 μ thick and 1 μ wide. At the critical temperature and critical current a film of this kind recorded 150-800 eV neutral argon and helium atoms and argon and helium ions with an approximately 100% efficiency.

One of the sections in the conference was entirely devoted to superconducting resonators.

REGULAR SESSION OF TECHNICAL COMMITTEE 45 OF THE IEC

V. V. Matveev and L. G. Kiselev

The 13th Session of Technical Committee 45 of the IEC (International Electrotechnical Commission), whose task is to draw up recommendations on standardization in nuclear instrumentation, was held at Rome and Milan on November 14-23, 1974. The Subcommittees on reactor instrumentation and dosimetry and the Working Groups of the Committee and Subcommittees met at the same time. More than 75 representatives of 12 European, American, and Asian countries took part in the Meetings.

The Meetings summarized the work completed during the past year. Six publications have been issued in the past year, as compared to 27 publications since the formation of the TC-45 till 1973. Among the latter is Publication 340A which expands the Basic Publication on the methods of testing preamplifiers and amplifiers operating with semiconductor detectors. In particular, Publication 340A establishes methods of measuring the transfer constant and the effective feedback capacitance of preamplifiers.

Publication 462 sets forth standard methods of testing photomultipliers used with scintillation and Cherenkov counters, and standardizes the methods of measuring amplitude and time response, noise characteristics, the variation of the characteristics with time and under load, etc.

Publication 460 establishes specifications on portable radiation meters for geological explorations operating with scintillation detectors. The publication indicates the desired operating and test conditions, and lists the parameters which should be given in the operation manual.

General specifications, the names of parameters, and their measurement in radioisotopic instruments designed, in particular, for thickness, density, level, etc., measurements are set forth in Publication 476. Publication 498 covers high-voltage connectors used in nuclear measuring instruments. The Publication establishes the basic dimensions and construction of connectors, their basic electrical specifications, and includes a Soviet high-voltage connector.

Publication 482 regularizes the dimensions of NIM and KAMAK system units, and the dimensions of Soviet units whose construction conforms to Section 5 of OST 95 88-73.

A supplement and correction have been prepared to Publication 323 concerning the ranges of analog and the levels of digital signals. The supplement includes a corrected edition of Sections 4.2 and 5 to which the load currents and resistances for digital signals have been added.

Several additional sections have been prepared to Chapter 39 of the 3rd International Electrotechnical Vocabulary (in Russian, English, and French) which covers the measurement of ionizing radiations with electronic devices. These sections contain definitions of terms on dosimetric and radiometeric devices and on reactor instrumentation.

Several documents of the Central Bureau prepared by TC-45 have been sent in 1974 to National Committees for voting. They include a document which establishes characteristics of testing methods of dc preamplifiers [45 (CB) 87]. The documents concern reactor instrumentation: 45A (CB) 25 (Radiation Detectors in Instrumentation and Protection of Nuclear Reactors. Characteristics and Testing Methods), and 45A (CB) 26 (Design Principles of Pressurized-Water Reactors).

TC-45 has begun to include in IEC recommendations the standards of ESONE Committee which regularize the principles and norms of the KAMAK system. In particular, document 45 (CB) 83 based on EUR 4100e defines the intrarack organization of the KAMAK system.

Translated from Atomnaya Énergiya, Vol. 38, No. 5, pp. 353-354, May, 1975.

The Meetings also discussed comments of national committees on the large number of documents issued by the TC-45 Secretariate. The discussions resulted in 12 documents being given the status of CB documents with the purpose of distributing them to National Committees for voting in accordance with the six-months rule. These documents include the "Organization of Multiframe Devices in KAMAK System and Structure of Control Device for Type A Racks." This document is based on the EUR-4600 standard of the ESONE Committee. Another document standardizes the dimensions and construction of 19-inch racks for NIM and KAMAK units.

TC-45 prepares a number of documents concerning the dimensions of cells used with radioactive materials, measuring glasses for liquid scintillators and radioactive samples, and test tubes for radioactive samples.

The document "Multichannel Amplitude Analyzers. Types and Basic Parameters" is to be distributed for voting in accordance with the six-months rule; the document is based on the Soviet GOST 16957-71 standard and includes the names and definitions of certain parameters of amplitude analyzers.

To the status of CB documents has been transferred the document which establishes the specifications of aerosol radion meters, and also several documents on instrumentation, in particular, the document "Instruments for Intrareactor Monitoring of Neutron Fluxes," which contains term definitions, recommendations on the design of monitoring systems, and basic detector parameters.

The document "The Use of Reactor Protection Systems for Purposes Other Than Safety" is a Supplement to Publication 231 A. The document establishes the principles of interaction between the reactor protection system and other reactor systems and equipment.

A document on the design principles of instrumentation for heavy-water boiling reactors has been drawn up as an Appendix to Publications 231 and 231A. One of the documents gives general recommendations on the accumulation and evaluation of data for the determination of reliability characteristics of reactor protection equipment.

The Chairman of TC-45, A. Reece informed the delegates on the growing activity of the Technical Committee 85 of ISO, in particular, of Subcommittee 3 (SK-3) on Reactor Design.

Several tens of documents are to be drawn up in the next year as documents of the TC-45 Secretariate, of Subgroups Secretariates, or Working Goups (WG).

WG-3 (interchangeability) prepares documents on the KAMAK system. They include a document establishing the principles of sequential organization of multirack KAMAK systems. The Group discussed the advisability of issuing various documents concerning NIM and KAMAK system in the form of two IEC publications both of which contain all documents on both systems.

WG-5 (geological exploration equipment) is preparing a new edition of the document which establishes types and basic parameters of radiation meters used in ore sorting.

WG-9 (detectors of ionizing radiations) has decided to revise Publication 340 (Standard Methods of Testing Amplifiers and Preamplifiers for Semiconductor Detectors) in view of the recent appearance of new and improved methods of parameter testing. It is planned to discuss a document which sets forth specifications for cryostats and Dewar vessels for semiconductor detectors. WG-9 prepares the issue of a vocabulary of terms used in the documents published by this group.

WG-10 (multichannel analyzers) continues the discussion of a corrected edition of the document on testing methods for amplitude analyzers, an another document on the types, basic parameters, and testing methods of devices used with multichannel analyzers operating at high load conditions.

In addition, WG-10 is expected to begin the discussion of a document that standardizes the testing methods of generators for measuring the integral and differential nonlinearity of multichannel amplitude analyzers.

The Plenary Meeting of SC-45 A has resolved to set up a new group and entrust to it the preparation of a document on testing methods for pulse rate meters with a logarithmic scale. Working groups of Subcommittee SC-45 (reactor instrumentation), WG-A1, WG-A2, and WG-A3, continue the discussion of documents including "General Principles of Communication Lines for Reactor Safety Systems," Application of Computers in Reactor Control," "Intrareactor Temperature Measurements," "Periodical Testing and Inspection of Safety Systems, and "Inspection of Airtightness of Fuel Elements."

Working groups WG-B3 and WG-B4 of Subcommittee SC-45B are to discuss, among others, a document on basic parameters and methods of testing of absorbed-dose dosimeters. A resolution has been adopted about the gradual transition to SI units in absorbed dose meters. Documents will be discussed on establishing the basic parameters of instrumentation for monitoring the radioactivity of gas discharges and instruments for continuous monitoring of the concentration of gaseous tritium in the atmosphere. The discussion of documents on the specifications of instruments for monitoring the α, β, and α, β contamination of soil and on neutron dose monitors continues.

Other documents are also to be discussed.

It should be noted in conclusion that throughout the Meetings, the work of TC-45 proceeded quite smoothly. The USSR delegation, consisting of V. V. Matveev, L. G. Kiselev, L. M. Isakov, and Yu. K. Kulikov, actively participated in all Meetings.

THE FIRST ASIATIC REGIONAL CONGRESS ON RADIATION PROTECTION

E. D. Chistov

The First Asiatic Regional Congress on Radiation Protection (15-20 December, 1974) was organized under the direction of the International Commission for Radiation Protection (ICRP), the Indian Association for Radiation Protection in conjunction with the Department of Atomic Energy and was held in the Nuclear Research Center in a suburb of Bombay.

The Congress attracted great attention from specialists, not only from the countries of Asia, but also from Europe and America. Delegates from 24 countries participated, in particular representatives of the IAEA and of the World Health Organization (WHO). Altogether, 300 persons participated in the work of the Congress.

At the five plenary sessions and in the subcommittees, 180 reports were read (130 from India, 13 from USA, 5 from France, about 4 from Japan, the Federal German Republic and Bangladesh; other countries presented one to three reports).

General problems of radiation safety were discussed, viz: the organization of radiation protection services on a country-wide scale; the most important problems and investigations into radiation safety: coordination of research, mutual aid, training; individual dosimetry; the nuclear industry (risks and benefits); legislation on radiation protection.

In addition to the plenary sessions, six subcommittees functioned. In these committees, problems of radiation safety, radiobiology, radiation physics, shielding and dosage calculations, the radioactivity of the surrounding medium, individual dosimetry, increase of the qualifications of the staff of radiation-safety units monitoring-measurement equipment and neutron dosimetry were reviewed. Standards of x- and γ-radiation, thermoluminescent dosimetry etc.were also considered.

Interesting reports were presented by individual scientists (K. Nambi, S. Sunty, A. Ganguly, S. Dua, et al.) on thermoluminescent dosimetry based on CaF_2, $CaSO_4$ and LiF. Almost all the reports of the Indian scientists were devoted to the analysis of radioactive contaminants of the air medium. Their careful approach to problems both of equipment and procedure should be mentioned. The Japanese scientist I. Hirovami spoke about a system for the training and preparation of staff serving radiation safety units. The extent of the program and of the instructional procedures was given. The French specialists shared their experience in operating a centralized service of radiation safety and spoke about its equipment and the extent of monitoring. In almost all the reports presented by the Asian countries, by participants in the Congress, the organization of radiation safety on a country-wide scale was reported. Some interesting data were presented on the extent of operations, radiation loadings and the number of staff occupied in the spheres of application of radioactive isotopes and sources of ionizing radiations.

An exhibition of dosimetric and radiometric instruments was organized for participants in the Congress, in which Indian-manufactured equipment mainly was demonstrated. An automatic ozone gas-analyser deserves mention. It permits the concentration of ozone to be measured in the presence of oxides of nitrogen.

The Nuclear Research Center complex was shown in which, in addition to nuclear reactors, experimental and industrial power-generating radiation facilities were operating, designed for conducting radiation—biological and radiation—chemical processes. Great interest was created by a commercial facility

Translated from Atomnaya Énergiya, Vol. 38, No. 5, pp. 554-555, May, 1975.

for the sterilization of medical products. Its high technology and culture of production should be mentioned. There are also two facilities at the Center, with a fixed irradiator (the irradiators are assembled from Co-60 radioisotopes), a facility with a Cs-137 irradiator, a facility of the fixed type with an irradiator of Co-60 isotopes and a radiation facility of the "gamma-field" type. These facilities are being used for experimental purposes.

The Congress promoted the establishment of contacts between scientists of different countries. It was particularly useful for the Indian scientists, who stressed that the successful solution of the problem of ensuring radiation safety, depends on the establishment of even closer contacts between the scientists of the whole world.

Verbatim reports will be published and sent to the USSR.

SOVIET SPECIALISTS ON GAS-COOLED REACTORS VISIT SWITZERLAND

I. Kh. Ganev

From January 22 to 29, 1975 V. A. Chebotarev, I. Kh. Ganev, E. V. Kusmartsev, and M. V. Mal'ko visited Switzerland to become acquainted with the state of the work on fast and thermal helium-cooled reactors and plans for the future. The delegation visited the Swiss Institute for Reactor Research (IRR) in Wuerenlingen, Brown Boveri Co. in Baden, and the Sulzer Co. in Winterthur; it recieved information on the activities of the Charmilles Co. on refueling machines and the work of the Zurich branch of BBRV on prestressed concrete (PSC) vessels; it was shown around the atomic power plant construction in Gosgen.

The 600 workers at IRR are concerned mainly with physics research and calculations, thermohydraulics, fuel, technological plans, and the dynamics of future HHT and GCFR installations with high-temperature reactors. It is proposed to use a direct cycle gas turbine with the following helium parameters before the turbine: 850°C and 60 bars in the HHT, and 680°C and 90 bars in the GCFR, with efficiencies of 37.5 and 30% respectively. The three-loop 1050 MW(e) HHT reactor with three horizontal turbines is completely contained in a PSC building 40 m in diameter and 45 m high. The fuel elements, developed by the NUKEM Co. of West Germany, consist of microscopic pellets of uranium dioxide with double cladding. Lumped fuel elements were not chosen for technical reasons, but because of the succession of decisions taken for HTGR reactors in the United States. Spherical fuel elements permit higher temperatures, and it is proposed to use them later, for example in the West German THTR reactor. It is planned to construct the HHT reactor in West Germany in 1980-1986 without first building a prototype reactor, since the basic conponents of the installation (the PSC vessel, the lining, the thermal shield, the supporting structure, the core, and the elements of the auxiliary equipment) are regarded as having been mastered by Swiss, West German, and United States industry. Work on helium turbines will be performed on experimental assemblies with nonnuclear heating at Oberhausen for parameters of 50 MW and 750°C, and at Julich for parameters of 40 MW and 850-1000°C, with startup planned for 1976.

A nonintegral arrangement is planned for the 1000 MW(e) four-loop GCFR, the design work on which was completed in 1972. The core is contained in a PSC vessel, the turbine and the heat exchanges are between the vessel and the safety shell, and the generators are placed outside the safety shell. The safety of the arrangement in case of piping ruptures, confirmed by dynamic calculations, is ensured by check valves at the entrance and gas-dynamic seals with nozzle linings in the exit pipes. The GCFR core is similar to cores of modern sodium-cooled oxide-fueled breeders. The main difference is in the roughening of part of the surface of the fuel elements by circumferential ridges of height 0.1, width 0.35, and pitch 1.12 mm. A machine in IRR forms these ridges by the simultaneous treatment of the surface with an electrolyte and a diamond polishing disk. Test unit AGATHE with a power of 950 kW is being prepared for startup in the Heat Engineering Laboratory. It contains 37 mockups of GCFR fuel elements 8.4 mm in diameter with tantalum cores heated by a current of 600 A. Twelve thermocouples are attached to each fuel element with leads to a small computer, thus permitting processing of the results during the experiment. All thermal test units in the laboratory use air and carbon dioxide instead of helium, with scaling to the helium parameters.

The IRR fuel program for the GCFR consists in developing methods for making microspheres of uranium—plutonium carbide approximately 50 and 700 μ in diameter with a steel cladding to obtain a fuel density of 10.2 g/cm^3, and in performing post reactor research on the fuel elements. In the opinion of

Translated from Atomnaya Énergiya, Vol. 38, No. 5, pp. 355-356, May, 1975.

Swiss specialists reactors of the GCFR type have a number of advantages over sodium-cooled breeders, including a higher conversion ratio. The introduction of GCFR reactors is planned for 1990-1995.

The Charmilles Co. designed and built a refueling machine for the Dragon reactor which is still operating successfully. The solutions of the problems of rubbing of surfaces and compression were used in the design of the GCFR refueling machine placed under the core. The fuel element assemblies are fastened in the upper support plate by couplings of the bayonet type.

BBRV manufactured most of the equipment and machines used to construct the PSC vessels. The company was involved in the manufacture of 45 protective shells and five PSC reactor vessels, including those for the Fort St. Vrain and THTR reactors. It is proposed to make the vessel of the second THTR unit by a new technology using an SW-8500 machine with a coil winding on the outer surface of the vessel.

Brown Boveri is manufacturing turbogenerator assemblies for various atomic power plants including some with helium coolant in the primary loop (AVR, THTR, HTR-1160). The company has supplied steam turbines and generators for 55 atomic power plant units with a total power of 37 million kW. Recently the unit power of the asemblies has been increased to 1300 MW at 3000 rpm. The company is carrying on design and research work on gas turbines, and manufacturing them in Mannheim, West Germany. Designs have been developed for a 250 MW machine for the GCFR, and for 350 and 500 MW machines for the HHT. It is assumed that the helium turbine power can be brought up to 1500-2000 MW. The optimum parameters of helium turbines are: temperature to 1200°C with a 4% increase in efficiency per 100°C, expansion coefficient 2.5; one terminal heat exchanger is used as a compromise between efficiency and complexity of manufacture.

The Sulzer Co. manufactures vessels for light water reactors with wall thicknesses up to 220 mm and 7-10 mm thick stainless steel sheet lining. A considerable fraction of the company's effort is directed toward the design, experimental development, and manufacture of single-pass steam generators for atomic power plants with carbon dioxide (five stages) and helium coolants (Fort St. Vrain power plant and THTR and HTR designs). Steam generators made by this company are characterized by trifoliate longitudinal-radial spacer plates with a helical arrangement of tubes (up to 15 radial layers), easily accessible tube sheets, and a single-pass scheme with sections for reheating the steam passing to the high pressure turbine. The company pays special attention to the selection of materials and the quality of the welding of the steam generator tubes. Ten meter tubes are welded into 100 m lengths automatically in an atmosphere of argon, helium, or a mixture of 90% argon and 10% helium. The dynamical rigidity, vibrations, and aerodynamics of the steam generators have been studied in most cases by replacing helium by CO_2, but a number of experiments were performed with helium or in a vacuum. The company also designs and develops helium gas blowers and accessories such as check and regulator valves etc. A horizontal gas blower with gas bearings has been built for the Dragon reactor. At the present time helium vertical gas blowers have been designed with powers up to 10 MW. They have electric drives with a frequency control of the number of rpm, oil thrust bearings, and gas radial bearings. Gas blowers developed by the Sulzer Co. do not have check valves. In case of failure of one of the gas blowers operating in parallel it is slowed down as a result of the choice of the shape of the rotor blades, ensuring a high resistance to reverse flow of gas, and also by a hydraulic brake.

Our delegation visited the atomic power plant construction area in Gosgen. The PWR with a power of 920 MW(e) will simultaneously produce 40 T/h of steam for a nearby carton factory. The steam will be obtained by using a special heat exchange after the high pressure turbine stage. The reactor will be contained in a spherical steel shell 32 mm thick encased in a supporting concrete shell 1.6 m thick underneath and 1.2 m on top, designed for protection against the possible fall of an airplane.

The heat is removed by a dry cooling tower 150 m high natural air circulation. The station is compact, occupying an area of 10^5 m^2.

In conclusion I should like to note the great consideration and goodwill shown the Soviet delegation by the leading members of IRR and the Division of Science and Research. It is assumed that the collaboration between the USSR and Switzerland will continue.

THE EXHIBITION "RADIOISOTOPE TECHNOLOGY IN THE COMPLEX AUTOMATION OF INDUSTRY"

K. A. Nekrasov

In May 1975, in the "Atomic Energy" Pavilion of the Exhibition of Achievements of the National Economy of the USSR (VDNKh), the thematic exhibition "Radioisotope Methods in the Achievement of the Complex Automation of Industry" will be opened.

Currently, more than 5000 organizations and firms of the USSR are successfully using radioisotope technology, which has boosted the production of plant, economy of raw and finished materials, improved quality of manufacturing production and increased production culture." Experience shows that the period of compensation of radioisotope technology is not more than one year.

The exhibits presented in the division of the metallurgical industry demonstrate the application of radioisotopic substances for the complex automation of the crushing mill of the Kachkanarsk Mining-Concentration Combine. Sixty-two radioisotope instruments have enabled the number of maintenance personnel to be reduced and an annual economy of 125,000 rubles to be effected.

In the "Krasnoe Sormov" factory, an automatic plant is operating for the continuous casting of steel. The radioisotope instruments in the continuous steel casting process are carrying out successfully the following operation: monitoring of the liquid metal level in the crystallizer, automatic control by servo-drawing of the dolly, computation of the finished production and automatic optimum coloring of the ingot, automation of cutting, and automatic control of the roller bed, tilter and auxiliary cage.

The high reliability of radioisotope slave level-meters URMS-2M (Fig. 1) has allowed them to be included in the automation complex of the blast furnace at the Zhanovsk "Azostal" factory.

At the Il'ich Metallurgical Plant, Zhdanovsk, 57 radioisotope instruments and nuclear-physical research methods are used. The economic effect of their introduction amounts to 1 million rubles.

Gamma-relays are installed on the conveyor lines, which clearly register flow blockages and issue the order to shut down the conveyor in order to carry out clearing operations. The use of gamma-relays (Fig. 2) has enabled a reliable automatic cycle of operations of the force and exhaust pumps in the slag basins to be ensured.

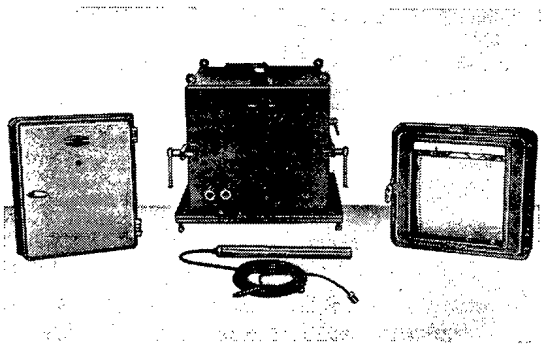

Fig. 1. Multichannel URMS-2M slave equipment.

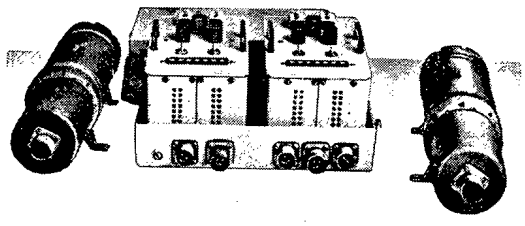

Fig. 2. The GRP2-1 Gamma-relay instrument.

Translated from Atomnaya Énergiya, Vol. 38, No. 5, pp. 357-358, May, 1975.

In order to improve the efficiency indexes of blast furnace smelting, a neutron meter is used in the plant to measure the moisture content of the skip-coke; this is based on the "Neutron-3" type of radioisotope hygrometer.

The use of a radioisotope thickness gage of the zinc-covered RGTsP-1 type in a continuous galvanizing unit enables the coating thickness at any point over the width of the band to be determined and the information to be issued. As a result of the introduction of the device, the plant productivity has been increased, the consumption of zinc has been reduced and the production quality has been improved.

In the exhibits on automation of the coal concentration industry, the use of radioisotope devices in the Cherepovets metallurgical plant are shown by: automation of the drying section and loading of the bunkers, the signalling and remote control panel, the charge dumper with belt conveyor and the system for the automatic discharge of coagulated sludge from the radial thickeners.

Radioisotope technology is used widely in the chemical industry for regulating the density and level of liquids, solids and friable substances.

At the Severodonets Chemical Combine plant, 206 different gamma-relays and slave level-gages are operating, monitoring the level of corrosive media and giving advance warning of a state of emergency.

By means of radioisotope gamma-relays, level meters and densimeters, filling of the railway tankers has been automated at the Chernorechensk Chemical Combine plant and the level and density of the products in the tanks is continuously monitored.

In this same section, an automatic level control system in a vinyl chloride polymerization reactor by the suspension method is exhibited; this uses a gamma-relay and an automatic system of control of the ammonium sulfate wastes from the evaporating plant.

About 800 radioisotope instruments for the monitoring and automation of technological processes are functioning in 140 plants in the food industry.

Stocktaking of sunflower oil in the Vinits Lubricant Combine has been automated by means of radioisotope instruments.

In the sugar industry, automation has been effected of the loading of the limestone-roasting furnaces and the bunkers over the beet choppers, by means of radioisotope gamma-relays.

Automation of production stocktaking of liqueur-brandy firms by means of RRP-2 radioisotope instruments makes an annual average saving of 3000 rubles per instrument.

In the machine construction industry, radioisotope technology finds widescale application for the solution of problems associated with the monitoring and automation of technological processes.

The I. A. Likhachev Automobile factory, Moscow, utilizes 238 radioisotope instruments of various designations.

Diagrams, photographs and models show how the complex automation process is accomplished for supplying the suspension in the ZIL cast body and which eliminates hazardous overflows, improves the working conditions and reduces time-wastage.

The introduction of radioisotope instruments enables the process of mixture preparation in the casting shop to be automated, its high quality to be ensured and the working conditions to be improved. The presence of the mixture components in the sealed tanks is displayed at the control desk and the absence of any component is recorded by a level-meter and leads to shutdown of the entire line; the simplicity of design and the high reliability permits these instruments to be installed at the most inaccessible places.

By means of radioisotope level meters, the level of sand in the quencher and the sand cooling process for the ZIL cast body can be monitored; this enables hazardous situations to be eliminated and work conditions to be improved.

It can be seen from the data on the exhibition, that in the coal industry of the USSR, about 2000 different radioisotope instruments are functioning. For example, at the "Severn" (Northern) mine of the Vorkutaugol Combine, the process of coal and rock transportation to the surface has been automated by means of radioisotope technology.

A special place is assigned to the department displaying "Activities of the All-Union Society Izotop" the specialized organization set up to render technical and practical assistance to firms and organizations through the introduction of the achievements of nuclear science and technology into the national economy of the Soviet Union.

The exhibition "Radioisotope Technology in the Complex Automation of Industry" will be open until November, 1975.

SEMINARS AND EXHIBITIONS OF THE ALL-UNION SOCIETY "IZOTOP"

A Seminar on "Experience in the Application of Radioisotope Methods and Instruments in the Fishing Industry" was held at Riga in October, 1974 by the Leningrad Inter-Republic Section of the All-Union Isotope Society in conjunction with the Main Administration for the Fishing Industry in the Western Basin, the Riga Scientific Research Institute for Radioisotope Instrument Manufacture, and the Construction Board of the Ministry of Maritime and River Transport for chief engineers and chiefs of control and measuring instruments and automatic equipment services of fish-canning enterprises in the Western Basin. More than 60 specialists from industrial enterprises took part in the work of the Seminar.

A Seminar on "Application of Radioisotope Preparations in the Practice of Medical Establishments in Central Asia and Kazakhstan" was held at Tashkent in November, 1974. It was organized by the Inter-Republic Section of the All-Union Isotope Society in conjunction with the Kazakhstan Ministry of Health. Specialists of many medical institutions at Moscow, Leningrad, Kiev, and other cities spoke at the Seminar. The participants prepared recommendations which will be circulated among the medical institutions of Central Asia.

An Exhibition and Seminar on "Materials Produced by the All-Union Isotope Society for the National Economy" was held at Irkutsk in October, 1974 by the Sverdlovsk Inter-Regional Section of the All-Union Isotope Society for specialists of scientific research institutes, design institutes, and industrial enterprises. The purpose of the Exhibition and Seminar was to acquaint the specialists with the materials produced by the All-Union Isotope Society. During the Exhibition, requests were submitted and accepted for the Society's materials in the amount of more than 50,000 rubles.

A Seminar on "Application of Radioisotope Methods and Instruments in Industry" was held at Tula in November, 1974 by the Moscow Inter-Regional Section of the All-Union Isotope Society in conjunction with the Municipal Council of Specialists of the Tula Municipal Committee of the Communist Party of the Soviet Union and the Tula Center for Scientific and Technical Research. More than 60 specialists from 25 organizations at Tula and in the Tula region took part in the work of the Seminar. The reports and statements delivered at the Seminar commented on the promising outlook for the utilization of isotope methods and instruments at industrial enterprises of the city and the region.

Isotope materials and instruments supplied to the national economy of the country by the All-Union Isotope Society were exhibited and demonstrated during the Seminar.

A Seminar on "Operating Experience, Nomenclature, and Level of Advancement in Radiation Shielding Technology" was held in November, 1974 at the Demonstration Hall of the Kiev Inter-Republic Section of the All-Union Isotope Society. Those participating in the Seminar included representatives of various Kiev organizations and enterprises which use radioactive substances, as well as representatives of the Development Institute, manufacturing plants, the All-Union Isotope Society, and health supervision authorities. The Seminar adopted recommendations which will be published and circulated to the enterprises concerned.

Seminars on "Problems of Radiation Safety," "Radioisotope Instruments Used in the Automatic Equipment of the Tallinn Regional for Plant for the Manufacture of Control and Measuring Instruments," and "Radioisotope Instruments for Automatic Control Systems at Enterprises of the Ministry of Nonferrous Metals" were held at the Demonstration Hall of the Sverdlovsk Inter-Regional Section of the All-Union Isotope Society in November and December, 1974 for specialists of Sverdlovsk industrial enterprises.

Translated from Atomnaya Énergiya, Vol. 38, No. 5, pp. 358-359, May, 1975.

Approximately 400 specialists from various Sverdlovsk organizations took part in the Seminars.

A Seminar on "Use of the SURM-2 Radioisotope Level Gauge in Shipbuilding" was held by the Kiev Inter-Republic Section of the All-Union Isotope Society at Nikolaev in December, 1974. Participants in the Seminar included representatives of the Central Design Office, the "Ocean" and "61st Communard" plants, and other shipbuilding organizations. The Seminar adopted recommendations concerning the wider use of the SURM-2 instrument in shipbuilding, and requests for the instrument for 1975 were received from a number of shipbuilding organizations (190 instruments requested by the Kherson Shipbuilding Plant, 120 instruments by the "61st Communard," and 220 instruments by the "Ocean" plant).

A Seminar on "Automatic Fire-Protection Equipment Systems and Automatic Fire-Extinguishing Equipment" was held at Kiev in December, 1974 by the Kiev Inter-Republic Section of the All-Union Isotope Society with specialists of design organizations. Participants in the Seminar included 80 specialists from 70 design institutes. They witnessed a demonstration of the RUOP-1 apparatus in action.

A Seminar on "Use of the RUOP-1 Radioisotope Fire Protection Apparatus" was held at Leningrad in December, 1974. It was organized by the Leningrad Inter-Republic Section of the All-Union Isotope Society in conjunction with the Fire Protection Department of the Leningrad Internal Affairs Administration for the chief power engineers of the city's industrial enterprises. More than 70 specialists participated in the Seminar. They observed the apparatus in operation.

INFORMATION: CORRESPONDENCE

STARTUP OF CYCLOTRON IN FINLAND

L. G. Zolinova

A small isochronous cyclotron with regulated particle energy was put into operation in late 1974 at the city of Turku, Finland; the energy range is 5 to 20 MeV for protons, 3 to 10 MeV for deuterium ions, and 8 to 26 MeV for helium ions.

The cyclotron is a universal source of radiation for activation analysis and for medical purposes.

The cyclotron was developed, prepared, installed, and put into operation through the efforts of specialists of the D. V. Efremov Scientific Research Institute of Electrophysical Apparatus.

Participants in the startup ceremony, held on December 12, 1974, included representatives of the Government of Finland and scientists from other countries. According to representatives of the USSR Ministry of Foreign Trade who attended the ceremony, the high technical parameters of the Soviet cyclotron aroused great interest among the scientists of Finland and the other Scandinavian countries.

Translated from Atomnaya Énergiya, Vol. 38, No. 5, p. 359, May, 1975.

The Plenum/China Program

Research in the medical, life, environmental, chemical, physical, and geological sciences from the People's Republic of China

The 15 major scientific journals published in China since the Cultural Revolution are being made available by Plenum in authoritative, cover-to-cover English translations under the Plenum/China Program imprint.

These important journals contain papers prepared by China's leading scholars and present original research from prestigious Chinese institutes and universities. Their editorial boards are affiliated with such organizations as the Chinese Chemical Society, the Academia Sinica in Peking and its Institutes, and the Chinese Microbiological Society.

The English editions are prepared by scientists and researchers, and all translations are reviewed by experts in each field.

Journal Title	No. of Issues	Subscription Price
Acta Astronomica Sinica	2	$65
Acta Botanica Sinica	4	$95
Acta Entomologica Sinica	4	$95
Acta Genetica Sinica	2	$65
Acta Geologica Sinica	2	$75
Acta Geophysica Sinica	4	$95
Acta Mathematica Sinica	4	$75
Acta Microbiologica Sinica	2	$55
Acta Phytotaxonomica Sinica	4	$125
Acta Zoologica Sinica	4	$125
Geochimica	4	$110
Huaxue Tongbao — Chemical Bulletin	6	$95
Kexue Tongbao — Science Bulletin	12	$175
Scientia Geologica Sinica	4	$125
Vertebrata PalAsiatica	4	$95

For further information, please contact the Publishers.

SEND FOR YOUR FREE EXAMINATION COPIES

plenum
PLENUM PUBLISHING CORPORATION
227 West 17 Street, New York, N.Y. 10011
In United Kingdom 8 Scrubs Lane, Harlesden, London, NW10 6SE, England

Declassified and Approved For Release 2013/09/25 : CIA-RDP10-02196R000400050003-3